Sunday, October 27, 2013 Session 1

Pulp Cell tracking by Nuclear Imaging for Dental Tissue Engineering

Jean-Baptiste Souron[1,2], Anne Petiet[3], Franck Decup[1,2], Julie Lesieur[1], Anne Poliard[1], Didier Letourneur[4], Catherine Chaussain[1,2], Francois Rouzet[4,5], Sibylle Opsahl Vital*[1,2]. [1]EA2496, Pathologies, Imaging and Biotherapies of the Tooth, Dental school, University Paris Descartes PRES Sorbonne Paris Cité, [2]AP-HP Services Odontologie HUPNVS and Charles Foix, [3]Institut Claude Bernard - ICB 2, [4]Inserm, U698, Cardiovascular Bioengineering; and University Paris Diderot-Paris 7, [5]Department of Nuclear Medicine, Bichat-Claude Bernard Hospital, AP-HP, University Paris Diderot-Paris 7, France

Introduction: The most common treatment of pulp infection, endodontic treatment, consists in pulp removal, mechanical enlargement of the canal and placement in the cleaned pulp cavity of a bio-inert material sealed with root canal cement. Such treatment does not exploit the high regenerative cellular potential of the pulp. The present study is part of a larger research project aiming to develop a pulp equivalent implantable in the injured dental pulp, based on the use of mesenchymal pulp stem cells. In tissue engineering, it is a major issue to determine the fate of implanted cells in a living organism. **Purpose:** To track by nuclear imaging ^{111}indium-oxine (^{111}In-oxine) radiolabeled pulp cells after implantation in the rat emptied pulp chamber. **Methods:** Rat pulp cells were radiolabeled with ^{111}In-oxine. Their viability and proliferation rate were controlled in vitro. Then, labeled cells were added to polymerizing type I collagen hydrogel in order to obtain a pulp equivalent. This scaffold was then implanted in the emptied pulp chamber space in the upper first rat molar, after performing pulpotomy. Labeled cells were tracked by Nuclear Imaging (Nano SPECT/CT plus, Bioscan®) for 3 weeks. Negative controls were performed using radiolabeled cell lysates. Treated rats were sacrified at 4 weeks after surgery. Maxillary were isolated, demineralized before embedding in paraffin for histological staining and immunohistochemistry studies. **Results:** *In vitro* studies showed that ^{111}In-labelled pulp cells viability and cell proliferation were similar to unlabeled cells. *In vivo* imaging performed sequentially over a month showed a significant increased radioactivity level from labeled pulp equivalent into the pulp chamber, compared to controls. This labeling was clearly detectable for 3 weeks, which indicates that implanted cells remained viable in the pulp space. At all-time points, whole-body acquisitions by SPECT/CT showed no signal outside of the pulp chamber, suggesting that most radiolabeled cells remained located in the tooth. Histological and immunochemistry studies showed limited inflammation, proliferation and angiogenesis in the cellular scaffold. **Conclusions:** Our study demonstrates for the first time that efficient tracking of pulp cells implanted in the dental pulp can be achieved by Nuclear Imaging. Importantly, our data indicate that the grafted cells were viable and remained located in the dental pulp. These results open a promising avenue in the treatment of pulpal dental diseases by tissue engineering.

Mineral association changes the secondary structure and dynamic properties of amelogenin

Wendy Shaw*1, Yimin Sharon Xu1, Jun-xia Lu1, Barabara J Tarasevich2, Garry W. Buchkol1. 1Fundamental Sciences Directorate, 2Energy and Environment Directorate, Pacific Northwest National Lab, Richland, WA, USA.

Introduction: Biomineralization proteins control the exquisite structures and properties of hard tissues such as bones, teeth, egg shells and nacre. Protein structure is often implicated in the control of mineral properties, however very little structural data is available due to the difficulty in determining structures of proteins interacting with biomineral surfaces. Solid-state NMR (SSNMR) is uniquely suited to the study of the structure of proteins bound to surfaces as demonstrated by studies that determined the structure and orientation of the mineralization proteins statherin and the amelogenin, LRAP onto hydroxyapatite (HAP). While these data are some of the only structural data available for adsorbed biomineralization proteins, the experiments are limited to proteins smaller than 60 residues and are often expensive and time consuming, due to the need to prepare and measure samples with isolated spin pairs. Amelogenin is an important protein in the development of enamel, but its large size and formation of a quaternary structure composed of multiple monomers (nanospheres) have precluded the collection of structural data in solution in addition to the structure of the adsorbed protein. Purpose: We utilize a combination of 1D and recently developed 2D SSNMR techniques along with a sparsely labeled sample to characterize the structure and dynamics of potential HAP binding domains of the 180 residue enamel protein, amelogenin. Methods: The nanosphere sample was prepared at pH=8.0 in 20 mM Tris buffer at ~1.5 mg/mL and ultracentrifuged at 259,000g. The HAP bound sample was prepared by precipitating amelogenin with calcium phosphate, following Fang et al, PNAS, 2011, 108, 14097. NMR studies were conducted at 500 and 900 MHz 1H frequency using published techniques. Results: The nanosphere sample was largely unstructured and highly dynamic, with a small fraction of β-strand present. The HAP bound amelogenin was in a largely β-strand configuration, with a second structural component, identified as a protein overlayer, in a random coil structure. The HAP associated protein was much less mobile than amelogenin in the nansophere. Conclusions: This work provides the first molecular level structure and dynamics information of full-length amelogenin within the nanosphere and on the surface of HAP. We found that amelogenin interactions with HAP resulted in a switch from random coil structure to β-strand structure along with a decrease in protein mobility. This work demonstrates the utility of SSNMR to evaluate structural characteristics of large biomineralization proteins bound to their physiologically relevant surfaces. Supported by the National Institutes of Health, grant number DE-015347.

Multiscale Phenotypic Analysis of Osteogenesis Imperfecta in Murine Bone

Joseph M. Wallace*1,2, Zachary R. Bart1, Max A. Hammond 2,1 Biomedical Engineering, Indiana University - Purdue University Indianapolis, IN; 2 Biomedical Engineering, Purdue University, West Lafayette, IN

Introduction: Bone is a flexible collagen matrix reinforced by mineral. Type I collagen is synthesized as α chains of amino acids forming heterotrimeric helices (2-α1;1-α2) which wind into fibrils. Osteogenesis Imperfecta murine (oim/oim) has a point mutation in col1α2 leading to α1 homotrimers. Heterozygous oim/+ contain one mutant allele, resulting in an intermediate phenotype. Purpose: To investigate how a defined molecular change in collagen alters bone composition, morphology and mechanics throughout the tissue hierarchy. Methods: 12 week old male mice (n=15/gp) were used. Femora and tibiae were harvested and stored at -20°C. Left bones were scanned by μCT (12 μm voxel) then tested to failure in 3 (femur) or 4 (tibia) point bending. Right femora (n=6) were scanned by Raman spectroscopy at 5 points along the posterior surface, then underwent reference point indentation (RPI) at 4 of these locations. Additional right femora (n=5) were briefly demineralized and imaged using atomic force microscopy. D-periodicity of individual fibrils was measured (~50 per sample). Statistical analyses were performed (One Way ANOVA for means, Kolmogorov–Smirnov (KS) tests to assess D-spacing distributions). Results: There was a significant decrease in D-spacing between WT and oim/+ (66.0±0.2 vs. 65.6±0.1 nm), which further decreased in oim/oim (65.4±0.5 nm). KS tests showed significantly altered D-spacing distributions in both disease states vs. WT and vs. each other. In the distal femur, there was a significant decrease in BV/TV and trabecular thickness in oim/oim vs. WT which was intermediate in oim/+. Similar trends were noted in femoral and tibial cortical geometry. Tibial (not femoral) bone mineral density increased with disease severity (WT:1749±24; oim/+:1789±54; oim/oim:1846±38 mg/cm3), and Raman spectroscopy revealed decreased crystallinity in oim/oim femora. Mechanical testing showed a significant increase in elastic modulus in oim/+ vs. WT (12.26±0.75 vs. 13.76±1.68 GPa) which decreased in oim/oim (10.73±1.96 GPa) in the femur and tibia (tibial data shown). RPI unloading slope mirrored these results in the femur (WT: 0.265±0.016; oim/+: 0.271±0.023; oim/oim: 0.211±0.021 N/μm). Postyield displacement and toughness were also decreased in both disease states in the femur and tibia. Conclusions: Altered collagen nanoscale morphology created structural and mechanical deficits at all interrogated length scales. A disease-specific shift in collagen D-periodicity caused by the increasing presence of α1 homotrimers mirrored alterations in mineralization levels. As mineralization increased to pathological levels in oim/oim, an initial increase in modulus in oim/+ was reversed and intensified suggesting that collagen-driven changes in mineral were responsible for decreased tissue-level mechanical properties. Experiments are underway to interrogate the structure and mechanical properties of non-mineralized tendon collagen from these animals. Supported by an IUPUI Research Support Funds Grant.

Heterotopic ossification and Raman spectroscopy: early diagnosis, age, and burn injuries

Katherine E. Cilwa[*1], Jonathan R. Peterson[2], Benjamin Levi[2], Stewart C. Wang[2], Michael D. Morris[1]. [1]Department of Chemistry, University of Michigan, [2]Department of Surgery, University of Michigan Medical School, Ann Arbor, MI, USA.

Introduction: Heterotopic ossification (HO) is the pathological formation of bone in soft tissue and is a debilitating sequela of trauma, burns, amputations, and orthopaedic surgery. HO is a secondary condition with particularly high incidence in young adults and is associated with combat related injuries (62-65%) and severe burns (60%). Diagnosis generally occurs late in disease progression, prophylaxis is limited, and overall prognosis is characterized by impaired rehabilitation and functional deficits. Identifying patients at high risk for developing HO will aid in earlier diagnosis and improved patient outcome. Understanding of the pathogenesis of HO is an important step toward identifying high risk populations and developing therapeutic treatments and prophylaxis. Recent developments in the study of HO utilize Raman spectroscopy to aid in both the detection and investigation of HO mineralization. **Purpose:** We present the application of Raman spectroscopy for detection and characterization of HO in mouse models and human specimens. **Methods or Approaches:** Raman microscopy and Raman fiber optic probe technology were used to examine a variety of excised mouse and human tissue specimens. Effects of age, type of trauma, and time since trauma were studied. In a mouse model, effects of administration of the anti-inflammatory agent Apyrase were examined. **Results:** Systematic measurements in mouse specimens demonstrated the ability of Raman to differentiate between areas of varied HO maturity, cortical bone, and soft tissue. Early HO showed low crystallinity and mineral-to-matrix ratios compared with more advanced stages and with normal tissue. Increased HO development was seen both in young specimens as well as in the case of burn accompanying injury. Apyrase, an ATP hydrolyzing agent administered post injury, reduced HO formation. Transgenic mice with Bmpr1a knockout demonstrated reduced HO formation even following burn injury. Low crystallinity and mineral-to-matrix ratios are also found in measurements of human specimens excised from patients with injuries originating from car accidents and are markers for HO. **Conclusions:** Raman spectroscopy aids in the detection and characterization of HO. Inflammatory responses to burn injury increase the formation of HO, particularly in young, healthy organisms. Supported by the National Institute of Health.

Monday, October 28, 2013 Session 2

Regulation of calcium phosphate formation by native amelogenins in *vitro.*

Henry C. Margolis*1, Seo-Young Kwak1, Sonia Kim1, 2, Elia Beniash3, Yasuo Yamakoshi4 and James P Simmer5.
1Center for Biomineralization, Dept. of Applied Oral Sciences, The Forsyth Institute, Cambridge, MA, 2Boston University Goldman School of Dental Medicine, Boston, MA, 3Dept. of Oral Biology, University of Pittsburgh, Pittsburgh, PA, 4School of Dental Medicine, Tsurumi University, Yokohama, Japan, 5Dental Research Lab., University of Michigan, Ann Arbor, MI.

Introduction: Full-length amelogenin and key amelogenin degradation products are believed to play essential roles in the formation of the highly ordered enamel structure. *In vitro* studies in our laboratory have also shown that recombinant full-length porcine amelogenin rP172 transiently stabilizes amorphous calcium phosphate (ACP) and can guide the formation of well-aligned bundles of hydroxyapatite (HA) crystals, as seen in the secretory stage of developing enamel. This functional capacity was found to be dependent on the hydrophilic C-terminal domain of amelogenin. However, we have found that native phosphorylated (single site on S-16) forms of full-length (P173) and cleaved (P148) amelogenins can stabilize ACP for > 1 d and prevent crystal formation. **Purpose:** To test the hypothesis that native full-length P173 also has the capacity to guide the formation of bundles of ordered HA crystals, under specified conditions generated via proteolysis or at reduced concentration. **Methods:** Calcium and phosphate were sequentially added to solutions of P148 or P173 (2 mg/mL, 60 ㉦L) with and without MMP20 to yield 2.5 mM calcium, 1.5 mM phosphate, 50 mM Tris-HCl, pH 7.4, at physiological ionic strength (163 mM) and 37oC. Protein degradation with time was assessed by gel-electrophoresis and mineral products formed were characterized by TEM and SAED. The effect of P173 concentration (0.2 – 2 mg/mL) on mineralization was assessed under similar conditions. **Result**s: Under mineralizing conditions, P148 underwent limited MMP20 proteolysis and only ACP particles were observed up to 48 h. In contrast, P173 was progressively degraded over time, resulting in the transformation of initially formed ACP particles into bundles of ordered HA crystals (seen at 18 h). In the absence of MMP20, bundles of ordered HA crystals also formed at lower P173 concentrations, although the rate, shape and organization of forming crystals were highly dependent on P173 concentration. **Conclusions:** The formation of the hierarchical enamel structure may be regulated by the partial degradation of full-length amelogenin via MMP20 proteolysis during secretory stage enamel formation. At the same time, predominant amelogenin degradation products, like P148, may serve to prevent uncontrolled crystal formation. These results have important implications with respect to the mechanism of amelogenesis. Supported by NIDCR grants R56-DE016376 and R01-DE023091.

Proinflammatory Cytokines Induce Amelotin Transcription in Human Gingival Fibroblasts.

Yohei Nakayama*[1,3], Hideki Takai[1,3], Sari Matsui[1], Liming Zhou[1,4], Yoshimitsu Abiko[2,3], Bernhard Ganss[5], Yorimasa Ogata[1,3]
Departments of [1]Periodontology, Biochemistry and Molecular Biology, and [3]Research Institute of Oral Science, Nihon University School of Dentistry at Matsudo, Chiba 271-8587, Japan; [4] Stomatological Hospital of Anhui Medical University, Anhui, China; [5]Matrix Dynamics Group, Faculty of Dentistry, University of Toronto, Toronto, Ontario, Canada.

Introduction: Amelotin (AMTN) protein is secreted by ameloblasts and has been localized at the enamel surface in a basal lamina-like layer at maturation stage of amelogenesis and in the junctional epithelium in molars of similar to odontogenetic ameloblast-associated/amiloid in Pindborg tumors (ODAM/APin). We recently have described that over-expression mice of AMTN gene have irregular and thinner enamel due to hypomaturation caused by AMTN expression at the secretory stage and the induction of mineral deposition by AMTN using mouse calvaria-derived osteogenic cell line MC3T3-E1. Thus, AMTN has been suggested as a regulator of final enamel formation, ameloblast-mineral. However the role of AMTN in the junctional epithelium has remained unclear. **Purpose:** We aimed to study the differences in gene expression between inflamed gingiva from chronic periodontitis patients and non-inflamed gingiva. **Methods:** Total RNAs were isolated from both gingival tissues from chronic periodontitis patients and non-inflamed gingiva. The gene expression profiles were monitored by DNA microarray. The total RNA was also utilized to confirm the induction of AMTN mRNA levels in inflamed gingiva by real-time PCR. Transient transfection assays were performed using chimeric constructs of mouse AMTN gene promoter fragments linked to a luciferase reporter gene in the cultured human gingival fibroblasts (HGF). To determine the ATG start codon of mouse AMTN gene promoter, primer extension analysis was carried out. **Results:** Among many differentially expressed genes we found significantly increased amelotin (AMTN) mRNA level in inflamed gingiva. Interleukin-1β (IL-1 β), Interleukin-6 (IL-6) and tumor necrosis factor-α (TNF-α) induced AMTN mRNA levels in HGF. Treatment of HGF with IL-1β, IL-6 and TNF-α increased the luciferase activities of the AMTN promoter constructs. The position of the major labeled product showed the transcription start site at position -91 to -93 relative to the translation start codon ATG of mouse AMTN gene promoter in the results of primer extension

analysis. **Conclusions:** These findings established that proinflammatory cytokines induce AMTN gene expression in human gingival fibroblasts and suggest the possibility of a role for AMTN in gingival inflammation. This work was supported in part by a Grant-in-Aid for Scientific Research (C; No.22592319), a supportive grant for young investigators from Nihon University School of Dentistry at Matsudo and Canadian Institutes of Health Research.

Ameloblast Transcriptome Changes from Secretory to Maturation Stages.

James P. Simmer*, Amelia S Richardson, Bryan M. Reid, Jan C-C. Hu. University of Michigan School of Dentistry, Ann Arbor, MI.

Introduction: The major stages of enamel formation are the secretory stage, when enamel mineral ribbons are extended from dentin to the surface of the crown, and the maturation stage, when the crystals deposited during the secretory stage grow in width and thickness and the enamel layer hardens. Although mineralization occurs in both stages, ameloblast activities change dramatically, and many of the key secretory and maturation stage proteins involved in secretion, proteolysis, endocytosis, ion movement, etc, are unknown. **Purpose:** To identify the major molecular components in the secretory and maturation stages of amelogenesis by stage-specific transcriptome analyses. **Methods:** Day 5 and Days 11-12 mouse heads were demineralized, fixed with methacarn, embedded in OCT, and cryosectioned. Ameloblasts (40 sections per age group) were laser micro-dissected from Day 5 (secretory stage) and Days 11-12 (maturation stage) first molars from the cusp slopes near the roots. The captured cells were lysed, RNA was extracted with a PicoPure isolation kit, and amplified using the NuGen WT (whole transcriptome)-Ovation Pico RNA Amplification System to generate a cDNA library. DNA sequences were obtained using next generation sequencing on an Illumina Sequencer. The DNA sequences were analyzed to identify genes whose expression had significantly increased or decreased in maturation stage ameloblasts relative to the secretory stage. **Result**s: 614 and 373 genes identified with a greater than 2-fold increase or decrease in expression, respectively, in the maturation relative to the secretory stage. 32 ion transporter genes with increased expression were identified, including *Slc31a2*, *Slc6a8*, *Slc24a4*, *Slc23a2*, *Slc4a11*, *Slc26a7*, *Slc34a2*, *Cnnm2* and *Cnnm4* and *Cftr*. 25 protease genes with increased expression were identified, including *Bmp1*, *Adamts1*, *Adamts2*, *Mmp13*, *Mmp15*, and *Mmp23*. Other upregulated genes were associated with endocytosis (*Sorl1*, *Tfrc*, and *Ldlr*) and signaling (*Shh*, *Fxyd4*, *Atp6v1a*, *Batf3*). The results were cross-checked against a comparable incisor transcriptome of enamel organ epithelia (EOE) [Lacruz *et al.* (2012) *J Cell Physiol.* 227, 2264-75] and 34 increasing and 26 decreasing expressors common to the two studies were identified. **Conclusion:** By comparing the two ameloblast stage-specific transcriptomes we have identified numerous molecular candidates for important roles in ameloblast function. Confirmation of their differential expression and function is required to accertain their importance in amelogenesis. Supported by NIDCR/NIH grant DE015846.

Moonlighting Enamel Proteins - the Systemic Expression of Amelogenin and Ameloblastin.

J Jacques[1], D Hotton[1], M De la Dure-Molla[1], AB Kulkarni[2], C Gibson[3], S.J. Brookes[4], S Petit[1] and A Berdal[1]. 1. Laboratory of Molecular Oral Physiopathology, Inserm UMRS 872, Universities Paris 5 and 7, France; 2. NIDCR NIH, Bethesda, MD, USA, 3. University of Pennsylvania School of Dental Medicine, Philadelphia, PA, USA and 4. Leeds Dental Institute, University of Leeds, UK.

Introduction: Growing evidence indicates that enamel matrix proteins (EMPs) exhibit biological activity in non-enamel tissues (e.g. EMPs in bone regeneration). EMPs have been shown to modulate various cell signaling pathways but their functional significance in non-enamel tissues, if any, is unclear. **Purpose:** To revisit the spatiotemporal expression of *Amelx* and *Ambn* in non-enamel tissues in order to better understand any potential physiological function(s) outside amelogenesis. **Methods:** Craniofacial bones (cranial, mandible alveolar and basal bone), appendicular skeleton (tibia) and a series of non-mineralized tissues were obtained from WT mice (3 days - 15 weeks of age) using manual and laser-capture microdissection. Tissues were screened for *Amelx* and *Ambn* expression using RT-PCR, RT-qPCR and Western-blotting. *In situ* hybridization and immunohistochemical analysis (light and fluorescence confocal microscopy) were carried out using epithelial dental cells as positive controls and amelogenin null mice as negative controls. The impact of Msx2, a transcription factor repressor of *Amelx* in dental epithelium, was analyzed in the Msx2 knock-in null mouse bone where modeling is impaired. **Results:** RT-qPCR (with sequenced cDNA) showed that significant expression of *Amelx* and *Ambn* is not restricted to enamel alone and gave their relative levels. Expression levels of both genes varied according to the ontogenic stage (decreased with age), and tissue type (epithelial dental cells with higher expression than bone and non mineralized tissues). *In situ* RNA and protein studies confirmed that *Amelx* and *Ambn* are expressed in non dental tissues. They evidenced cellular heterogeneity in bones, especially in adult mice. Bone Western blot analysis identified immunoreactive bands at molecular weights corresponding to those previously reported for AMELX and AMBN extracted from developing enamel. Their overall abundance relatively to enamel extracts was lower as judged by staining intensity. Bone AMELX and AMB expression was decreased in 3 month-old Msx2 null mice, contrary to the observed increased expression in epithelial dental cells of the same Msx2 null mice. **Conclusion:** Our data provides a survey of the expression of *Amelx* and *Ambn* in extradental tissues such as bones, eye and epidermis. Dental epithelial and bone expression

was reversely influenced in Msx2 null mouse jaw where dental crowns are dramatically abraded. Thus, their levels would be controlled by a number of factors which combine biomechanics and transcription factors. Elucidation of the distribution, concentration and most importantly the functional role of EMPs in extradental tissues will allow for a more rationalised approach for EMPs in pathophysiological and therapeutic contexts.

Uncoupling Protein-2 is an Antioxidant that is Upregulated in the Enamel Organ of Fluoride-Treated Rats

Maiko Suzuki[1], Megan L. Sierant[1] Jerry V. Antone[1] Danielle V. Riley[2], Kathleen Ryan[3], Eric T. Everett[3] Gary M. Whitford[2], John D. Bartlett [*1]. [1]Forsyth Institute, Department of Mineralized Tissue Biology & Harvard School of Dental Medicine, Cambridge, MA, USA; [2]Georgia Health Sciences University, Department of Oral Biology, School of Dentistry, Augusta, GA, USA; [3]Department of Pediatric Dentistry and The Carolina Center for Genome Sciences, University of North Carolina, Chapel Hill, NC, USA.

Introduction: Dental fluorosis is characterized by subsurface hypomineralized enamel with high protein content. Previously, we showed that fluoride (F^-) exposure causes endoplasmic reticulum (ER) stress. ER-stress is caused by improper folding of nascent proteins but, it is unclear how F^- affects protein folding. F^- exposure generates reactive oxygen species (ROS) and generation of ROS is known to cause ER-stress. We therefore screened oxidative stress arrays using stringent conditions to identify if any genes within the rat enamel organ are regulated by F^- exposure. Vitamin E is an antioxidant and a diet high in vitamin E was demonstrated to: promote plasma membrane repair, attenuate pulmonary fibrosis, reduce glomerular hypertrophy, and ameliorate diabetic mouse skin fragility. We also asked if a diet high in vitamin E would attenuate dental fluorosis in mice. **Purpose:** To identify novel F^- regulated oxidative stress gene(s) and to determine if vitamin E ameliorates fluorosis. **Methods:** Maturation stage incisor enamel organs were harvested from rats exposed for six weeks to 0, 50 or 100 ppm F^- as NaF in drinking water. mRNA was converted to cDNA for use in Rat oxidative stress RT^2 Profiler PCR Arrays (Qiagen). Arrays were performed in triplicate and any gene with an average cycle threshold of >30 for any treatment group was eliminated. Positive results were confirmed by qPCR analysis. Mice were treated with 0 or 50 ppm F^- and were also treated or not with chow containing vitamin E (500 IU d,l-α-tocopherol acetate/kg chow). Quantitative fluoresce (QF) was used to assess the level of fluorosis in mice. **Results:** Uncoupling protein-2 (*Ucp2*) was significantly upregulated (~1.5 & 2.0 fold for the 50 or 100 ppm F^- treatment groups respectively). *Ucp2* downregulates mitochondrial production of ROS and its activation decreases ATP production necessary for such activities as glucose metabolism. Thus, in addition to reduced protein translation caused by ER-stress, a reduction in ATP production by *Ucp2* may contribute to the inability of ameloblasts to remove protein from the hardening enamel. The fluoride treated mice had significantly more enamel fluorescence than the untreated. However, no significant difference was observed between similarly treated mice with or without added vitamin E. Bone and plasma F^- levels were also similar among vitamin E treatment groups. **Conclusions:** We have identified a novel oxidative stress response gene (*Ucp2*) that is upregulated *in vivo* by F^-. Activation of this gene may adversely affect ameloblast function. Vitamin E does not appear to attenuate dental fluorosis. We Gratefully Acknowledge Support From NIDCR Grant DE018106.

Monday, October 28, 2013 Session 3

Identifying Protein -Protein Interactions at the Dentogingival Attachment Site

James Holcroft, Symone San Miguel, Bernhard Ganss*,
Matrix Dynamics Group, Faculty of Dentistry, University of Toronto, Toronto. ON, Canada

Introduction: The junctional epithelium (JE) is the anatomical attachment site of the gums to the teeth, and as such a very important barrier against invasion of oral microorganisms. Only few proteins such as laminin 5 (Lam332) and more recently Odam, Amelotin(AMTN) and FDC-SP have been localized to the interface between epithelial cells and the mineralized tooth surface, but their interactions and thus the detailed nature of the dentogingival attachment apparatus remains unresolved. **Purpose**: To determine whether AMTN, Odam and FDC-SP interact with Lam332 subunits, particularly LamB3 and LamC2. **Methods**: We have used the stringent Matchmaker™Gold Yeast Two-Hybrid System (Clontech) to probe for all possible permutations of interactions between all four proteins, followed by co-immunoprecipitation (co-IP) assays in murine ameloblast-like cells . Immunogold-TEM was used to determine ultrastructural co-localization of the four proteins in native human tissue. **Results**: Yeast-two-hybrid experiments have demonstrated interactions between AMTN and Odam, and have shown that ODAM interacts with LamB3 and FDC-SP interacts with LamC2. FDC-SP further interacts with the enamel proteins amelogenin (AMEL), ameloblastin (AMBN) and enamelin (ENAM), but not with AMTN or Odam. Most of these interactions have been confirmed by co-IP of proteins in transfected ALC cells. Immunogold TEM has further demonstrated co-localization of AMTN, Odam, LamB3 and FDC-SP in the internal basal lamina of the JE. **Conclusions**: This work has identified new protein interactions in the internal basal lamina of the JE. These interactions may be functionally important for the attachment of the gingiva to the tooth and open new avenues toward preventive strategies against gingival recession and dentogingival attachment loss. Supported by the Canadian Institutes of Health Research (CIHR), National Science and Engineering Research Council

(NSERC) and an IADR-GSK Innovation in Oral Care Award.

Characterization of Peritubular Dentin: An enigmatic, non-collagenous mineralized tissue.

Jason R. Dorvee, Alix Black, Lauren Gerkowicz, Arthur Veis. Feinberg School of Medicine, Department of Cell and Molecular Biology, Northwestern University, Chicago, IL. 60611, USA.

Introduction: Tooth matrix formation initiates at the boundary between epithelial preameloblasts and mesenchymal preodontoblasts (pOD), initially separated by a basement membrane at the dentin-enamel junction (DEJ). The pOD polarize and begin to secrete a collagenous intertubular dentin matrix (ITD) that pushes the main OD cell body away from the DEJ, leaving behind a thin connecting cell process attached to the DEJ as the OD moves in the direction of the pulp chamber. As the tooth matures, the process retracts partially in the pulpal direction, leaving a tubule surrounded by collagen. Thus the dentin is penetrated by a dense network of tubules, connected to the odontoblast layer, and partially filled by the cell processes. The perimeter of the tubule space becomes filled with a material called peritubular dentin (PTD), hyper-mineralized with respect to the ITD. It does not appear to have the structural integrity to enhance the mechanical properties of the mineralized ITD. **Purpose:** To isolate and determine the composition and structure of PTD. **Methods:** The coronal dentin of erupted bovine molars was sectioned in 1 μm slices ⊥ to the long axis of the tubules, yielding cross sections of the 1-2 μm diameter tubules. A Zeiss PALM microdissection laser system was utilized to cut these tubules from their surrounding ITD. Similar sections were cut from the ITD. The excised tubule sections were captured separately in the capture tubes, or on a coated electron microscope grid inserted in the capture tube. The PTD and ITD were examined by scanning transmission electron microscopy (STEM) and other imaging techniques. STEM yields insight to both structure (electron density and selected area diffraction) and composition via electron dispersion x-ray spectroscopy of the PTD. Based on these EM results further chemical analysis was pursued. Separate polished molar sections from the same region of the tooth, with tubules still intact, were analyzed by TOF-SIMS for both positive and negative secondary emission ions. **Conclusion**: It is evident that the PTD collar around the OD processes are higher in mineral than the surrounding ITD, as shown by many others. However, the PTD is irregular and not uniformly placed within the tubule. The texture of the PTD mineral is different than that of the ITD mineral, and the PTD is porous. The PTD is calcified, but all of the calcified material is not apatite mineral, as shown by the Ca/P ratio's. Earlier work had shown that the PTD contained phospholipids. In this work the presence of a sulfated component (chondroitin sulfate) within the PTD was detected. Thus, the PTD is a quite distinct, but non-uniform material. It is difficult to suggest any function for the PTD except possibly, through its porosity, providing for the transport of ions and other components between the OD processes and the dentin matrix. Supported by the National Institute for Dental and Craniofacial Research, Grant DE-01374(to AV).

Ultrastructural Organization of Dentin in Mice Lacking Dentin Sialoosphoprotein Gene.

Pingan Fang1, Xu Yang1, Lyudmila Lukjashova2, Adele Boskey2, Kostas Verdelis1, Elia Beniash1
1- Center for Craniofacial Regeneration, Department of Oral Biology, University of Pittsburgh School of Dental Medicine, Pittsburgh, PA 2- Musculoskeletal Integrity Program, Hospital for Special Surgery, 535 E 70th Street, New York, NY

Introduction: Osteopontin (OPN) is an acidic phosphoglycoprotein that is believed to play a critical role in the prevention of calcium oxalate kidney stone formation. In vitro studies have shown that OPN can inhibit the formation of calcium oxalate monohydrate (COM) and that this inhibitory activity is dependent upon the phosphorylation of the protein. Our laboratory has previously synthesized peptides corresponding to a sequence 220-235 of rat OPN (SHESTEQSDAIDSAEK) and containing 0, 1 or 3 phosphate groups (P0, P1, P3). Using these peptides, we investigated the effects of varying degrees of phosphorylation on adsorption to and growth modulation of COM crystals. Our results show that all three peptides bind to the {100} faces of the COM crystals. However, the degree of growth inhibition perpendicular to this face increases with peptide phosphorylation. Purpose: To determine the mechanism by which phosphorylation inhibits {100}-face growth of COM. Methods: Atomic scale molecular dynamics (MD) simulations were performed using the GROMACS suite. The {100}-face of COM was taken from previously solved coordinates. Simulations were performed in which P0, P1 or P3 was initially placed in an extended conformation parallel to the surface at a distance of approximately 3 nm. Each system was solvated with explicit water and counter-ions were added to maintain a charge-neutral state. Simulations were run for 50 nsec each. Results: All three peptides demonstrated an affinity for the {100} face in the simulations performed. Centre of mass trajectory analysis showed that P3 settles closer to the crystal surface (0.668 nm) than P1 (0.732 nm) or P0 (0.975 nm). Root mean squared distance (RMSD) analysis showed that peptide conformational stability is positively correlated with the degree of phosphorylation. Residue distribution analysis showed that carboxylate-containing residues form closer and more stable contacts to the crystal surface than phosphorylated residues (P0: D12, E15; P1: E3, E6, E15; P3: E3, E6, D9, E15). Conclusions: The results indicate that phosphorylations increase the charge density of the peptide to facilitate bulk transport to the crystal surface whereas carboxylate-containing residues form the close, stable interactions. This suggests separate roles for both phosphate and carboxylate groups,

providing a possible explanation for the extensive phosphorylation found in many mineral-binding proteins. These simulations demonstrate the great potential of molecular dynamics in understanding protein-crystal interactions and provide a paradigm of computer-aided biomineral inhibitor design. Supported by the Canadian Institutes of Health Research.

Matrix Metalloproteinase-20 is enriched in the dentin-enamel junction of mature teeth where it could play a role in enamel delamination following radiotherapy

A.A. MOUSA[1], B. ZHANG[1]; J. D. MCGUIRE[1]; N. HUFFMAN[1], A. KEIGHTLEY[2], Y. WANG[1], M.P. WALKER[1], and J.P. GORSKI[1], [1]Department of Oral and Craniofacial Sciences, University of Missouri-Kansas City, Kansas City, MO, [2]Biological Mass Spectrometry and Proteomics Facility, School of Biological Sciences, University of Missouri-Kansas City, MO

Introduction: In general, the enamel layer is quite stable. Biomaterial and biochemical studies suggest that an organic layer extending from the dentin-enamel junction (DEJ) outward about 400 μm into the bulk enamel may contribute to this stability. Specifically, propagation of cracks produced in enamel was impeded upon reaching this layer. Also, high dose radiation therapy can cause enamel delamination particularly in cuspal regions. We speculate that radiotherapy may cause degradation of the DEJ and associated enamel organic matrix leading to full thickness defects and delamination. Radiation is also known to induce matrix metalloproteinase (MMP) expression as well as activation of MMP precursors. The purpose of this study was to characterize metalloproteinases localized to the DEJ and enamel phase of mature human teeth. **Methods:** Intact third molars were either exposed to a fractionated 70 Gy radiation dose and incubated for 3 or 12 months at 37˚C, or were not irradiated or incubated to serve as control. A third group of post-oral cancer radiotherapy extracted teeth were also included in the study. Roots and pulp tissue were removed and individual crowns were processed for protein extraction. Extracts were analyzed by liquid chromatography-tandem mass spectrometry (LC-MS) for protein characterization. Western blotting and immunoprecipitation for MMP-20 was done with antibodies specific for the N-terminus. Enzymatic activity was analyzed with casein or gelatin gel zymography. Extracts from crown sections processed mechanically to remove all or most of the dentin, yet preserve the DEJ, were also immunoblotted for MMP-20. MMP-20 was also immunofluorescently localized in decalcified crown sections with confocal fluorescence microscopy. **Results:** MMP-20 was the only protease detected in relative high abundance by LC-MS in in vitro irradiated crowns where characteristic bands at 44, 24-20, and 19-17 kDa were identified by casein gel zymography. Neither casein nor gelatin gel zymography detected substantial quantities of other MMPs in dental extracts. Western blotting routinely detected six bands at 53, 43, 41, 22, 19 and 11 kDa; the first five bands are identical with the sizes of MMP-20 precursor and four activated forms, respectively. These bands were largely absent when the DEJ was removed from crown sections prior to extraction and western blotting. After immunoprecipitation, the three major bands at 43, 41 and 22 kDa were identified as catalytically active MMP-20. Consistent with this assignment, MMP-20 forms were not detected in gelatin gels and activity was only detected in the presence of calcium and zinc. Importantly, immunoflourescently labeled MMP-20 could be localized prominently to the DEJ by confocal microscopy. Finally, MMP-20 protein and activity could be readily identified in extracts from in vitro and in vivo irradiated teeth, however, they contained less of the higher molecular weight species and more of 20 kDa MMP-20. **Conclusion:** MMP-20 protein and associated proteolytic activity was readily detectable in extracts of control and irradiated mature human tooth crowns where MMP-20 was prominently localized to the DEJ. We propose that 20 kDa MMP-20 could play an active degradative and destabilizing role leading to enamel delamination after oral radiotherapy.

Monday, October 28, 2013 Session 4

Quantification of clonal heterogeneity of mesenchymal progenitor cells in Dental Pulp and Bone Marrow

Rachel Waddington, Jodie Harrington and Alastair Sloan. Tissue Engineering and Reparative Dentistry, School of Dentistry, Cardiff University, UK.

Introduction: The multipotential nature of mesenchymal stem / progenitor cells (MSCs) isolated from bone marrow (BMSCs) and dental pulp (DPSCs) provides attractive prospects for their clinical applications in bone repair and regeneration. We have previously reported that MSC clones in dental pulp exhibit different cellular characteristics in terms of their embryonic nature. Further, there are suggestions that MSCs can be arranged into a lineage hierarchy with heterogeneous trilineage potential. **Purpose:** To compare "classical" stem cell characteristics of several clonal MSCs isolated from dental pulp and bone marrow. **Approaches:** BMSCs and DPSCs were obtained from femurs and teeth of 21 day old rats. Mononuclear marrow cells were separated using histopaque density-gradient centrifugation. Pulp cells were dissociated by collagenase/dispase. Immature MSCs were selected by preferential adherence to fibronectin and clonally expanded. Colony forming efficiencies (CFEs) and long term population doublings (PDs) were determined. Clones were analysed at 8, 18, 30, 41PDs for a range of MSC markers by RT-PCR and qPCR. Cell potentiality was assessed by culture in osteogenic, adipogenic and chondrogenic media. **Results:** CFEs for cells

isolated from dental pulp was 0.088, whilst bone marrow was 0.007, significantly lower. However, clonal expansion of isolated colonies was 7 times more successful for BMSCs compared with DPSCs. Clonal BMSCs had on average 1.5 times higher PDs compared with clonal DPSCs. DPSC clones also exhibited high and low proliferative characteristics. All clones expressed mesenchymal markers VCAM1, MSX2 Fgfr1, Snai1, MCAM, Nanog. BMSC clones additionally expressed Sox2. All markers were maintained to 41PDs. However, quantitative differences were observed between all clones in the levels of VCAM1 and MSX2, with no clone showing similarity to another. All BMSC clones readily differentiated towards osteoblasts, chondrocytes and adipocytes. Of three DPSC clones analysed, only one clone demonstrated tripotentiality, with the other clones capable of osteogenic differentiation, but poor potential for chondrogenesis and adipogeneis. Cell differentiation was slower for DPSC clones compared to BMSC clones. **Conclusion:** Whilst dental pulp appeared to contain a high number of colony forming immature progenitor cells, examination of the resultant clonal populations indicated that dental pulp contained MSCs with a more heterogeneous nature compared to bone marrow, with an overall lower capacity for proliferation and osteogenic differentiation. These differences may reflect the relative contribution of the respective MSCs in maintaining tissue integrity; BMSCs required for continual bone remodeling, whilst DPSCs are only stimulated in response to trauma to produce a reparative mineralised matrix. The observed heterogeneity of these cells for the various tissue sources will provide better selection of cells with therapeutic potential. Funded by the Medical Research Council UK.

Variations in Dental Pulp Stem Cell Ageing and Response to Oxidative Stress Influence Regenerative Potential

Alastair J Sloan[1,2], Amr Alraies[1,2], Rachel Waddington[1,2], Ryan Moseley[1,2]. 1Tissue Engineering and Reparative Dentistry, School of Dentistry, 2Cardiff Institute for Tissue Engineering and Repair, Cardiff University, UK

Introduction: Dental pulp progenitor cells (DPSCs) are among many stem cell sources with potential therapeutic benefits however a significant limitation of stem cell therapy is extensive in vitro expansion necessary to produce sufficient cell numbers for clinical use, leading to proliferative/regenerative decline and cellular senescence. Despite heterogeneous DPSC populations being capable of >120 population doublings (PDs) in vitro before senescence, only 20% of DPSC clones undergo >20PDs, suggesting that DPSC subset populations exist that differ in their proliferative /regenerative capacities. **Purpose:** As ageing and oxidative stress are well-established senescence mediators, we assessed proliferative / senescence profiles and differentiation properties of DPSC clones and clonal susceptibilities to continued expansion, oxidative stress-induced senescence, telomere length and differentiation. **Methods:** DPSC clones were isolated from third molar pulps by collagenase/dispase digestion and fibronectin adhesion and maintained in the absence / presence of sub-lethal doses of hydrogen peroxide (0-200μM) throughout culture. Population doublings (PDs) were monitored, as was expression of stem cell markers (CD105/CD90/CD73) by RT-PCR. Senescence was determined at <0.5PD/week and confirmed by senescence-associated-β-gal staining and telomere restriction fragment analysis. Abilities of each clone to undergo osteogenic, adipogenic and chondrogenic differentiation were assessed at early and late PDs by culture in appropriate media and expression of specific cell markers, alizarin red, oil-red-o and alcian blue staining. **Results:** Highly proliferative clones exhibited greater proliferation (>100PDs) under normal and oxidative stress conditions, compared to low proliferative clones (<10PDs). All clones were telomerase negative, however highly proliferative clones possessed inherently longer telomeres (≈12-20kb) and maintained stem cell marker expression and osteogenic/chondrogenic differentiation for longer periods in culture. In contrast, low proliferative clones had shorter telomeres (<10kb), reduced stem cell marker expression and exhibited increased adipogenesis. Highly proliferative clones resisted H2O2-induced senescence (>40PDs) and maintained stem cell marker expression and telomere length. Only 200μM H2O2 exposure impaired differentiation. Low proliferative clones were highly susceptible to senescence (<25PDs), with reduced stem cell marker expression, telomere length and differentiation. **Conclusions:** Results indicate significant variations in the proliferative/differentiation capabilities of DPPC clones, explained by differences in telomere length and cellular ageing. In addition, significant variations exist in DPPC clonal susceptibilities to oxidative stress-induced senescence. Identification of the underlying mechanisms behind contrasting clonal proliferative/regenerative capabilities provides opportunities to develop screening strategies for the selective isolation of DPPCs for clinical use.

Insights into the effects of Fibroblast Growth Factor (FGF) signaling on odontoprogenitors in the dental pulp.

Karen Sagomonyants* and Mina Mina. School of Dental Medicine, University of Connecticut Health Center.

Introduction: Odontoblast differentiation during physiological and reparative dentinogenesis is dependent upon multiple signaling molecules. Previous studies have demonstrated that Fibroblast Growth Factor 2 (FGF2) is an important regulator of dentinogenesis, having both positive and negative effects on odontoblast differentiation. Our recent studies demonstrated that exposure of dental pulp cells to FGF2 during the proliferation and differentiation phases of growth markedly decreased the extent of mineralization, expression of markers of dentinogenesis (*Dspp, Dmp1*) and various GFP transgenes, including DSPP-GFP and DMP1-GFP. These negative effects of FGF2 on mineralization and dentinogenesis included a transient stimulatory effect at day 7 suggesting that the effects of FGF2 on mineralization depend on the stage of differentiation/maturity of cells and/or are mediated through distinct signaling pathways. **Purpose:** To gain insight into 1) the stage-specific effects of FGF2 on different

subpopulations of odontoprogenitors in the dental pulp and 2) the signaling pathways mediating stimulatory effects of FGF2 on dental pulp cells. **Methods:** Primary cultures from P5-7 pups from various transgenic mice, in which GFP expression is under the control of promoters that results in the expression of transgenes at specific stages of odontoblast differentiation, were prepared and treated with vehicle (control) and FGF2 (20 ng/ml) during the proliferation phase of growth (between days 3-7). The effects of FGF2 on dental pulp cells were examined using a wide variety of assays. **Results:** FGF2 increased expression of *Dmp1*, *Dspp*, the number of DMP1-GFP^{+} and DSPP-GFP^{+} cells as compared to the control. DNA content/cell cycle and FACS analyses showed that the increase in the number of DMP1-GFP^{+} cells in FGF2-treated cultures was primarily due to activation of DMP1-GFP in new cells. FACS-sorted studies showed that FGF2 stimulated dentinogenesis in both undifferentiated (Cola12.3-GFP^{-}) and more committed (Cola12.3-GFP^{+}) populations. Additional experiments using various inhibitors (SU5402, U0126 and noggin) showed that stimulatory effects of FGF2 on dentinogenesis were mediated through FGFR-MEK/Erk1/2 and BMP2/MEK/Erk1/2 signaling pathways. The presence of potential AP-1 and CRE-like binding sites within *Dmp1* and *Dspp* promoter regions has also been showed. **Conclusions:** FGF2 stimulated dentinogenesis by undifferentiated and committed (not differentiated) odontorogenitors in the dental pulp through ERK signaling that is activated by both FGFR and BMP pathways. Supported by R01-DE016689 & R90-DE022526 grants.

Gain of Function MDA5 Mutation Affects Cell Survival and Collagen Expression in Human Dental Cells

Changming Lu[1], Frank Rutsch[2], Mary MacDougall[1] . [1]Institute of Oral Health Research, School of Dentistry, University of Alabama at Birmingham. [2]Münster University Children's Hospital, Germany

Introduction: Melanoma Differentiation-Associated protein 5 (MDA5), a cytoplasmic sensor for double-strand RNA, has a broad effect on innate immune response by inducing interferon (IFN) and other numerous proinflammatory cytokines. Recently, our consortium has identified a heterogeneous p.R822Q mutation of MDA5 association with Singleton-Merten Syndrome (SMS; MIM 182250), a rare autosomal-dominant disorder with aortic calcification, localized osteoporosis, psoriasis, dentin dysplasia, rapid periodontitis and root resorption. **Purposes:** (1) to determine the functional significance of the p.R822Q MDA5 mutation; (2) to investigate the potential roles of MDA5 in the disease development. **Methods:** MDA5 from a normal (MDA5) and SMS patient (SMS-MDA5) was cloned, sequenced and inserted into expression vectors. The SMS-MDA5 mutation was corrected by PCR site-directed mutagenesis (ΔSMS-MDA5). MDA5 constructs were transiently or stably over-expressed in HEK293T cells, primary dental pulp cells by lipofectamine transfection or lentiviral transduction. Cell proliferation and apoptosis were determined by MTT assay and Annexin-V/PI staining respectively. Gene expression level was determined by real-time PCR or western blot analysis. **Results:** Over-expression MDA5 in HEK293T resulted in a dose-dependent pattern of increased IFN-β production in the cells. Interestingly, over-expression of the SMS- MDA5 led to ~ 15-20 times higher level of IFN-β or TNF-α levels than MDA5, while over-expression of ΔSMS-MDA5 resulted in similar levels as the control. Furthermore, transfection of self-RNA or poly (I: C) also showed higher levels of IFN-1β and TNF-α in HEK293T cells with SMS-MDA5 than the ΔSMS-MDA5. Consistently, pulp cells with over-expression of SMS-MDA5 produced higher level of IFN-1β and TNF-α than pulp cells with ΔSMS-MDA5 before or after poly (I: C) stimulation. Although there was no difference in cell proliferation and apoptosis before stimulation, compared with the cells with ΔSMS-MDA5, the cell proliferation and cell apoptosis were significantly reduced and elevated respectively in pulp cells with SMS-MDA5 after poly (I: C) stimulation. In agree with this, there was higher protein level of phosphorylated IRF3 in pulp cells with SMS-MDA5 than that in control cells after poly (I: C) stimulation. Blocking of IFN-β signaling or Fas signaling reduced cell apoptosis mediated by MDA5 signaling. Finally, SMS-MDA5 signaling up-regulated the expression of matrix metalloproteinase 13 and down-regulated the expression of type 1 collagen. **Conclusions:** This is the first report of a gain-of-function MDA5 mutation associated with SMS inducing IFN-1β and TNF-α expression through MDA5 binding to self/ non-self-RNA. The elevated MDA5 function by p.R822Q mutation may impair dentinogenesis through affecting cell apoptosis and type 1 collagen expression.

Stuctural and Molecular Basis for Control of Mineralization at the Periodontal Ligament-Cementum Junction

*Eli D. Sone[1,2,3], Bryan D. Quan[1], Alexander J. Lausch[1]. [1]Institute of Biomaterials & Biomedical Engineering , [2]Department of Materials Science & Engineering, [3]Faculty of Dentistry, University of Toronto, Toronto, ON, Canada.

Introduction: The anchorage of periodontal ligament (PDL) fibers to the tooth via the insertion of bundles of collagen fibrils into root cementum is critical to the function of teeth. The attachment involves a highly controlled mineralization process, in which unmineralized collagen fibrils widen and become a fully-mineralized part of the cementum layer of the tooth at a well-defined mineralization front. It has been proposed that the initiation of mineralization is related to loss of proteoglycans in the PDL and/or the presence of acidic phosphoproteins at the PDL-cementum junction. Others attribute the onset of mineralization to structural changes in the collagen fibrils themselves, which are wider in cementum than in the ligament. However, none of these hypotheses has been convincingly validated for two main reasons: (i) collagen structure is distorted during sample processing, complicating ultrastructural analysis; and (ii) there is no *in-vitro* model that accurately reproduces the features of the PDL-cementum junction and that would allow the many potential variables in the system to be evaluated separately. **Purpose:** To determine the extracellular factors controlling mineralization at the PDL-cementum junction by: (i) characterization of collagen structure under near-native conditions using cryo-TEM; and (ii) developing an *in-vitro* remineralization model to evaluate the roles of different non-collagenous macromolecules in the spatial control of mineralization. **Methods:** Sections of fixed, demineralized periodontial tissues from three-week old CD-1 mice were obtained. For cryo-TEM, sucrose-protected cryo-

sections were washed in water, plunge frozen in liquid ethane, and examined in the TEM at ~-180 °C. For remineralization experiments, cryo-sections were washed of sucrose and exposed to calcium and phosphate-containing mineralizing solutions and examined by TEM. **Results:** We find that the D-spacing of collagen fibrils examined by cryo-TEM contracts by ~3 nm from the PDL to cementum, accompanied by an increase fibril width of ~40%. The decreased periodicity results from a contraction of the gap region. In our *in-vitro* model, we find the previously mineralized tissues (cementum, dentin, bone) are remineralized while the PDL is not. This indicates that the fixed extracellular matrix contains sufficient information to direct mineralization. **Conclusions:** By examining collagen in a frozen-hydrated state, we are able to observe the structure and organization of collagen fibers free from artifacts introduced by the dehydration and embedding processes of conventional TEM sample preparation. Using the remineralization model described here, we plan to selectively remove different macromolecular components from the periodontal tissues to see at what point spatial selectivity is lost.

Characterization of the Bone Sialoprotein (*Bsp*)-null Phenotype: Role in Periodontal Tissue Integrity

Y. Soenjaya[1], E. Holm[2], B. L. Foster[3], F. H. Nociti, Jr.[3], K. R. Kantovitz[3], J. E. Aubin[4], D. W. Holdsworth[5], G. K. Hunter[1,2,6], M. J. Somerman[3], H. A. Goldberg[1,2,6 *]. [1]Biomedical Engineering Program, [2]Dep't of Biochemistry, [5]Imaging Research Lab, Robarts Research, [6]School of Dentistry, University of Western Ontario, London, Canada, [4]Molecular Genetics, University of Toronto, Canada, and [3]NIAMS, National Institutes of Health, Bethesda, USA.

Introduction: Bone sialoprotein (BSP) is an acidic phosphoprotein with collagen-binding, cell-binding and hydroxyapatite (HA)-nucleating properties, localized primarily in mineralized tissues. The *Bsp*-null mouse has been shown to have decreased bone mineral density, reduced formation rates and impaired bone healing. Our recent studies on the *Bsp*$^{-/-}$ mice have shown that in addition to bone defects, a periodontal tissue phenotype is evident. This includes a dramatic loss of functional acellular cementum, which we postulate gives rise to the observed decrease in periodontal ligament (PDL) integrity and insertion into the tooth, as well as a decrease in surrounding alveolar bone. **Purpose:** To provide a more in depth analysis of the *Bsp*$^{-/-}$ mice to delineate the role of BSP in mineralized tissue formation. **Methods:** *Bsp*$^{-/-}$ mice were maintained on a mixed 129/CD1 background. Tissues from *Bsp*$^{-/-}$ mice and wild-type littermates were studied by histology, immunohistochemistry, micro-computed tomography (μCT), SEM and TEM. **Results:** Contrary to previous reports, *Bsp*$^{-/-}$ mice on soft diets, but not hard-pellet diets, were of similar size and weight as wild types over the 12 weeks of study. Hard diets exacerbated the malocclusion rates (30% vs. 3% on soft diets). However, alveolar bone loss and tooth pitting in *Bsp*$^{-/-}$ mice fed soft diets were equivalent to that seen in mice fed hard-pellet diets with defects increasing with age. Osteoclast-like RANKL-positive cells on the root surfaces were likely the cause of the observed pitting. We also noted enhanced incisor enamel development, loss of pulp and increased thickness of incisor dentin in *Bsp*$^{-/-}$ mice fed either hard or soft diets, which may be the consequence of the increased trauma on the tooth due to decreased PDL attachment. At 20 weeks, μCT scanning showed alveolar bone loss of greater than 60% in relation to root length. To determine whether addition of exogenous BSP rescued the periodontal phenotype, in a pilot study, 10 or 20 μg rat BSP (recombinant or native) was injected subcutaneously starting at postnatal day 5 (coinciding with root development) and followed by additional injections (9 or 16) over 5 weeks. The mice at 6 weeks of age were sacrificed and analyzed by μCT. The extent of alveolar bone loss, apparent in *Bsp*$^{-/-}$ mice given saline, was markedly reduced in mice receiving BSP. This suggests that BSP rescues the periodontal phenotype. **Conclusions:** Based on the established functional properties of BSP, our current findings suggest that BSP plays a non-redundant role in acellular cementum formation by binding collagen and initiating mineralization on the root surface, which in turn stabilizes the insertion of the PDL collagen into the cementum. Supported by CIHR and the Intramural Research Program of NIAMS (NIH).

Tuesday, October 29, 2013 Session 5

Gain of mineral and loss of non-mineral material in enamel depend on ameloblastin.

Yong-Hee P Chun*[1], John D Teepe [1, 2], Yuanyuan Hu [3], James Schmitz [4], Roberto J Fajardo [4], Charles E Smith [5]
[1]Department of Periodontics, University of Texas Health Science Center at San Antonio, San Antonio, TX, USA, [2]Airforce Lackland, San Antonio, TX, USA, [3] Department of Biologic and Materials Sciences, University of Michigan, Ann Arbor, MI, USA, [4] Department of Orthopedics, University of Texas Health Science Center at San Antonio, San Antonio, TX, USA, 5 Department of Anatomy & Cell Biology, McGill University, Montreal, QC, Canada

Introduction: In enamel formation, the deposition of mineral in crystallites starts when the mineralization front forms in secretory stage. During maturation, the enamel layer accumulates significant new mineral when the crystallites grow in volume. Inversely related to mineral gain is loss of protein and water from the forming enamel. Ameloblastin (Ambn) is required for a functional mineralization front; Ambn mutant mice (missing exons 5 + 6; Ambn-/-) lack this mineralization front. Ambn is critical in enamel formation even though it constitutes only 5% of enamel proteins; amelogenin accounts for 90% of these proteins. The importance of this disproportionate expression of enamel proteins is unclear. **Purpose**: To determine the proportion of mineral and non-mineral material in developing enamel depending on the concentration of Ambn by microcomputed tomography. **Methods**: Ambn mutant mice were mated with mice overexpressing full-length Ambn from the mouse amelogenin promoter. Three independent transgenic (Tg) mouse lines expressed Ambn in concentrations of lower (+), similar (++) or higher

(+++) than normal. Mandibular incisors (age: 7 wks, n=8) were fixed and scanned in a Skyscan 1172 instrument. The enamel was analyzed from the apical to the incisal edge in 1.0 mm tall volumes of interest. The mineral density was determined using HA phantoms (0.25 to 2.9 g HA/cm^3). The following parameters were analyzed: volume, mineral weight, % mineral by volume and % non-mineral material by volume. The % mineral and % non-mineral material were calculated from the discrepancy between observed and expected mineral weight in a volume of interest. The expected enamel mineral weight was estimated from cross-sectioned wildtype mandibular incisors in 1.0 mm tall volumes of interest. **Results**: At the eruption site, the enamel volume, mineral weight, and mineral density were reduced in the mandibular incisor when Tg Ambn was expressed lower or higher than normal. While in wildtype the % mineral was >95, it was negligible in Ambn-/-, 22.7% in Ambn-/-, Tg(+), 78.4% in Ambn-/-, Tg(++), and 64.4% in Ambn-/-, Tg(+++). Conversely, the non-mineral content was increased in Ambn-/-, Tg(+) and Ambn-/-, Tg(+++). **Conclusion**: The deposition of mineral and removal of non-mineral components via the mineralization front are both very sensitive to expressed Ambn concentrations. Ambn concentration appears to directly or indirectly control the level to which enamel will ultimately mineralize overall. This study was supported in part by NIDCR K08DE022800.

Shedding Light on the Chemical Diversity of Ectopic Calcifications in Kidney Tissues: Diagnostic and Research Aspects

Arnaud Dessombz* [1,2], Dominique Bazin [2], Paul Dumas [3], Christophe Sandt [3], Josep Sule-Suso [4], Michel Daudon [5]. [1] Centre de Recherche des Cordeliers, Université Paris 5, Université Paris 6, Inserm, Université Paris 7, Paris, France, [2] Laboratoire de Physique des Solides, Bat. 510, Université Paris Sud, Orsay, France, [3] Synchrotron SOLEIL, L'Orme des Merisiers, Saint-Aubin - BP 48, Gif-sur-Yvette, France, [4] Cancer Centre, University Hospital of North Staffordshire, Newcastle Road, Stoke-on-Trent, Staffordshire, United Kingdom, [5] AP-HP, Hôpital Tenon, Service d'Exploration Fonctionnelle, Paris, France

Introduction: Chronic renal failure is increasing in most industrialized countries as a consequence of acquired systemic diseases such as type II diabetes, which is now the first cause for end stage renal failure. A number of other causes may be responsible for the loss of kidney function and tubular interstitial nephritis, but they are less frequent. Among them, lithogenic diseases may induce intratubular crystallization, which may finally result in end-stage renal failure (ESRF). The diagnosis of such pathological conditions is of a prime importance before kidney transplantation in order to treat efficiently the disease and protect the grafted kidney against recurrence of crystallization. Often, crystals are found in kidney biopsies performed in order to understand the mechanism of the loss of renal function. However, only few histochemical tests are available to attempt an identification of the crystals. For these reasons, it is of clinical importance to accurately identify crystals found in the tissue as they can help to early characterization of a disease, which may be efficiently treated by specific drugs. **Purpose**: The aim of this work is to emphasize and explain the chemical diversity of ectopic calcifications present in kidney tissue by a synchrotron FTIR study. **Methods**: 24 kidney biopsies were investigated by FTIR spectroscopy. The measurements were carried out at SOLEIL-Synchrotron (St Aubin-Gif sur Yvette, France) on the SMIS beamline, in reflection mode. The data were analyzed by OMNIC. **Results**: Twelve crystalline species were identified and in two cases, precipitates of proteins in tubular lumens were observed. Some phase were never described before in a tissular context, as Octacalcium phosphate. This phase is metastable and is a precursor of apatite. For the first time, the heterogeneity of intratissular calcification is underlined. Two or more phases were observed in 7 samples. Immuno-suppressed patients under treatment for infection show apatite calcifications in tubular tissues. **Conclusion**: this study gives the first structural evidence of a chemical diversity for mineral deposits in the kidney tissue. New crystalline phases were described such as amorphous silica, sodium hydrogen urate, methyl-1 uric acid and three different Ca2+ phosphates namely whitlockite, OCP and ACCP. We propose mechanisms of formation for these phases and suggest an explanation for these ectopic calcifications induced by drugs or specific pathologies.

The Role of phosphorylation in Dentin Phosphoprotein peptide absorption to hydroxyapatite surfaces: A molecular dynamics study.

Eduardo Villarreal-Ramirez*[1], Ramon Garduño-Juarez[2], Luis Javier Alvarez[3] and Adele Boskey[1]. [1]Mineralized Tissue Research Laboratory, Hospital for Special Surgery, New York, NY, USA, [2]Instituto de Ciencias Físicas, UNAM, Cuernavaca, México, [3]Instituto de Matemáticas,UNAM, Cuernavaca, México.

Introduction: Dentin Phosphoprotein (DPP), is a protein expressed mainly in dentin and to a lesser extent in bone. It is the most acidic protein ever discovered to date. DPP has a disordered structure, rich in glutamic acid, aspartic acid, and phosphorylated serine/threonine residues. It has a high capacity for binding to calcium ions and to hydroxyapatite (HA) crystal surfaces. A detailed atomistic description of the binding mechanisms and the anchoring points occurring between DPP motifs and calcium phosphates is lacking. **Purpose**: Our goal is to elucidate the key interactions between DPP and HA. **Methods:** To study the physical processes involved in these interaction we have designed a research strategy based on molecular dynamics (MD), Small Angle X-ray Scattering (SAXS) and Fourier Transform Infrared Spectroscopy (FTIR). Here, we only present results of MD simulations. For these simulations we have considered five peptides from the sequence of DPP, specifically, #1-DSSDSDSSDSSDSD, #2-SSDSKSDSSKSESDS, #3-SSDSSDSSSSSDSSN, #4-SSNSSDSSNSSDSSN, and #5-SSDSSDSSDSSDSSD. The peptides were modeled and phosphorylated using the xLeap module of AmberTools, PyMol and

YASARA. MD simulations were performed using the GROMACS version. 4.5.3 suite, the peptides were oriented parallel to the {001} HA crystal surface where the distance between the HA slab and the peptide was 3 nm. The system was simulated for 3ns. **Results:** Preliminary results show that for the unphosphorylated peptides, the acidic amino acids present an electrostatic attraction where their side chains are oriented towards HA, however this attraction not is strong enough to facilitate bulk transport to the crystal surface. On the other hand, the phosphorylated (PP) peptides are absorbed on the surface of the HA slap and their centers of mass are closer to the HA surface. More importantly, the root mean square distances (RMSD) indicate that the structures of the phosphorylated peptides are very stable, while the RMSD for the un-phosphorylated peptides are unstable. Radius of gyration (Rg) analysis showed that phosphorylated peptides are absorbed to the HA surface, stabilizing Rg values, more quickly, than un-phosphorylated peptides. The absorption process is a rapid process occurring in picoseconds. **Conclusion:** Phosphorylation of the DPP peptides is necessary for binding to HA surfaces. It appears that phosphorylation of the disordered peptides is as important for binding as phosphorylation of the intact protein. The absorption process is quick process occurring in picoseconds. Supported by the National Council of Science and Technology of Mexico (PFP-186957), PAPIIT IN221913, and the National Institutes of Health (DEO22716).

Dark-field transmission electron microscopy of cortical bone reveals further hierarchical detail

Henry P. Schwarcz[1, 2], Elizabeth A. McNally[2,3], Gianluigi A. Botton[2,3], [1]School, of Geography and Earth Sciences, McMaster University, Hamilton, ON, L8S 4K1, [2]Department of Materials Science and Engineering, McMaster University, Hamilton Ontario, Canada, L8S 4M, [3]Canadian Centre for Electron Microscopy,. McMaster University, Hamilton Ontario, Canada, L8S 4M

Introduction Bone is hierarchically structured so that, viewed at successively higher magnification, smaller-scale structural elements can be visualized. In previous papers [1.2] we have shown that ~80% of the mineral component of bone lies external to the collagen fibrils in the form of "mineral structures" (MSs), 5 nm thick, ~60 nm wide and hundreds of nm long. These are arranged around the collagen fibrils while lesser amounts of mineral occur in the gap zones within the fibrils. Dark-field imaging suggested that the mineral structures are polycrystalline. Here we further investigate their internal structure. **Purpose** To determine the size and form of the mineral (apatite) crystals within individual mineral structures. **Methods** Ion-milled sections were prepared of human cortical bone, and viewed in bright-field and dark-field illumination, the latter using electrons scattered from the 002 reflection of the apatite structure. Dimensions of single crystals were measured using Photoshop Version 12.0 X64, using calibrated images. **Results** Component crystals in MSs can only be seen in edge-on images of MSs oriented in plane of section and with their 60 nm dimension oriented normal to section. MSs display single homoaxial domains averaging 5.8 ± 2.7 nm in width and 28 ± 19 nm in length, the long axis being oriented parallel to the mineral structure. Some appear to be pairs of co-aligned crystals as thin as 2 nm. Size and shape of these smaller crystals agrees with published data obtained using wide-angle X-ray analyses. Images of MSs lying flat in plane of section display complex moiré patterns due to interference of superimposed, quasi co-aligned MSs. Individual homoaxial domains (single crystals or aligned pairs) span the width of the MSs **Conclusions** Most of the apatite in bone bone occurs as plate-like single crystals 5 nm thick and 10's of nm wide, intimately intergrown within mineral structures. Dark-field imaging guarantees that illuminated areas must be single regions of homoaxially oriented apatite; Mineral in gap zones is not illuminated in dark-field using 002 reflections and its nature is still uncertain. **References:** 1. McNally EA et al. (2012) A Model for the ultrastructure of bone based on electron microscopy of ion-milled sections. Plos1, Volume 7 , Issue 1 | e29258. DOI 10.1371/journal.pone.0029258; 2. McNally EA et al. Transmission Electron microscopic tomography of cortical bone using Z-contrast imaging. Micron, in press. DOI 10.1016/j.micron.2013.03.002

Correlative Microscopy and Spectroscopy of Buried Interfaces in Tooth Enamel

Michael J. Cohen1, Lyle M. Gordon1, and Derk Joester1

1. Department of Materials Science and Engineering, Northwestern University, Evanston, IL 60208.

Introduction: Tooth decay, also known as dental caries, is the most pervasive infectious disease in humans. With billions of dollars being spent on dental services in the US alone, there is no question that a significant demand exists for improved dental treatment and preventative measures. Tooth enamel is composed of layers of woven 3-5μm diameter rods, each comprised of thousands of hydroxyapatite nanowires. This architecture is accompanied with a network of buried interphases between the crystals. Despite decades of research on enamel, the complex nanoscale structure and chemistry of the intercrystalline space is not well understood. **Purpose:** A more complete understanding of the interphase structure and chemistry is a fundamental milestone in creating novel and effective preventative techniques. **Methods:** Atom-probe tomography (APT) is uniquely capable of providing the necessary structural insight at the atomic scale by directly probing the location and chemical identity of the atoms within a small sample of material. By field evaporating ions successively from a sharp sample tip, time-of-flight mass spectrometry gives high accuracy spatial resolution and chemical information across the periodic table. **Results**: We report on the application of correlative characterization techniques to probe native mammalian enamel. The unique sensitivity of APT reveal numerous inorganic substituents (such as Na+, Mg2+, CO3 2-) accumulated at grain boundaries and triple junctions. Correlative transmission electron microscope (TEM) imaging of samples reveal grain boundaries consistent with chemical segregation observed in the APT reconstructions, suggesting a magnesium-rich buried interface. This correlative technique allows us to match APT chemical positioning definitely with traditional TEM imaging of grain boundaries. By further correlating to

synchrotron extended X-ray absorption fine structure (EXAFS) of this magnesium-rich intercrystalline space, we can further comment on the local chemistry including bond distance, coordination number and valence state. We will discuss combining structural insight from APT reconstructions with chemical information gleaned from EXAFS and our preliminary model of the intercrystalline space in enamel. **Conclusion:** This correlative method has elucidated new information concerning the critical buried interphase. Our findings suggest the existence of a magnesium-rich interphase, which may play a critical role in dissolution process. We look to use this better understanding of the intercrystalline space to develop novel and effective preventative measures in combatting this pervasive malady.

Tuesday, October 29, 2013 Session 6

MEPE-derived ASARM peptide impairs mineralization in tooth models of X-linked hypophosphatemia

B Salmon[1,2]*, C Bardet[1], M Khaddam[1], B Baroukh[1], J Lesieur[1], BR Coyac[1,6], D Le-Denmat[1], A Nicoletti[3], A Poliard[1], S Opsahl Vital[1,2], PS Rowe[4], A Linglart[5], MD McKee[6] and C Chaussain[1,2]. [1]Faculty of Dentistry, Paris Descartes University, France [2]Odontology Department, Paris Nord Hospital, AP-HP, France [3]Inserm UMRS698, France [4]University of Kansas, USA, [5]Paris Sud University, France, [6]Faculty of Dentistry, McGill University, Canada.

Introduction: Mutations in the *PHEX* gene cause X-linked familial hypophosphatemic rickets (XLH) with severe bone (osteomalacia) and tooth abnormalities being the distinguishing features of this disease. Histological dentin examinations indicate unmerged mineralization foci or calcospherites surrounded by large non-mineralized interglobular spaces. The *PHEX* mutations lead to an increase in ASARM peptides (acidic serine- and aspartate-rich motif) and osteopontin fragments which both inhibit bone extracellular matrix mineralization. MEPE-derived ASARM has been shown to accumulate in tooth dentin of patients with XLH where it may impair dentinogenesis. **Purpose:** Here, we investigated the effects of ASARM peptides on odontoblast differentiation and matrix mineralization. **Methods:** Dental pulp stem cells obtained from human exfoliated deciduous teeth (SHEDs) were first characterized for mesenchymal stem cell markers by cell sorting analysis. The cells were then seeded into a 3D collagen-tooth slice scaffold, and induced towards odontoblastic differentiation using appropriate culture conditions (supplements). Cultures were treated with synthetic ASARM peptides (phosphorylated -p- and nonphosphorylated –np-) derived from the human MEPE sequence. In parallel, MEPE-derived ASARM peptides were implanted in the injured pulp of rat molars and their effects on reparative dentin formation were evaluated. **Results:** p-ASARM peptide inhibited SHED differentiation, with no mineralized nodule formation, decreased odontoblast marker expression, and upregulation of MEPE. When implanted in a tooth pulp injury model, this peptide impaired reparative dentin formation and mineralization, and increased MEPE immunohistochemical staining was detected. In addition, the pulp volume was significantly higher in p-ASARM samples (1.03 mm3 +/- 0.04) when compared to both control and np-ASARM conditions (0.88 mm3 +/- 0.06 and 0.86 mm3 +/- 0.05, respectively). **Conclusion:** In conclusion, using original models to study tooth dentin abnormalities observed in XLH, we show that the MEPE-derived ASARM peptide inhibits both odontogenic differentiation and matrix mineralization, while increasing MEPE expression. These results provide a partial mechanistic explanation of XLH pathogenesis; that direct inhibition of mineralization by ASARM peptide leads to the mineralization defects observed in XLH teeth. This process appears to be positively reinforced by the increased MEPE expression induced by ASARM. This peptide, previously identified in XLH dentin, constitutes therefore as a key molecule in the pathogenesis of tooth dentin abnormalities and should be considered as a potential therapeutic target for treatment of XLH.

Osterix Deficiency Disrupts Ameloblast and Odontoblast Maturation but Not Tooth Morphogenesis

Ji-Myung Bae[1], Mitra Adhami[2], Harunur Rashid[2], Christopher Clarke[2], Amjad Javed*[2], Dobrawa Napierala[2], Soraya Gutierrez[3], Krishna Sinha[4], Benoit de Crombrugghe[4], Haiyan Chen[2].
1Dental College, Wonkwang University, Iksan, Korea. 2Department of Oral and Maxillofacial Surgery, School of Dentistry, University of Alabama at Birmingham, AL, USA. 3Universidad de Concepción, Concepción, Chile. 4University of Texas M. D. Anderson Cancer Center, Houston TX, USA.

Introduction: Runx2 and its downstream target Osterix (Osx) are essential for skeletogenesis. In humans, mutations in Runx2 and Osx are associated with CCD and osteogenesis imperfecta respectively. Tooth development in Runx2 null mice is arrested at late bud stage. Unlike Runx2, nothing is known about Osx role in tooth morphogenesis or differentiation of ameloblasts and odontoblasts. During skeletogenesis, Osx functions downstream of Runx2 but it remains unknown if Osx act independently or is part of the same pathway that controls development of tooth organ. **Purpose:** Investigate regulatory functions of Osterix during tooth development. **Methods:** Molecular, biochemical, and histological approaches were used to evaluate odontogenesis in Osterix-null mice. **Results:** We established Osx-null mice that are devoid of mineralized tissue and died within minutes after birth due to respiratory failure. Newborn heads were sectioned sagitally to evaluate tooth development. In sharp contrast to Runx2, tooth development in Osx null mice progressed till late bell stage. Surprisingly, normal tooth morphogenesis was noted in

incisors, and multi-cusped first and second molars of the Osx homozygous mutants. It is important to note that despite progression of tooth morphogenesis, mineralization was completely absent in alveolar tissues of Osx-null mice. These data demonstrate that tooth morphogenesis is not a prerequisite for formation of alveolar bone. Despite normal shape, position and number, Osx-null tooth-organs were significantly smaller in size. We investigated reasons for difference in size by performing BrdU-labeling assays at E18, a stage by which basic morphogenesis is established. Significant numbers of BrdU positive cells were observed in growing incisor of the WT mice. However, BrdU signal was barely detected in Osx-null littermates, suggesting Osx role in regulating cell proliferation. Moreover, Osx deficiency results in accelerated cell death in growing incisor as noted by increased expression of apoptotic-marker, caspase-3. We next followed differentiation status of ameloblasts and odontoblasts. Maturation of both cell types progressed simultaneously in WT mice that showed well separated, polarized ameloblast and odontoblast. Osx null mutants on the other hand showed only cuboidal and disorganized cells in epithelial and mesenchyme portions of teeth. Impaired differentiation and matrix synthesis was further confirmed by reduced collagen production and loss of expression of stage and cell-specific markers such as DSPP, DMP1, Amelogenin and Enamelin in Osx-null incisors. Analysis of WT and Osx-null incisor mRNA further established failed maturation, with reduced expression of key odontoblast and ameloblast markers by 5-10 fold. Finally, we show that Osx promote odontogenesis by regulating expression of inductive ligands FGF3, and FGF8. **Conclusions:** We report for the first time that tooth morphogenesis is not essential for alveolar bone formation and that Osterix is obligatory for maturation of both odontoblast and ameloblast.

Osterix is Essential for Stability and Function of Runx2 Protein During Bone Formation

Harunur Rashid*[1], Haiyan Chen[1], Changyan Ma[1], Krishna Sinha[2], Benoit deCrombrugghe[2], Amjad Javed[1]. [1]Department of Oral and Maxillofacial Surgery, School of Dentistry, University of Alabama, Birmingham, AL, USA, [2]Department of Molecular Genetics, University of Texas M. D. Anderson Cancer Center, Houston TX, USA.

Introduction: Runx2 and Osterix (Osx) transcription factors are essential for skeletogenesis as null models for both genes exhibit complete lack of bone tissue. However, molecular mechanisms responsible for surprisingly similar phenotype by two unrelated proteins remain unknown. Osx a downstream molecule is not expressed in Runx2 null mice. Thus Runx2 null model represent a compound phenotype of loss of both proteins. Interestingly, Osx null mice expresses Runx2 mRNA but fail to develop bone tissue. **Purpose:** To decipher molecular reasons for functional incompetency of Runx2 in Osx null mice. **Methods:** Cellular, genetics, biochemical and in vivo approaches were used. **Results:** We first analyzed Runx2 expression in skeletal tissues of Osx null mice by RT-PCR and western blot analysis. Similar levels of Runx2 mRNA were consistently noted in bones of wild type and Osx null mice. To our surprise Runx2 protein was barely detected in Osx null mice. These in vivo data strongly suggests that Osx regulates Runx2 protein stability. We experimentally tested this by using human & mouse osteoblast where both proteins are expressed endogenously. Cells were transfected with increasing amount of Osx specific siRNA. We find a dose dependent and potent reduction in Osx protein in both cell types. Surprisingly a concomitant decrease in Runx2 protein was also noted. It is possible that reduction of Runx2 in Osx knock-down cells is related to transcriptional regulation of Runx2 by Osx. To test this possibility, parallel cultures of osteoblasts transfected with Osx siRNA were used for both RNA and protein. A dose dependent decrease in Osx mRNA was evident but the levels of Runx2 mRNA remain unchanged. Thus Osx mediated regulation of Runx2 protein is post-transcriptional. The involvement of Osx in regulating Runx2 stability was further confirmed by coexpression studies. HeLa cells were transfected with increasing concentration of Osx and fixed amount of Runx2 plasmid. We find a dose dependent increase of Osx protein. To our surprise, a progressive increase in Runx2 protein ~20 fold was also noted. Thus Osx is required for stability of Runx2 protein. To understand how Osx stabilize Runx2 protein, reciprocal Co-IP studies were performed in osteoblasts. Our data indicate endogenous Runx2 and Osx protein forms a molecular complex. Deletion mutagenesis identified that runt homology domain of Runx2 and transactivation domain of Osx are involved in physical association. We next tested if Osx regulate Runx2 stability, by competing with E3-ligase mediated degradation of Runx2. Our results shows that Osx protects Runx2 protein from smurf1 mediated ubiquitination and degradation. We further demonstrate that Osx-Runx2 physical interaction is essential for protecting Runx2 protein from degradation, as mutant Osx protein that lack Runx2 interaction domain, fail to block Runx2 protein degradation. Finally, we show Osx-Runx2 interaction results in synergistic regulation and maximal induction of cell phenotype-restricted genes such as OC, ColX and FGF3. **Conclusion:** Multiple line of evidence demonstrates that, Osterix forms a molecular complex with Runx2 to regulate Runx2 protein stability and osteogenic functions in skeletal tissues.

Dental Tissue Phenotype and Ultrastructural Changes in Mouse Brtl/+ Teeth

Adele L. Boskey[1], Kostas Verdelis*[2, 3], Lyudmila Spevak[1], Lyudmila Lukashova[1], Elia Beniash[3], Xu Yang[3], Wayne A Cabral[4], Joan C. Marini[4] [1]Musculoskeletal Integrity Program, Hospital for Special Surgery, 535 E 70th Street, New York, NY [2]Department of Endodontics and [3]Department of Oral Biology, School of Dental Medicine, University of Pittsburgh, PA [4]Bone & Extracellular Matrix Branch, NIH/ NICHD, Bethesda, MD

Introduction: The Brtl/+ mouse is a knock-in model for osteogenesis imperfecta type IV in which a Gly349Cys substitution was

introduced into one Col1a1 allele. **Purpose**: The objective of this study was to characterize the changes in dental tissues structure and mineral composition in these transgenic mice, and compare them to those described for the dentinogenesis imperfecta (DGI) mouse models and DGI associated with OI typeIV in humans. **Methods**: Hemi-mandibles from 2 and 6 months of age normal and transgenic mice were imaged by microcomputed tomography (Scanco µCT 35) at a 12µm voxel size and 55 kVp and crown/root volumes as well as enamel and dentin volumes and densities were measured. 1st and 2nd molar crown and root areas from the same specimens were analyzed by Fourier Transform Infrared Imaging for characterization of the hydroxyapatite quality and co-localization with mineral density, after PMMA embedding and sectioning at 2µm. Backscattered SEM imaging was also performed on 2 month-old 1st molars on polished PMMA blocks for dentin and enamel ultrastructural analysis. **Results**: The Brtl/+ molars showed decreased crown volume and reduced mineralized tissue volume without changes in enamel properties. Increased mineral content and acid phosphate content was noted at 2 months by FTIRI, the latter suggesting a delay in the mineralization process, most likely associated with the defect in the collagen structure. The presence of globular dentin was observed adjacent to the predentin in the cervical portions of the root of Brtl/+ molars by SEM. Although there were no major histological or organization (dentinal tubule density/orientation) changes in the circumpulpal dentin of these molars, the majority of them presented pulp micro-exposures to the oral environment in the enamel-free areas of the cusps and signs of necrotic pulp and apical periodontitis spread into the adjacent trabecular bone. The shape of the molars (shape of crowns, cervical constriction, root length) was altogether normal. **Conclusions**: Although not paralleling the dental phenotype in humans with type IV OI, this condition in the Brtl/+ mice shares some of the features described for a DGI-type II-like phenotype described for dentin sialophosphoprotein knockout animals, without the distinct hypomineralized areas and defective tubule organization throughout dentin characteristic for the last mouse model.

Tuesday, October 29, 2013 Session 6

Cortical Bone Matrix Composition in Cynomolgus Monkeys Treated with Sclerostin Antibody

R. Ross*[1], M. Ominsky[2], A. Acerbo[3], L. Miller[3], D. R. Sumner[1]. [1]Rush University, Chicago, IL, [2]Amgen, Thousand Oaks, CA, [3]Brookhaven National Lab, Stony Brook, NY

Introduction: Sclerostin antibody (Scl Ab) is a potent anabolic agent known to up-regulate bone formation and increase bone volume. Previously, we found that global cortical mineralization in rats was unaffected by Scl Ab treatment, an unexpected finding as increased bone formation should decrease the average tissue age, leading to lower global mineralization. Rat bone tends to mineralize rapidly which may be a confounding factor. **Purpose:** To evaluate the effects of Scl Ab treatment on cortical mineralization in a primate model. **Methods:** Femoral diaphyseal samples from a previous fibular osteotomy study in which 4-5 year old male cynomolgus monkeys were treated with vehicle or 30 mg/kg Scl Ab (romosozumab) once every 2 weeks for 10 weeks (n=10 per group) were examined. Global bone mineral density distribution (BMDD) was assessed using backscattered SEM. The kinetics of mineralization, collagen-crosslinking, carbonate substitution, and crystallinity were assessed by examining tissue between fluorochrome labels given 0.5, 2, 6.5 and 8 weeks prior to sacrifice with Fourier-transform infrared microspectroscopy (FTIRM) within the endocortical and intracortical compartments. **Results:** Scl Ab treatment increased the cortical bone area by ~3% (NS) and the bone formation rate by 4- and 7-fold within the endocortical compartment for each series of labels ($p<0.001$). Despite these increases in bone formation rate, neither the measures of central tendency for the global BMDDs (mean and mode, $p=0.604$ and 0.760, respectively) nor the shape of the BMDD (skewness and standard deviation, $p=0.585$ and 0.601, respectively) were affected by Scl Ab treatment. Within the endocortical compartment, FTIRM showed that tissue between 6.5 and 8 weeks old was more mineralized than tissue between 0.5 and 2 weeks old ($p=0.023$) with no group ($p=0.648$) or group-by-tissue age interaction ($p=0.451$). Within the intracortical compartment, interstitial tissue (>8 weeks old) was more mineralized than tissue between 0.5 and 2 weeks old ($p<0.001$). There was also a trend towards significance for the group difference ($p=0.068$), with Scl Ab causing increased mineralization compared to controls for the tissue formed between 0.5 to 2 weeks ($p=0.001$), but no significance in the group-by-tissue age interaction ($p=0.509$). None of the other FTIRM matrix composition parameters were affected by Scl Ab. **Conclusions:** Despite large increases in the endocortical bone formation rate, Scl Ab did not affect mineralization kinetics at this surface. Intracortically, however, Scl Ab appears to accelerate primary matrix mineralization. These results suggest that while treatment with Scl Ab does not affect global mineralization in the primate cortex, it did accelerate early mineralization in Haversian systems. This interesting compartment-specific effect may be due to differences in the mode of formation (with or without prior resorption) or to differences in exposure to sclerostin protein.

Inactivation of Gnas alters postnatal bone quality

Girish Ramaswamy,[1,4] Deyu Zhang,[1,4] Frederick S Kaplan[1,2,4]Robert J. Pignolo,[1,2,4] Eileen M. Shore*[1,3,4] Department of [1]Orthopaedic Surgery, [2]Medicine, [3]Genetics, and the [4]Center for Research in FOP and Related Disorders, Perelman School of Medicine at the University of Pennsylvania, Philadelphia, PA

Introduction: Progressive osseous heteroplasia (POH), Albright hereditary osteodystrophy (AHO), osteoma cutis (OC), and

pseudohypoparathyroidism 1a/1c (PHP) form a spectrum of disorders that are caused by heterozygous inactivating mutations in *GNAS*, a gene that encodes multiple transcripts including the α-subunit of the stimulatory G-protein ($G_s\alpha$) of adenylyl cyclase. All these disorders exhibit subcutaneous heterotopic ossification (HO); however, POH is the most severe form and is characterized by HO progression into deeper connective tissues including muscle and fascia. The *GNAS* gene shows genomic imprinting and POH is associated with paternal inheritance of the mutation. Mice with paternal inheritance of heterozygous deletion of exon 1 (Gnas $Ex1^{+/p-}$) have lower body weight and length, and develop subcutaneous ossifications with age. But whether reduced Gnas expression leads to alterations in the formation or quality of skeletal bone remains undetermined. **Purpose:** To investigate the effects of paternally inherited *Gnas* inactivation (+/p-) on early skeletal development. **Methods:** We performed μCT and histology on developing bone and cartilage of Gnas $Ex1^{+/p-}$ mice. μCT scans were taken at distal epiphyseal and mid-diaphyseal regions in femurs from postnatal day 14 (P14) mice to assess trabecular and cortical bones respectively. Alcian blue staining was performed on paraffin sections from hindlimbs of P14 mice. **Results:** $Ex1^{+/-}$ mice weighed significantly less than wild-type (wt) littermates at both P1 and P14 days. Tibiae from $Ex1^{+/-}$ mice at these ages were significantly shorter in length (15% ± 4). Trabecular bone parameters at the distal epiphyseal region in P14 mice, revealed dramatic reductions in bone volume (36% ± 11) and bone volume fraction (20%±12). Trabecular microarchitecture was altered with a significant decrease in trabecular thickness and a concomitant increase in the structure model index, suggesting that trabecular bone is more rod-like in these mutants than wt. μCT of femoral mid-diaphysis showed reduced cortical thickness (20%±10) and cortical bone volume (35%±8) in P14 mutants. No differences in bone mineral density of cortical and trabecular bone were observed. Histology from P14 mice showed a marked decrease in the length of the hypertrophic zone of the growth plates of $Ex1^{+/-}$ mice. The calvaria of P1 and P14 heterozygous mutants were reduced in size in both antero-posterior and medial-lateral dimensions. **Conclusion:** Taken together with our previous findings, heterozygous paternal allele inactivation of Gnas not only alters post-natal progenitor cells to form heterotopic ossification, but also adversely affects normal skeletal development and postnatal bone quality that impacts both endochondral and intramembranous bone formation.

Bone-Specific DMP1 Overexpression: Implications on Endochondral Ossification

Joshua D. Padovano*[1], Sriram Ravindran[1], Amsaveni Ramachandran[1], Ana Bedran-Russo[2], Anne George[1]
[1] Brodie Tooth Development Genetics & Regenerative Medicine Research Laboratory, Department of Oral Biology, [2]Department of Restorative Dentistry, College of Dentistry, University of Illinois at Chicago, Chicago, IL, USA

Introduction: Dentin matrix protein 1 (DMP1) is a noncollagenous protein that plays a regulatory role in mineralization. In-vitro studies show that DMP1 can bind type I collagen and initiate the calcium phosphate nucleation process. **Purpose:** To determine if bone-specific overexpression of DMP1 induces altered bone biochemistry, bone architecture, and increased bone mechanical properties that may be adventageous for applications in tissue engineering. **Methods:** Transgenic mice overexpressing DMP1 via the osteocalcin promoter were generated. Protein expression was analyzed by isolating total proteins from the femurs of 15, 30, and 60-day post-natal transgenic and wild type mice. Tissues were homogenized and proteins isolated, separated on SDS-PAGE gel, and analyzed by western blot. Bands of interest were normalized to tubulin and quantified using Image J. Histological analysis was performed on 15, 30, and 90-day femurs demineralized with 14% EDTA. Subsequently, samples were paraffin embedded and 7μm thick sections were prepared. Sections were stained with H&E and proteins investigated with immunohistochemistry and immunofluorescence. Micro-CT analysis was performed on 30, 45, 60, and 90-day femurs for analysis of trabecular and cortical bone architecture. Femoral shaft toughness of 30-day femurs were assessed by 3-point bend test under hydrated conditions. Cortical bone hardness and elastic modulus of 90-day femurs was measured by nano-indentations under hydrated conditions. Statistical analysis was performed using two-way ANOVA followed by Student's t-test post-hoc analysis. **Results:** Western blotting revealed a significant increase in DMP1 expression in 15 and 30-day mouse femurs when compared with the wild type (n=3, p=0.02, p=0.04, respectively). H&E staining of 15 and 30-day distal growth plates revealed altered proliferative and hypertrophic zone morphologies. Immunohistochemical analysis indicated significant DMP1 and Runx2 expression in the hypertrophic zone of 15 and 30-day transgenic growth plates. Micro-CT analysis indicated a significant increase in transgenic trabecular BV/TV and mean cortical thickness at 90-days of age in transgenic mice. Three-point bend test showed increased femoral shaft toughness in transgenic femurs, but not significant (n=4, p=0.17). Nanoindentation of 90-day cortical bone showed no difference in hardness or elastic modulus. **Conclusions:** These data suggest that transgenic mice overexpressing DMP1 using an osteocalcin promoter demonstrate increased matrix synthesis by osteoblasts at the growth plate and that femur trabecular architecture is altered during early post-natal development. Supported by: NIH-NIDCR DE11657, 5T32DE018381, and The Brodie Endowment Fund.

Regulatory circuity of Msx 1 and Msx2 homeogenes in bone.

Sylvie Babajko[1], Stéphane Petit[1], Fleur Méary[1], Ali Nassif[1], Ibtisam Senussi[1], Sophia Loiodice[1], Alba Bolanos[3], Dominique Hotton[1], Benoît Robert[2], Ariane Berdal[1] [1]Team "Molecular Oral Pathophysiology" INSERM UMRS872 Paris-Diderot University, France [2]Institute Pasteur, Paris, France [3]University Carabobo, Valencia, Venezuela.

Introduction: Homeobox genes are instrumental in skeletal morphogenesis. The present study characterizes Msx1 in bone modeling using a transgenic mouse slightly overexpressing Msx1 in the osteoblasts (Msx1-Tg with the COL1A1 2.3 kb promoter) and compare the data with Msx1 and Msx2 -/- bone phenotype. On the other hand, Msx expression is driven by

circumstantial cross-talks with growth factors and a tight retrocontrol involves a cis-antisense non coding RNA which modulates Msx1 protein expression levels. The study explored the putative conservation of this regulatory loop via antisense RNAsMsx1 role was explored in Msx1-Tg and wild-type mice during PN growth. **Methods:** Micro-CT, histomorphometrical, molecular histology and RT-qPCR characterized bone phenotype. Results were compared to Msx1 and Msx 2 -/- data. As done for Msx1, Msx2 antisense RNA was searched by RT-PCR and *in situ* hybridization. Msx1 antisense regulation was further analyzed *in vitro*. A 664bp sequence corresponding to the putative Msx1 antisense promoter was cloned and inserted in front of the luciferase reporter gene in order to study transcriptional regulations by Msx1 and Msx2 homeoproteins. **Results:** As previously documented in Msx2 -/- mice, Msx1 controlled bone modeling rates. This was attested by increased osteoblast and osteoclast number and activity (trabeculae size, cell proliferation and apoptosis, TRAP and COL1A1 expression) in Msx1-Tg mice. Bone mineralization was also abnormal, decreased in Msx1-Tg and increased in Msx1 -/- mice. Bidirectional transcription previously evidenced for Msx1 intervened also for Msx2. But, Msx2 antisense transcripts appeared to be more complex (multiple initiation sites and differential splicing) than that of the single, tightly controlled, Msx1 antisense RNA. In vitro, both Msx1 and Msx2 proteins were shown to stimulate Msx1 antisense promoter transcriptional activity, thus potentially co-decreasing Msx1 protein levels. **Conclusion:** Msx1 (this study) and Msx2 modulate bone modeling and mineralization. Msx1 and 2 osteoblast targets might be common and their site-specific impact, in fact secondary to a differential expression. The underlying regulatory loops involve antisense non-coding RNAs, apparently more critically for Msx1 protein. Future studies will explore these regulatory pathways as key-factors in the known Msx differential impact in jaw and long bones.

Characterization of DSPP-Cerulean/DMP1-Cherry reporter mice.

Mina. Mina[1], Sean. Ghassem-Zadeh[1], Barbara. Rodgers[1], Karen, Sagomonyants[1,] Y. Fu[2], Xi. Jiang[2], Peter. Maye[2].Departments of Craniofacial Sciences[1] and Reconstructive Sciences[2,] School of Dental Medicine, University of Connecticut, Farmington, CT,

Introduction: Transgenic mouse lines in which Green Fluorescence Protein (GFP) expression is under the control of tissue- and stage specific promoters have provided powerful experimental tools for identification and isolation of cells at specific stages of differentiation along many lineages including odontoblast lineage. Our previous studies showed that the 2.3-GFP, 3.6-GFP and DMP1-GFP transgenes could be used for isolation and identification of odontoblasts at early and late stages of differentiation. However these transgenes similar to expression of the endogenous proteins are expressed by both odontoblasts and osteoblasts and therefore make it difficult to distinguish between the two cell types. **Purpose:** To generate and characterize a new fluorescent protein reporter transgenic mouse that allows identification and isolation of odontoblasts at later stages of differentiation and to distinguish between odontoblasts and osteoblasts. **Methods**: DSPP-Cerulean/DMP1-Cherry transgenic mice were generated using a bacterial recombination strategy with the mouse BAC clone RP24-258g7. The expression of both fluorescent reporters in the mandibular teeth was examined in frozen sections at various stages of tooth development. Primary cultures from Dental Pulp (DP) and Bone Marrow Stromal (BMS) cells from these animals were used to examine the stage-specific activation of both Fluorescent reporters during *in vitro* mineralization and compared to the expression of endogenous *Dspp* and *Dmp1*. **Results**: DSPP-Cerulean and DMP1-Cherry were not expressed in pre-odonblasts, ameloblasts or dental pulp. The expression of both reporter genes was first detected in functional odontoblasts associated with pre-dentin and increased in newly differentiated odontoblasts. Fully differentiated odontoblasts exhibited high levels of DSPP-Cerulean and reduced levels of DMP1-Cherry expression. DMP1-Cherry (but not DSPP-Cerulean) was expressed at high levels in the osteoblasts and osteocytes within the alveolar bone. In DP cultures DMP1-Cherry+ cells appeared before DSPP-Cerulean+ cells. Some (not all) of the DMP1-cherry positive cells differentiated into and DSPP-Cerulean+ cells. Expression of both transgenes was affected by FGF2 in primary pulp and bone marrow stromal cell cultures. In BMS cultures only DMP1-Cherry was in mineralized nodules. **Conclusions:** In DSPP-Cerulean/DMP1-Cherry transgenic mice DSPP-Cerulean transgene can be used for identification and isolation of secretory/functional odontoblasts and DMP1-Cherry for isolation of functional odontoblasts, osteoblasts and osteocytes. This transgenic animal provides a new experimental model to study the molecular mechanisms that regulate the progression of progenitors into odontoblasts vs. osteoblasts/osteocytes. Supported by a Grant R01-DE016689.

An Essential Role of Bmp Receptor1A (ALK3) in Postnatal Skeleton Formation

J. Jing*[1,2], Z. Zong[1], C. Liu[3], N. Kamiya[4], Y. Liu[1], X. Zhou[2], and J.Q. Feng[1].[1] TX A&M Baylor College of Dentistry, Dallas, TX; [2] State Key Laboratory of Oral Diseases, West China School of Stomatology, Sichuan University, China; [3] Orthopaedic Surgery, New York University School of Medicine, New York, NY; and [4] Texas Scottish Rite Hospital for Children, Dallas, TX

Introduction: ALK3 plays a critical role in both chondrogenesis and osteogenesis during embryonic development but its role in the postnatal stage is still unclear. **Purpose:** To test the postnatal role of ALK3 in skeletal tissues formation. **Methods:** The skeletal phenotype was studied in 2-wk, 4-wk and 8-wk in Alk3 conditional knockout (cKO) mice, which were crossed between $Alk3^{fl}$ and aggrecan-Cre^{ER} (specific for cartilage tissues) and induced by tamoxifen at postnatal day 3. Histological analysis such as H&E and Toluidine Blue staining and immunostaining were performed. X-ray and μCT were also performed to characterize the bone phenotype. **Results:** The X-ray and μCT images displayed a reduced bone length in null femora and vertebrae, 40% and 30% reduction, respectively. There was no apparent change in the cortical bone quantity as well as other flat bones such as calvarial and alveolar bones as assessed by bone volume/total volume. H&E and Toluidine Blue staining showed no evidence of chondrocytes in the null epiphysis and metaphysis, suggesting a complete block of endochondral bone formation in Alk3-cKO mice. Moreover, sulfated proteoglycan and Sox9 (an essential early transcription factor for chondrogenesis) were undetectable in the cKO epiphyseal and growth plate cartilage. Interestingly, mice lacking Alk3 in the late chondrocyte obtained from the offspring of mice crossing between Col X-Cre & $Alk3^{fl}$ showed no apparent change in the cartilage, suggesting an essential early

(but not late) role of ALK3 in controlling postnatal chondrogenesis, likely via regulation of SOX9. Of note is that the ribs are composed of true (bonny) and false (cartilage) components, whereas ribs are known to undergo intramembranous ossification. Surprisingly, the inactivation of Alk3 in early cartilage led to a sharp cortical bone volume increase in the boney ribs, indicating that rib ossification is cartilage-dependent and regulated by ALK3. **Conclusions:** Inactivation of Alk3 in cartilage led to a switch from the epiphysial perichondrium to a periosteum-like structures such as the lack of cartilage and great expansions of the bone bark (>10-fold increase) as evidenced by X-rays, uCT, immunostaining, Safranin O and Toluidine Blue staining. Our data support the vital role of ALK3 in postnatal endochondrogenesis via regulation of Sox9. The finding that severe defects in rib ossification but not in other flat bones suggest that rib bone formation is chondrocyte-dependent, in which ALK3 plays an essential role. This research was supported by NIH/NIDCR grant DE018486.

Wednesday, October 30, 2013 Session 7

Postnatal Osteoblast Function and Skeletal Homeostasis is Dependent on Runx2

Mitra Adhami*, Haiyan Chen, Harunur Rashid, and Amjad Javed.
Department of Oral and Maxillofacial Surgery, School of Dentistry, University of Alabama at Birmingham, AL, USA

Introduction: Runx2 is an essential transcription factor for commitment and differentiation toward the osteoblast, chondroblast, and odontoblast lineages. Global gene deletion of Runx2 results in a complete failure of development of mineralized tissue. Due to early lethality of null models, specific roles of Runx2 in mineralizing cell types remain unknown. Previous studies with Runx2 transgenic models are contradictory. Osteoblast specific overexpression or blockage of endogenous Runx2, results in similar decreased bone density. Thus, the osteoblast-specific function of Runx2 remains unclear. **Purpose:** Identify physiologic roles of Runx2 in committed osteoblast for skeletogenesis. **Methods:** Newly developed Runx2-floxed mice and 2.3kbCol1a1-Cre line were used to achieve osteoblast-specific conditional ablation of Runx2 gene. Cellular, biochemical, histological and micro-CT approaches were employed to evaluate skeletogenesis. **Results:** We recently show that chondrocyte-specific deletion of Runx2 gene results in failed endochondral ossification and perinatal lethality. To our surprise, at birth osteoblast-specific Runx2 null mutants ($Runx2^{F/F}$Col1a1) were essentially identical to WT littermates. Skeletal preps double stained with alizarin red/alcian blue showed intramembranous and endochodral ossification in Runx2 null was similar to WT mice. Histological analysis of newborn limbs further confirmed that length, width, proteoglycan content and the extent of calcification in Runx2 mutant bones is identical to WT littermates. Consistent with these observations, BrdU labeling revealed that loss of Runx2 does not affect proliferative capacity of osteoblasts. Furthermore, osteoblast cell death was not affected by loss of Runx2, as we noted similar levels of apoptotic marker Caspase-3. These results are not due to non-specific expression or poor cleavage efficiency of Col1a1-Cre, as two independent reporter lines confirmed robust and specific Cre-activity. Thus Runx2 activity in differentiated osteoblasts is not required for development and mineralization of embryonic bones. To understand if Runx2 actions in osteoblasts contribute to post-natal skeletogenesis, we monitored WT and $Runx2^{F/F}$Col1a1 littermates for 6 months. Interestingly, during postnatal development, both male and female $Runx2^{F/F}$Col1a1 drop off the growth curve. As mice reached skeletal maturity, a rapid weight loss in $Runx2^{F/F}$Col1a1 was observed with mutants weighing 70% less than WT. Signs of early skeletal aging in $Runx2^{F/F}$Col1a1 were evident with severe concavity in the spine and hunchback phenotype. Additionally, Runx2 loss also affected post-natal development of intramembranous bones. We noted significant decrease (~60%) in the thickness of calvarial bones of Runx2 null mutants. Consistent with these observations, double-calcein labeling showed a complete lack of bone synthesis in calvaria and endosteal surfaces of the limbs of Runx2 mutant mice. Consistent with this observation, micro-CT analysis revealed a striking decrease in both the cortical and trabecular bones of Runx2 mutant mice. **Conclusions:** Runx2 expression and functions in osteoblasts is not critical during embryonic skeletogenesis but is necessary for postnatal bone acquisition and maintenance.

Transcriptional Regulation of Dentin Matrix Protein 1 by TCF11 during osteoblast and odontoblast differentiation

Alexander Jacob, Youbin Zhang and Anne George*. Brodie Tooth Development Genetics & Regenerative Medicine Research Laboratory, Department of Oral Biology, University of Illinois at Chicago, Chicago, Illinois 60612

Introduction: Dentin matrix protein 1 is an acidic noncollagenous protein that plays a regulatory role during mineralization. Expression analyses demonstrate that DMP1 is differentially regulated in osteoblasts and odontoblasts. During osteoblast differentiation DMP1 is constitutively expressed whereas in differentiating odontoblasts the expression is temporally and spatially regulated. We had shown earlier that blocking DMP1 expression inhibits osteoblast differentiation. Results from earlier study indicate that c-Fos and c-Jun play an important role in early osteoblast differentiation, whereas they do not have a significant effect on the terminally differentiated osteoblasts. **Purpose:** To identify the transcription factors that regulate the expression of DMP1 in differentiating osteoblasts and odontoblasts. **Methods:** In-silico analysis of the 6.2kb DMP1 promoter to identify the transcription factor binding sites. The rat odontoblast cell line T4-4 and the mouse osteoblast cell line MC3T3-E1were used to demonstrate DMP1 promoter activity. Luciferase assays were performed to test the promoter activity. EMSA and ChIP analysis were performed to confirm the binding of the transcription factor to the DMP1 promoter. Immunofluoresence and siRNA were performed to confirm the presence of the identified transcription factor. **Results:** Examination of the transcription factor binding sites within the 6.24 kb upstream sequence of rat DMP1 promoter performed by Matinspector software revealed that TCF11 had the highest number of binding sites with 100% matrix similarity. Four of these sites are conserved in the mouse DMP1 promoter. Transient transfection experiments showed that TCF11 induces DMP1 promoter activity in odontoblasts and osteoblasts. However, the binding pattern was different when cells were cultured in the

differentiation media. EMSA and ChIP assay showed the differential interaction between TCF11 and its binding sites on the DMP1 promoter. Immunofluorescence experiments showed that TCF11 is predominantly localized in the nucleus of both T4-4 and MC3T3 cells in the presence or absence of mineralization conditions. SiRNA knock-down of TCF11conclusively demonstrated that TCF11 is indispensable for the expression of DMP1 in osteoblasts. **Conclusions:** TCF11 a member of the Cap-n-Collar (cnc) family of basic leucine zipper transcription factors can induce the promoter activity of DMP1 in osteoblasts and odontoblasts. Specifically, TCF11 is indispensable for the expression of DMP1 in osteoblasts, as evidenced by SiRNA transfection experiments. Supported by NIH-DE11657 and the Brodie Endowment Fund.

Hedgehog Regulated Matrix Metalloproteinases Expressed in Bone-Invasive KCOTs

Hope M. Amm, Mary MacDougall. Institute of Oral Health Research, School of Dentistry, University of Alabama at Birmingham, Birmingham, AL

Introduction: Keratocystic odontogenic tumors (KCOT) are highly proliferative, locally aggressive tumors of the jaw with a high rate of recurrence. Invasion of KCOTs has been associated with the expression of matrix metalloproteinases (MMPs), which degrade the extracellular matrix. KCOTs, both sporadic and syndromic (Gorlin's syndrome), are associated with mutations in Hedgehog signaling (HH) pathway receptors, PTCH1/2, related to increased HH signaling. HH signaling, regulated by Gli transcription factors, up-regulates MMP-2, 11, and 14. Therefore, the HH signaling characteristic of KCOTs may be associated with the invasive properties of the tumors. **Purpose:** To characterize HH and MMP expression profiles in KCOT cell populations. **Methods**: Four independently established KCOT primary cell populations were grown in DMEM supplemented with 10% FBS and antibiotics and in tumor sphere-forming assays. Cells were analyzed by qRT-PCR, immunohistochemistry (IHC) and cDNA microarray (KCOT-1; Affymetrix U133plus). **Results:** Active HH signaling was shown by sonic hedgehog, patched, smoothened, Gli-1 and Gli-2, expression in all KCOT primary cell populations by qRT-PCR and IHC. The HH-regulated MMPs (MMP-2 and MMP-14) were highly expressed in all KCOT populations, while MMP-1, 3, 11, 12, 16, 17, and 19 were moderately expressed. Most of the expressed MMPs have not been previously associated with KCOTs or odontogenic tumors in general. This expression was confirmed by microarray analysis of KCOT-1 cells. No significant differences in MMPS profiles were found between syndromic (KCOT-3) and non-syndromic populations (KCOT-1/2/4). Protein expression of MMP-3, MMP-12, and MMP-16 were confirmed in KCOT-1, KCOT-2, and KCOT-3 samples by IHC. KCOT cells with significantly higher HH activity (increased Gli-1 expression) were isolated and demonstrated significant increases in HH-regulated MMP-2, 11, and 14. **Conclusion:** KCOT cell populations have active HH signaling, which regulates MMP expression and may be associated with the invasive property of the tumors by regulation of MMPs. Supported by the NIDCR-DART32DE017601/T90DE022736 & UAB SOD IOHR.

Endothelin Signaling Promotes Osteogenesis via Wnt Signaling Derepression and Induction of IGF-1 and PGE2

Michael G. Johnson*, Jasmin Kristianto, Anne Gustavson, Kathryn Konicke, Baozhi Yuan and Robert BlankDepartment of Medicine University of Wisconsin-Madison

Introduction: Endothelin (ET1) promotes the growth of osteoblastic breast and prostate cancer metastases, an effect previously shown to be due in part to derepression of canonical WNT signaling. Conversion of big ET1 to mature ET1, catalyzed primarily by endothelin converting enzyme 1 (ECE1), is necessary for ET1's biological activity. We previously identified *Ece1*, encoding ECE1, as a positional candidate gene for a pleiotropic quantitative trait locus affecting femoral size, shape, mineralization, and biomechanical performance. **Purpose**: To test the hypothesis that ET1 signaling regulates osteogenesis in the normal state as well as in cancer. **Methods:** we exposed TMOb osteoblasts to 25 ng/ml big ET1 prior to and over the course of *in vitro* differentiation. Cells were grown for 6 days in growth medium and then switched to mineralization medium for an additional 15 days, by which time they form mineralized nodules. Cells were harvested every three days following the switch to mineralization medium. We measured mRNA levels of genes involved in the ET1 signaling axis, production of paracrine factors involved in osteogenesis, and miRNA expression. Data were analyzed by the rank sum test or nonparametric ANOVA. **Results:** TMOb cells exposed to big ET showed greater mineralization than control cells ($N = 6$, $p = 0.008$). The mineralization difference was specific to ET1 signaling, as it was blocked by pharmacological inhibition of ECE1 or endothelin receptor A. Under normal mineralization conditions, *Ece1* mRNA expression showed no change over the course of mineralization, ET1 was repressed and endothelin receptor A was induced. Addition of big ET1 repressed expression of all three genes. IGF-1 levels were significantly (1.3-1.8X) higher over time in the presence of big ET ($p<0.001$). PGE2 levels were significantly increased over time (1.2-1.4X) in the presence of big ET-1 while DKK1 and SOST production were repressed over time by 30-40% by big ET-1 ($p<0.001$). Big ET1 repressed anti-osteogenic miRNAs including miRNA 335-5p, which targets *Igf1* and *Runx2* transcripts, while miRNAs that target proteins involved in bone catabolism were induced by big ET1 exposure. Modulation of canonical WNT signaling could not fully account for ET1's osteogenic effects, as big ET1 produced a greater mineralization than treatment with LiCl. **Conclusion**: Our data show that osteoblasts express all the elements needed for ET1 signaling over the course of differentiation and that ET1 signaling promotes mineralization. Moreover, they suggest that ET1's osteogenic effects are mediated in part via IGF-1 and PGE2 induction, potentially through changes in miRNA expression previously unrecognized ET1 osteogenic mechanisms.

The Rapid 1α,25(OH)$_2$D$_3$-Mediated Activation of Phospholipaes A2 is Modulated by Ca2+/CaM-Dependent Protein Kinase II in Osteoblasts

Maryam Doroudi[1], Chas Plaisance[2], Subhendu De[2], Zvi Schwartz[3], Barbara D. Boyan[3]. [1]School of Biology, [2]The Wallace H. Coulter Department of Biomedical Engineering, Georgia Institute of Technology, Atlanta, GA. [3]School of Engineering, Virginia

Common Wealth University, Richmond, VA.

Introduction: Vitamin D plays an important role in maintaining bone and mineral homeostasis. 1α,25-dihydroxyvitamin D3 [1,25D3], one of the bioactive metabolites of vitamin D_3, mediates its effects via two different mechanisms: the classical pathway that is vitamin D receptor (VDR) mediated, and rapid membrane-mediated signaling. In 1,25D3 membrane-mediated signaling in osteoblasts, after 1,25D3 binds its membrane-associated receptor (Pdia3) in caveolae, phospholipase-A2 (PLA2)-activating protein (PLAA) is activated, stimulating PLA2, resulting in prostaglandin-E2 (PGE2) release and PKC activation. However, how PLAA mediates the signal to cPLA2 is not clear. Previous reports suggested norepinephrine-mediated CaMKII activation is required for activation of cPLA2. **Purpose:** The aim of the present study was to evaluate the role of CaMKII as the mediator of the 1,25D3-activated cPLA2. **Method:** To determine the time-point at which 1,25D3 and PLAA-peptide activate CaMKII, MC3T3-E1 osteoblasts were treated for various times with 1,25D3/PLAA-peptide and whole-cell-lysates assayed for CaMKII activity. To determine requirements for Cav-1, Pdia3 and PLAA in 1,25D3-mediated CaMKII activation, we measured CaMKII activity in osteoblasts silenced for Cav-1 (shCav-1), Pdia3 (shPdia3) and PLAA (shPLAA) or pretreated with anti-Pdia3 and anti-PLAA antibodies, and next treated with 1,25D3. To determine effects of caveolar disruption on 1,25D3/PLAA-mediated CaMKII activation, we measured CaMKII activity in cells pretreated with methyl-β-cyclodextrin and next treated with either 1,25D3 or PLAA-peptide. To investigate the effects of CaMKII inhibition, cells were pretreated with CaMKII-specific inhibitors, and next treated with 1,25D3. Activities of cPLA2 and PKC and PGE2 release were measured. **Results:** 1,25D3 and PLAA-peptide significantly increased CaMKII activity 9 minutes after treatment in a dose-dependent manner. Unlike wild-type cells, shCav-1, shPdia3 and shPLAA osteoblasts failed to activate CaMKII in response to 1,25D3. Similarly, pre-treating cells with anti-PLAA or anti-Pdia3 antibodies blocked 1,25D3-mediated CaMKII activation. Caveolae disruption abolished 1,25D/PLAA-mediated CaMKII activation. CaMKII-specific inhibitors reduced cPLA2 and PKC activities and PGE2 release in response to 1,25D3 in a dose-dependent manner. **Conclusion:** Taken together, the results suggest that 1,25D3 and PLAA-peptide rapid effects are mediated by CaMKII. PLAA, Pdia3, Cav-1 and caveolae are required for 1,25D3-mediated CaMKII activation. CaMKII mediates the signal from PLAA to cPLA2.

Osteocytes are Key to the Formation and Maintenance of Mineralized Bone

Y. Ren[1], S. Lin[1], X. Han[1], B. Yuan[2], Y. Jing[1], Y. Liu[1], MK. Drezner[2], P. Dechow[1], M. Liu[3], and J.Q. Feng[1]. [1]Baylor College of Dentistry, TX A&M Health Science Center, Dallas, TX 75246; [2]School of Medicine and Public Health, Univ. Wisconsin, Madison, WI; and [3]Department of Metabolic Disorders, Amgen Inc., Thousand Oaks, CA, USA;

Introduction: The theory that osteoblasts (Obs) regulate mineralized bone formation is a cornerstone of bone biology. However, the role that the osteocyte (Ocy), the most abundant bone cell, may play in bone formation remains speculative. Thus, we tested if the Ocy does, in fact, have a role in this vital function. **Purpose:** To investigate osteocytes' role in biomineralization. **Methods:** SEM and FITC (a fluoresce dye filling in Oycs and dendrites) are applied to view osteocytes maturation and lacuna-canalicular system, 3D quantitation of osteocytes is performed by Imaris 7.6 (Bitplane). Double labeling shows mineral deposition along osteocytes to the mineral front. IHC and serum biochemistry are used to analyse mice phenotype. **Results:** we documented a close association between Ocy maturation and the degree of bone mineralization by SEM and FITC. Quantitative data revealed that the mature Ocy cell volume was 50% reduced, and the volume vacated by the reduced cell body in the matrix was replaced by mineral. Confocal microscopic examination of DAPI nuclear stained bone, previously labeled with calcein/alizarin red revealed not only mineral deposition surrounding Ocy matrix, but also at the mineralization front surrounding cananiculae. For the Ocy to play such a central role in formation of mineralized bone, access to a mineral source is critical. Yet, it is widely believed that there are few blood vessels in bone. However, we demonstrated high vessel density and numerous dendritic connections between the vessels and Ocys. Moreover, a dye injection into the rabbit abdominal aorta revealed dye in the Ocy bodies and their dendrites in < 2 minutes, indicating a rapid exchange and delivery of mineral between capillaries and Ocys. The vital Ocy role in mineralization was further demonstrated in *Dmp1*mice, where Obs failed to form Ocys; where b-catenin levels are >10-fold higher than WT; and the mice are osteomalacic. Moreover, in the offspring of mice obtained by crossing *Dmp1*-Cre & $Catnb^{\Delta ex3}$mice, the elevated b-catenin levels recaptured an osteomalacia phenotype similar to *Dmp1* KO mice except without the FGF-23 abnormalities. Currently, imbalances of Obs and osteoclasts are implicated in osteoporosis, although neither cell is embedded in bone matrix where Ocys likely play a key pathological role. We then evaluated osteoporosis patients and ovariectomized (OVX) rats demonstrating distinct Ocy changes from a spindle to a round shape with >50% increase in Ocy volumes and reductions of Ocy #, unexpectedly, there were sharp reductions of blood vessels in Ovx bones as well. **Conclusion:** Our studies suggest that the Ocys, but not Obs, are the key cells building and maintaining mineralization, as such, defective Ocy function may underlie osteomalacia and possibly osteoporosis. Supported by NIH R01 DE018486.

Wednesday, October 30, 2013 Session 8

Examining if nanoscale mineral properties in bone formed in response to loading is altered by aging

Marta Aido*[1], Michael Kerschnitzki[2], Rebecca Hoerth[2], Peter Fratzl[2], Georg N. Duda[1], Wolfgang Wagermaier[2], Bettina Willie[1]. [1]Julius Wolff Institute, Charité - Universitätsmedizin Berlin, Germany, [2]Department of Biomaterials, Max Planck Institute of Colloids and Interfaces, Potsdam, Germany.

Introduction: Bone has the specific capability to adjust structure and shape to loading conditions. Exercise trials have shown that physical stimuli that enhance osteogenesis in young people aren't as effective in older individuals. Recently we showed that the bone formation response to tibial in vivo loading of female C57/Bl6 mice diminishes with age. However it remains unknown, to what degree the material composition of bone formed in response to loading is altered by aging. **Purpose:** We aimed at examining bone's mineral properties at a nanoscale level due to changed loading conditions and how this material adaptation is altered with age. **Methods:** We performed in vivo cyclic compressive loading of the left tibia of 10, 26 and 78 wks old female C57Bl/6J mice, 5d/wk for 2 wks (216 cycles/day; f = 4 Hz), with the right tibia as an internal control (n=2/age). Peak strains of 1200 με were engendered on the medial tibial midshaft for all ages (determined by in vivo strain gauging). Mice were given calcein 12 and 3 days before necropsy, to locate newly formed bone with fluorescent microscopy. Tibiae were PMMA embedded and 10 μm thick longitudinal sections were analyzed at the mid-shaft with Small-Angle X-Ray Scattering using a 1 μm size beam at the European Synchrotron Radiation Facility to measure mineral particle thickness (T parameter) and degree of alignment (Rho parameter). Approximately 15000 SAXS patterns were recorded per sample. 3 regions of interest (ROI) were measured: intracortical (30 μm from bone borders), endosteal (10 μm at endosteal border) and periosteal (10 μm at periosteal border). An ANOVA assessed effects of loading, age, ROI and interactions. **Results:** Neither age, nor loading altered T or Rho for the entire region or individual ROIs. A trend of increased T parameter with age was observed in the loaded limbs. The lack of significance may be related to small sample size, but requires further study. The T and Rho of new tissue formed with in vivo loading was not significantly different than tissue formed with normal growth in the 10wks old mice. However, newly formed tissue in the endosteal region (2.22±0.04 nm) had a significantly lower T compared to the one formed in the periosteal region (2.43±0.18 nm) in the loaded limbs. The endosteal region also had a significantly lower T and Rho (0.40 ± 0.16) compared to mature intracortical tissue (T: 2.40±0.12 nm, Rho: 0.53±0.05) of loaded and non-loaded limbs. **Conclusions:** Bone formation rates at the tibial mid-shaft in these mice are greater in the endosteal than periosteal region, which may account for the regional differences observed in mineral properties. Although some specific changes in nano-scaled mineral properties were observed, these findings suggest no influence of in vivo loading on mineral particle thickness and alignment.

Enamel Defects Reflect Perinatal Exposure to Bisphenol A

Jedeon Katia*1, De la Dure Molla Muriel1, Brookes Steven2, Canivenc-Lavier Marie-Chantal3, Kirkham Jennifer2, Berdal Ariane1, Babajko Sylvie1. 1Centre de Recherche des Cordeliers, INSERM UMRS 872, Laboratory of Molecular Oral Pathophysiology, Paris, F-75006 France. 2Leeds Dental Institute, Department of Oral Biology, University of Leeds, Leeds LS2 9LU, UK. 3Équipe Formation et dynamique du comportement alimentaire, Centre des sciences du gout et de l'alimentation, UMR 1324 INRA-Université de Bourgogne, 21 065 Dijon, France.

Introduction: Endocrine disrupting chemicals (EDCs) including bisphenol A (BPA) are environmental ubiquitous pollutants and associated to a growing health concern. Molar incisor hypomineralization (MIH) is a recent pathology of unknown origin affecting 1/5th of children. **Purpose:** Concurrent increases in MIH prevalence and health issues related to EDCs led us to investigate BPA as a causative candidate for MIH. **Methods:** Wistar rats were orally exposed daily to 5 μg/kg BPA from conception until P30 (post-natal day 30) or P100 mimicking human environmental exposure. BPA treated rats and MIH affected teeth, obtained after elective extraction, were investigated in parallel by scanning electron microscopy (SEM) and energy-dispersive X-ray spectroscopy (EDX) analysis. Organic content of rat incisors was analysed by quantitative approaches as qRT-PCR and western-blotting as well as qualitative procedures as immunohistochemistry for enamel matrix proteins and albumin. **Results:** At P30, BPA treated rats exhibited hypomineralized incisors similar to human MIH. SEM and EDX analysis showed an abnormal accumulation of organic material in erupted enamel. BPA affected enamel showed an abnormal accumulation of exogenous albumin in the maturation stage. RT-qPCR, Western blotting and immunohistochemistry showed increased expression of enamelin but decreased expression of kallikrein 4 (protease essential for removing enamel proteins). Data suggest that BPA exerts its effects on amelogenesis by disrupting normal protein removal from the enamel matrix. Interestingly, in P100 rats erupting incisor enamel was normal suggesting amelogenesis is only sensitive to MIH causing agents during a specific time window during development (as reported for human MIH). **Conclusions:** BPA has been shown to directly target enamel related genes and affect enamel matrix composition at a susceptible developmental stage. The present work documents the first experimental model that replicates MIH and presents BPA as a potential causative agent of MIH. As human enamel defects are irreversible, MIH may provide an easily accessible marker for reporting early EDC exposure in humans.

Raman spectroscopic analysis of combat-related heterotopic ossification development

Nicole J. Crane, PhD[1,4]; Elizabeth Polfer, MD[1,3,4]; Eric A. Elster, MD, FACS[1,2,4]; Benjamin K. Potter, MD[1,3,4]; Jonathan A. Forsberg, MD[1,3,4*]

[1]Department of Regenerative Medicine, Naval Medical Research Center, Silver Spring, MD; [2]Department of Surgery, Walter Reed National Military Medical Center, Bethesda, MD;

[3]Department of Orthopaedic Surgery, Walter Reed National Military Medical Center, Bethesda Maryland;
[4]Department of Surgery, Uniformed Services University of Health Science, Bethesda, MD

Introduction: Over 60% of combat-injured patients develop radiographically apparent heterotopic ossification (HO), defined as the formation of mature lamellar bone in the soft tissues. Nearly a third of these require surgical excision of persistently symptomatic lesions, a procedure that is fraught with complications and delays or regresses functional rehabilitation in many cases. Due to the high prevalence and the morbidity of surgical removal, prophylaxis would be much preferred to treatment. Unfortunately, for the combat injured, medical contraindications and logistical limitations limit widespread use of conventional means of primary prophylaxis. Better means of risk stratification are needed to both mitigate the risk of current means of primary prophylaxis as well as to evaluate novel preventive strategies currently in development. **Purpose:** We asked whether Raman spectral changes, measured *ex vivo*, correlated with histologic evidence of the earliest signs of HO formation using tissue biopsies from the wounds of combat casualties. **Methods:** In doing so, we compared normal muscle tissue to injured muscle tissue, unmineralized HO tissue, and mineralized HO tissue. **Results:** The Raman spectra of these tissues demonstrate clear differences in the amide I and amide III spectral regions of HO tissue compared to normal tissue, denoted by changes in the 1680/1445 cm^{-1}, 1660/1445 cm^{-1}, 1640/1445 cm^{-1}, 1340/1270 cm^{-1} and 1240/1270 cm^{-1} band area ratios (BARs). Additionally, analysis of the bone mineral in HO by Raman spectroscopy appears capable of determining bone maturity by measuring both the 945/960 cm^{-1} and the 1070/906 cm^{-1} BARs. **Conclusions:** Raman may therefore prove a useful, non-invasive, and early diagnostic modality to detect HO formation prior to it becoming clinically or radiographically evident. This technique could ostensibly be developed as a non-invasive means to risk stratify individual wounds at a time thought to be amenable to various means of primary prophylaxis. Supported by the U.S. Navy Bureau of Medicine and Surgery under the Advance Medical Development Program and Office of Naval Research work unit number (602115HP.3720.001.A1015), USAMRMC Military Medical Research and Development award OR090136, Defense Medical Research and Development Plan D10_I_AR_J2_501, as well as the Orthopaedic Trauma Research Program grant # OTRP W81XWH-07-1-0222.

The Character of Gene Expression of Human Periosteum Used to Form New Tissue in Allograft Bone.

William Landis[1], Jessica Kemppainen[1], Qing Yu[1], John Alexander[2], Thomas Scharschmidt[3], Robin Jacquet[*1]. [1]Department of Polymer Science, University of Akron, Akron, OH, United States, [2]College of Medicine and [3]Department of Orthopedic Surgery, The Ohio State University, Columbus, OH, United States.

Introduction: There are more than two million segmental bone defects repaired annually with bone autografts and allografts. Fifteen to forty percent of such repairs fail. A possible approach to improving healing rates is tissue engineering with use of periosteum overlying an allograft, for example. Previous work from this laboratory with human cadaveric periosteum-allograft constructs has demonstrated histologically that allograft remodeling occurs when such constructs are implanted in athymic (nude) mice for up to 20 weeks. Osteoblasts and new bone and osteoclasts and resorption pits are all found in the constructs and allografts without periosteum fail to remodel. **Purpose**: Document gene expression in human periosteum-allograft constructs compared to allografts alone. **Methods**: Human cadaveric periosteum (26 yo, f, distal femur) was dissected into tissue strips that were wrapped and sutured about sterilized human femoral cortical strut bone allografts (54 yo, m) segments. After construct incubation (M199 supplemented medium) for 8 days, constructs and allografts alone were implanted in nude mice. At 10 and 20 weeks, constructs (N = 4, each group) and allografts (n = 2, each group) were retrieved and placed in RNAlater for quantitative PCR to determine expression of human- and murine-specific genes relevant to remodeling. Specimens were frozen-ground to powder and RNA was extracted, purified, reverse-transcribed, and amplified. Ribosomal protein (P0) was used to normalize sample quantities. Fold change plots were generated to compare 20- to 10-week gene expression data. Statistical analysis of gene data utilized a student t-test with errors given as standard errors of mean values. **Results**: Allografts alone yielded no human-specific gene expression. Fold changes of human-specific *alkaline phosphatase, bone sialoprotein, type I collagen, decorin, RANKL, RANK, cathepsin K,* and *osteocalcin* in 20-week compared to 10-week specimens had respective values of 0.75 ± 0.24, 1.13 ± 0.33, 1.37 ± 0.70, 1.48 ± 0.28, 1.43 ± 0.36, 1.82 ± 1.05, 1.84 ± 0.56 and 2.26 ± 0.88. Murine-specific expression of genes indicative of host mouse vascularization (*RANK, type I collagen*) was detected in both allograft alone and periosteum-allograft samples. **Discussion**: Gene data confirm viable and productive periosteum in constructs after 20 weeks. Relatively higher fold change values of *RANK, RANKL* and *cathepsin K* indicate activities of osteoclast precursors, osteoclasts and osteoblasts involved in the allograft remodeling during implantation. All additional genes of interest indicate osteoblast activity in new bone matrix formation. Gene data are directly correlated with previous histology work. Extension of this study suggests autologous periosteum-allograft constructs could be utilized for healing bone defects.

Wednesday, October 30, 2013 Session 9

Proteomic analysis of skeletal organic matrix from the stony coral *Stylophora pistillata*

Jeana L. Drake[1*], Tali Mass[1], Liti Haramaty[1], Ehud Zelzion[2], Debashish Bhattacharya[1,3], Paul G. Falkowski[1,2,3], [1]Institute of Marine and Coastal Sciences , [2]Department of Ecology, Evolution, and Natural Resources, and [3]Department of Earth and Planetary Sciences, Rutgers University, New Brunswick, NJ, USA

Introduction: It has long been recognized that a suite of proteins exists in coral skeletons that is critical for the oriented precipitation of calcium carbonate crystals, yet these proteins remain poorly characterized. Using liquid chromatography-tandem mass spectrometry analysis of proteins extracted from the cell-free skeleton of the hermatypic coral, *Stylophora pistillata*, combined with a draft genome assembly from the cnidarian host cells of the same species, we identified 36 coral skeletal organic matrix proteins. The proteome of the coral skeleton contains an assemblage of adhesion and structural proteins as well as two highly acidic proteins that may constitute a unique coral skeletal organic matrix protein subfamily. We compared the 36 skeletal organic matrix (SOM) protein sequences to genome and transcriptome data from three other corals, three additional invertebrates, one vertebrate, and three single-celled organisms. This work represents a unique extensive proteomic analysis of biomineralization-related proteins in corals from which we identify a biomineralization **"**toolkit,**"** an organic scaffold upon which aragonite crystals can be deposited in specific orientations to form a phenotypically identifiable structure. **Purpose:** To determine the 'biomineralization toolkit' proteins retained in coral skeleton. **Methods:** After decalcifying clean coral skeleton in dilute HCl, TCA-acetone precipitated proteins were enzymatically digested and analyzed by LC-MS/MS. The data were searched against a draft gene model for *S. pistillata* using X! Tandem. Resulting proteins were blasted against NCBI and an in-house query database containing translated EST, transcriptome, and genome information for biomineralizers and non-biomineralizers. Presence of select proteins in SOM was confirmed by immunoblotting. **Results:** 36 predicted proteins were observed across six sequencing analyses; these included several collagens and cadherins, two novel coral acidic proteins (CARPs 4 and 5), and a carbonic anhydrase. Immunoblotting confirmed presence of several of these proteins in soluble and insoluble SOM. **Conclusions:** Although some proteins are common across calcium-bearing minerals, CARPs 4 and 5 are only found in Order Scleractinia (i.e. stony corals) and are members of a highly conserved CARP sub-family. Taken together, these 36 proteins constitute part of the biomineralization toolkit of Order Scleractinia. While almost certainly more proteins will be discovered in coral SOM, this initial set provides a basis for understanding the spatial relationships between the major components within the skeleton and how their relative expression influences rates of calcification. Supported by the U.S. National Science Foundation.

Crystal-Modulating Protein Films from Molluscan Nacre That Form Mesocrystalline Calcite Assemblies

Eric P. Chang*[1], Jennie A. Russ[2], Andreas Verch[3], Roland Kröger[3], Lara A. Estroff[2], John. S. Evans[1], Department of Basic Science and Craniofacial Biology – New York University[1], Department of Materials Science and Engineering – Cornell University[2], Department of Physics – University of York[3]

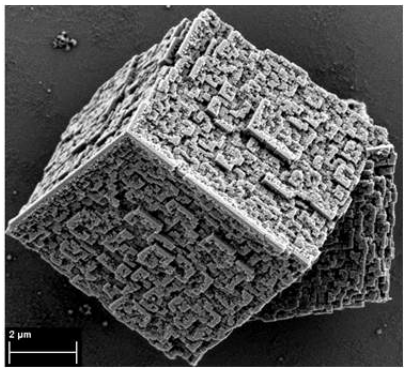

Introduction: AP7 is an intracrystalline, nacre-associated protein of the Pacific Red abalone (*Haliotis rufescens*) known to self assemble under in vitro mineralization conditions. When utilizing the $(NH_4)_2CO_3$ decomposition vapor method for producing $CaCO_3$, AP7 assemblies are known to stabilize aragonite and limit the growth of calcite. However, using solution-based experimental methods, precipitated films of AP7 unexpectedly promoted the growth of mesocrystalline calcite. **Purpose:** To structurally and chemically characterize novel mesocrystalline assemblies of calcium carbonate formed in the presence of AP7 protein films. **Methods:** Mineralization assays were conducted by mixing equal volumes of 20mM $CaCl_2$ x $2H_2O$ (pH 5.5) and 20mM $NaHCO_3/Na_2CO_3$ buffer (pH 9.75) in sealed polypropylene tubes and incubating at room temperature for one hour. Proteins were added to the calcium solution prior to the beginning of the reaction. The final pH of the reaction mixture was approximately 8.0-8.2. **Results:** The mixing of AP7 with the calcium solution caused the formation of an insoluble precipitate that was present throughout the duration of the mineralization reaction. Physical analysis of the crystals formed through this reaction by X-ray diffraction, electron diffraction, and Raman spectroscopy identified calcite as the primary product. SEM revealed unique morphologies of the calcite crystals appearing mesocrystalline in nature (insert). Elemental analysis of the mesocrystalline calcite shows the presence of sulfur arising from the Cys residues of the AP7 protein; however, it is unclear at this time how AP7 was associated with the mesocrystalline assemblies. **Conclusions:** The precipitation of the AP7 protein film prior to the onset of mineral nucleation, in conjunction with solution-based experimental conditions, caused the formation of mesocrystalline calcite. This result demonstrates that AP7 is a multifunctional protein capable of performing different tasks based on the conditions of the surrounding environment. Current studies are aimed at understanding the growth mechanisms that resulted in the intricately-

patterned mesocrystals formed in the presence of AP7 protein films. Portions of this work were supported by the U.S. Department of Energy under Award DE-FG02-03ER46099.

Meso-to-Nanoscale Structure and Mechanical Properties of Biogenic Crystals from Mollusks

Lara A. Estroff*[1], Stephan E. Wolf[1], Robert Hovden[2], Miki E. Kunitake[1], Hanying Li[1], Huolin Xin[3], Shefford Baker[1], David Muller[2]. [1]Department of Materials Science and Engineering, [2]Department of Applied and Engineering Physics, [3]Department of Physics, Cornell University, Ithaca, NY, USA.

Introduction: Biogenic calcite crystals are known to incorporate biomacromolecules and other organic molecules while still diffracting x-rays as single crystals. Such structures represent an interesting class of crystalline materials that can couple high surface areas with high degrees of long-range order. The formation mechanisms of these biominerals is still under debate. In addition, such biogenic crystals have been reported to have higher hardnesses and fracture toughnesses as compared to geologic calcite. **Purpose:** To compare the meso-to-nanoscale structure and mechanical properties of biogenic crystals from two different mollusks: *Pinna nobilis* and *Atrina rigida*. **Methods:** High angle annular dark field scanning transmission electron microscopy (HAADF-STEM) was used to examine thin sections of shell, prepared by either polishing or focused ion beam (FIB) milling. In both cases, multiple sections with different orientations with repect to the shell normal were prepared. Nanoindentation was used to determine the modulus and hardness of individual calcite prisms, indented on the {001} facet. **Results:** HAADF-STEM imaging reveals many interesting details of the internal structure of the calcite prisms and aragonite tablets as well as the transition zone between the prismatic and nacre layers. Both the prisms and the tablets have darker (corresponding to lower MW material) inclusions, which are identified as occluded macromolecules. Intriguingly, in the transition zone of *Pinna*, we observe fibrous structures (in cross-section) that appear to be forming the nacre tablets (Figure, right). These fibers correspond to more rod-like structures in the plane-view section. The hardness of both *Atrina* and *Pinna* prisms was greater than that of geologic control calcite, with *Pinna* slightly harder than *Atrina*. **Conclusions:** These results demonstrate the power of ADF-STEM imaging to reveal details about the nano-to-mesoscale structure of biominerals. In addition, insights provided by this work may help to elucidate the formation mechanism(s) and structure-property relationships of biogenic single crystals with incorporated organic material. Supported by the NSF.

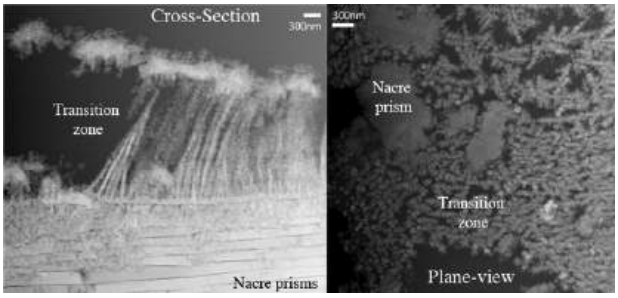

Microstructures, Phylogeny and Biomineralization Across the Regular Sea Urchins

Stuart R. Stock*, Dept. of Molecular Pharmacology, Northwestern Univ. Chicago, IL, USA

Introduction: Sea urchin teeth are an interesting biomineralization system because of the rich variety of structures within the teeth and the way in which the teeth reach high mineral density. Teeth of the regular sea urchins mineralize in two stages, the first stage consisting of arrays of plates and of needles/prisms and the second of columns (disks) that cement adjacent plates and prisms together. Each plate and needle/prism grows in an independent syncytial space, and very complex curvatures are routine and recapitulated in different individuals of a species. Mineral of both stages is calcite $Ca_{1-x}Mg_xCO_3$ with lower x in the first stage and higher in the second and diffract as single crystals. **Purpose:** To address the following unanswered questions: What defines the plate and prism orientations in their separate spaces and the microscopic morphologies of these tooth elements? What controls the very different geometry of tooth cross-sections? What triggers the change in calcite composition, and what determines the rate of column growth between plates? **Methods:** The above questions are studied with position-resolved x-ray diffraction, microComputed Tomography (microCT) and scanning electron microscopy (SEM). **Results:** X-ray diffraction of living teeth show single crystal calcite early in each tooth's growth, and these spatially-separate primary plates all possess the same crystallographic orientation. Further, diffraction shows that, from orders Cidaroida to Echinoida (across the phylogenic width of regular sea urchins), first and second stage minerals have the same crystallographic orientations and have a composition difference $0.20 < \Delta x < 0.30$. SEM demonstrates the second stage mineral grows from both adjacent plates, with a progression from small hemispheres to larger nodules with irregular surfaces to mesa-like structures joining the adjacent plates. Small hemispheres, nodules and mesas are often intermingled before columns grow laterally. Synchrotron microCT provides several quantitative measures. It measures how fast columns fill channels between adjacent plates and shows that growth is controlled by the flux of ions along the channels and slows dramatically when the columns block the channels. Numerical shape analysis of tooth transverse cross-section across Echinoidea reveals the expected phylogenic relationship between taxa. Observations of the transition from plumula to shaft suggest keel growth in Carinacea is governed by the presence of long prisms and geometrical constraint from the secondary plates. Finally, carinar process plate geometry differs quantitatively between families of Echinoida, and, if incorporated into numerical models, may provide mechanical insight into why some keels are short and broad and others long and thin. **Conclusions:** Microstructure provides important biomineralization insight but only in the context of tooth development and phylogeny. Support by NICDR DE001374 (to A. Veis); use of the Advanced Photon by US DoE, Office of

Sci., Office of Basic Energy Sci., Contract No. DE-AC02-06CH11357.

Sea Urchin Embryo Spicules: Buried Interfaces, Phase Transformations, and Mechanical Properties

C.-H. Wu,[1] R. Knapp,[1] C. Tester,[1] W. Gu,[2] D. Jang,[2] J. Greer,[2] and D. Joester*,[1]. [1] Department of Materials Science and Engineering, Northwestern University, Evanston, IL 60202; [2] Materials Science and Mechanics, Caltech, Pasadena, CA 91125.

Introduction: An important aspect of biomineral structure and function is the organic matrix that interacts with the forming mineral and is occluded during mineralization. The analysis of the role of matrix molecules has been a considerable challenge. For example, biomineralization in the sea urchin embryo results in single crystalline spicules with complex, branching shape and smoothly curving surfaces.[1] It has been shown that PMCs precipitate at least one transient amorphous phase that converts into the final biomineral.[2] The mechanism of the disorder-to-order transformation remains poorly understood. While the weight fraction of organics occluded in the final crystal is less than 0.5wt%, there are more than 200 different proteins present.[3] The role of these proteins is not known. We recently discovered that VEGF induces PMC to switch from linear growth along the calcite *c*-axis to triradiate growth parallel to the *a*-axes.[4] **Purpose.** To understand the role of proteins, individually and collectively, in modulating a) crystal growth direction; b) phase transformation kinetics; and c) mechanical properties. **Methods.** We use STEM-HAADF to investigate the distribution of organics in the biomineral after stimulation of PMC with different concentrations of VEGF. We investigate the evolution of order using Sr as a pulse-chase probe for X-ray absorption spectroscopy. Finally, we are developing a micro-mechanical three-point bending test to determine spicule mechanical properties. **Results.** There is clear evidence for preferential adsorption of proteins on specific crystallographic faces that are correlated with the spicule growth direction. At the same time, three-point bending tests of in vitro-grown single crystals indicate an important role of organics for the strength of the biomineral. Based on Sr K-edge XAS of cryo-frozen whole embryos, we propose a new model for the structural evolution from ACC to calcite.[5] **Conclusions.** The ability to stimulate and control the crystal deposition process with recombinant sea urchin VEGF *in vitro* sets the stage for an in depth analysis of a the spicule nano-composite. We are confident that in combination with knockdown experiments, our model system will enable unprecedented insights into the roles of protein in sea urchin embryo spicules. [1] F. H. Wilt, *Dev Biol 280*, (2005); [2] Y. U. T. Gong, C. E. Killian, I. C. Olson, N. P. Appathurai, A. L. Amasino, M. C. Martin, L. J. Holt, F. H. Wilt, P. Gilbert, *Proc. Natl. Acad. Sci. U. S. A. 109*, (2012); [3] K. Mann, F. H. Wilt, A. J. Poustka, P*roteome Sci 8*, (2010); [4] R. T. Knapp, C.-H. Wu, K. C. Mobilia, D. Joester, *J Am Chem Soc 134*, (2012); [5] C. Tester, C.-H. Wu, M. R. Krejci, L. Mueller, A. Park, B. Lai, S. Chen, C. Sun, M. Balasubramanian, D. Joester, *Adv Fun Mat*, (available online).

Influence of genetic selection and physical activity on bone properties of laying hens.

Alejandro B. Rodriguez-Navarro1, Heather McCormack2, Ian Dunn2, Julia Romero-Pastor1, Pedro Alvarez-Lloret1. 1Departamento de Mineralogía y Petrología, Universidad de Granada, 18002 Granada, Spain. 2Roslin Institute and Royal (Dick) School of Veterinary Studies, University of Edinburgh, Easter Bush, Midlothian, EH25 9RG, Scotland, UK.

Introduction: Laying hens are an interesting model for osteoporosis development studies. During the egg laying period, hens need to mobilize large amounts of calcium for eggshell formation. They cease forming cortical bone and start forming medullary bone which is used as a temporary storage of calcium. During eggshell formation, hens reabsorb medullary bone to release calcium need for the calcification of the eggshell. However, cortical bone reabsorption also occur which is gradually replaced by less organized and structurally weaker medullary bone. As a consequence of intensive egg production, laying hens can develop a severe form of osteoporosis. On the other hand, bone is a living tissue that responds to mechanical stimuli during physical exercise by stimulating bone growth and remodeling. Purpose: To determine how selective breeding and different levels of physical activity modify the structure and composition of bone and in turn its mechanical properties. Methods: Two White Leghorn lines were generated by divergently selecting hens based on high or low bone strength. Hens from both lines were raised either in cages with restricted movement or in aviaries to allow unrestricted physical exercise. The structure and composition of cortical and medular bone were characterised by 2D X-ray diffraction (2D-XRD) and infrared spectrometry (FTIR). Results: The type of housing has a great influence on bone properties. The aviary housed birds had stronger bones than cage birds due to a larger amount of cortical bone. FTIR analyses of bone showed that the aviary birds have a bone composition with a higher carbonate content and a higher collagen to phosphate ratio, indicative of an increased degree of bone remodeling. The cage birds of the low bone strength line have a composition indicative of decreased bone remodeling. Also in this line, bone mechanical properties are positively correlated to the degree of mineralization of medullary bone. 2D-DRX analysis showed that the cortical bone of caged birds have a higher degree of crystal and collagen fiber alignment than that of aviary birds. In both groups, the degree of crystal and collagen fiber alignment in cortical bone is negatively correlated with mechanical bone properties. Changes in bone properties evidenced the environmentally-induced plasticity of bone in laying hens. Conclusions: Our results indicate that genetic selection and physical exercise have a strong influence on bone metabolism and structural organization of bone in both lines. Housing in aviary systems promotes bone growth and remodeling. Structural organization of crystal and collagen fibers in cortical bone determines the mechanical properties of bone with stronger bones having a lesser orientation. Medullary bone contributes to bone strength only when present at greater amounts as in the case of cage birds.

Supported by Ministerio de Ciencia y Tecnologia (Spain).

Thursday, October 31, 2013 Session 10

Tensile force in collagen induced by osmotic pressure.

A. Masic, L. Bertinetti, R. Schuetz, H. Metzger, P. Fratzl, Department of Biomaterials, Max Planck Institute of Colloids and Interfaces, Research campus Golm, Potsdam, Germany;

Introduction: The collagen fibril is the fundamental structural building block for various types of tissues such as skin, tendon and bone. Its characteristic hierarchical structure allows for a variety of mechanical functions. In bone for example, it is known to interact with mineral to provide the stiffness and strength of bone tissue. Water is the third most important component adding up to 10% by mass even in fully mineralized tissue. Dry tissue is known to be stiffer and more brittle than hydrated tissue, but in general very little is known about the mechanical role of water in collagenous tissues. In this study, we explored effects of water on molecular and macroscopic behavior of collagen in rat tail tendon and cortical bovine bone by Raman and synchrotron x-ray scattering experiments during simultaneous control of hydration, temperature and force. **Methods:** The effects of hydration on backbone conformation in rat tail tendon were monitored by Raman scattering, while changes in triple helix parameters (radius, pitch and lateral spacing) were measured using synchrotron X-ray diffraction. At mesoscopic scales, small angle x-ray scattering revealed hydration dependent changes of the collagen staggering period (D) and of the relative lengths of gap and overlap in the fibrils. Macroscopic deformation and the forces generated were measured by a custom built micromechanical tensile tester in both tendon and bovine cortical bone. **Results:** Our results show that the interaction of the collagen molecule with water affects the structure of collagen at all hierarchical levels. Most of the vibrational modes of collagen change during drying which indicates that water not only modifies the chemical environment of the triple helix but also induces conformational changes. This is confirmed by the WAXS analysis of the triple helix reflections, showing that the distribution of helix pitches becomes broader with an average shortening of about 1% upon dehydration. At the fibril level, a decrease of 2.5% in the D period is measured under the same conditions. This is accompanied by a dramatic change in the gap/overlap lengths as measured from the intensity ratios in the 1^{st}, 2^{nd} and 3^{rd} order reflections of the axial staggering. If the tendon is not allowed to strain during drying, stresses up to 80 pN/molecule are measured, several tenfold the force generated by a myosin molecule in human muscle. Similarly large stresses were also found in fully mineralized bone tissue. **Conclusions:** This study shows that water plays a crucial role in stabilizing the structure of the collagen molecule and probably is an essential and active part of the protein unit. Its removal results in conformational changes of the collagen molecule, which is effectively shortened, producing large tensile stresses. This force generation is already significant at relatively low osmotic pressure changes which might occur even inside a fully hydrated environment, such as occurring in-vivo.

The High Resolution Xray Crystal Structure of Bovine 3 Glu Osteocalcin

Terry L. Dowd1, Vladimir Malashkevich2 and Steven Almo2, 1Department of Chemistry, Brooklyn College of CUNY, Brooklyn, NY, 2Dept. of Biochemistry, Albert Einstein College of Medicine, Bronx, N.Y.

Introduction: The 3 Glu form of osteocalcin is increased in serum during low Vitamin K intake or oral anticoagulant use (warfarin). Previous reports show it binds with lower affinity to bone mineral, is not a mineralization inhibitor and is less structured than 3 Gla Ca2+-osteocalcin as shown by circular dichroism. Recent studies have suggested a role for 3 Glu-Ost or 2 Gla-Ost as potential regulators of glucose metabolism. Animal and cell based studies report 3 Glu-Ost increased pancreatic β-cell proliferation, insulin secretion and insulin sensitivity. A G-protein coupled receptor, GPCR6a found in the pancreas and other tissues, was identified as the putative osteocalcin receptor. The 3 Glu-Ost can provide a useful model for Osteocalcin-mineral interactions and Osteocalcin-cell receptor interactions. No high resolution structure has been reported for this molecule. Purpose: To determine the high resolution structure of bovine 3 Glu-Ost, using x-ray crystallography, which may aid in understanding the lower affinity interaction with hydroxyapatite as well as molecular interactions between 3 Glu-Ost and 3 Gla Ca2+ - Ost with the GPCR6a receptor. Methods: Bovine osteocalcin was extracted from bone powder, purified and thermally decarboxylated using previously published methods. The protein, dissolved in 20 mM NaCl and 10 mM CaCl2, was concentrated to 13.3 mg/ml. Diffraction quality crystals were grown using vapour diffusion against a reservoir containing 2.5 M ammonium sulfate, 0.1 M Bis-Tris and propane at pH 7.0. Diffraction data were collected with 1.08 Å resolution on the X29A beamline (synchrotron light source, Brookhaven). The crystal structure was solved using the molecular replacement method with the structure of porcine osteocalcin as a starting model. Results:, The final refined structure contained residues 17-47 and consisted of 3 □-helices surrounding a hydrophobic core and a disulfide bond C23-C29 between the 3 helices. The bovine 3 Glu-Ost structure had no Ca2+ ions bound and contrary to previous reports, had a very similar structure to that reported for porcine 3 Gla Ca2+-Ost (97% sequence identity res. 17-47). Thus the helical structure of 3 Glu-Ost is independent of Ca2+ as opposed to 3 Gla-Ost which requires millimolar Ca2+ concentrations to form a similar conformation. Conclusions: Since the 2 structural forms were similar the lower affinity interaction with bone is most likely due to lower number of Ca2+ coordinating ligands on 3 Glu-Ost. Possibly the GPCR6a receptor may respond to helical osteocalcin. Reports show 3 Gla-Ost stimulates GPCR6a in the presence of Ca2+

with maximum stimulation at 5 mM, the concentration required for maximum □-helical conformation. The 3 Glu- Ost was shown to stimulate the GPCR6A receptor in pancreatic cells. In-vivo, with serum [Ca2+] =1 mM, helical 3 Glu-Ost may stimulate GPCR6a more strongly than 3 Gla-Ost and this may shed light on its role in glucose homeostasis.

Osteopontin as a Novel Substrate for Proprotein Convertase 5/6 (*PCSK5*) in Bone

Betty Hoac,*[,1] Delia Susan-Resiga,[2] Rachid Essalmani,[2] Edwidge Marcinkiweicz,[2] Nilana M.T. Barros,[3,4] Nabil G. Seidah[2] and Marc D. McKee[1,5]. [1]Faculty of Dentistry, McGill University, Montreal, QC, Canada, [2]Laboratory of Biochemical Neuroendocrinology, Clinical Research Institute of Montreal, Montreal, QC, Canada, [3]Departamento de Biofísica, [4]Departamento de Ciências Exatas e da Terra, Universidade Federal de São Paulo, Diadema, SP, Brazil, [5]Department of Anatomy and Cell Biology, Faculty of Medicine, McGill University, Montreal, QC, Canada.

Introduction: Seven proprotein convertases (PCs) cleave the basic consensus sequence K/R-X_n-K/R↓ (where n = 0, 2, 4 or 6 variable amino acids) to activate precursor proteins. Despite similarities in substrate specificity, basic amino acid-specific PCs have a distinct tissue distribution allowing for enzymatic actions on tissue-resident substrates. The proprotein convertase PC5/6 (*PCSK5*) exists as soluble PC5/6A or membrane-bound PC5/6B isoforms. *Pcsk5* is highly expressed in mouse bone development, but cellular localization and a substrate for PC5/6 have not been described in this tissue. *Pcsk5*-knockout mice die at birth with a bone phenotype that includes small size, retarded ossification and additional thoracic segments and ribs. Osteopontin (OPN) is an abundant bone extracellular matrix protein with roles in mineralization, cell adhesion and migration, and it has two consensus sequence sites for cleavage by PC5/6A which might modify its functions. **Purpose**: To determine whether OPN is a substrate for PC5/6A. **Methods**: *In situ* hybridization was performed on sections of normal mouse bone using *Pcsk5, Opn/Spp1* and *Dmp1* anti-sense and control sense cRNA probes. Quantitative RT-PCR for *Pcsk5* was performed on mouse RNA extracts from the osteoblastic MC3T3-E1 cell line and from primary osteoblast and osteoclast cultures. Enzyme-substrate assays using recombinant human PC5/6A and OPN were performed along with gel electrophoresis to visualize cleavage products. Immunoblotting for OPN was performed after SDS-PAGE of long-bone extracts from *Pcsk5*$^{\Delta 1/\Delta 1}$ (knockout) E18.5 embryos and wild type (WT) littermates. E18.5 embryos were also analyzed by micro-computed tomography. **Results**: *In situ* hybridization and quantitative RT-PCR showed expression of *Pcsk5* and *Dmp1* in bone-forming cells (similar to *Opn* expression) but not in osteoclasts. Cell-free *in vitro* digestions showed that PC5/6A efficiently cleaved OPN. Consistent with this finding, immunoblotting of mouse bone extracts confirmed an OPN fragment appearing at ~15 kDa in WT bone that was not present in PC5/6-deficient bone. By micro-computed tomography, PC5/6-knockout embryos had delayed skeletal mineralization. **Conclusions**: We show that *Pcsk5* is expressed in OPN- and DMP1-producing bone-forming cells, and that OPN is a novel substrate for PC5/6A. Cleavage of OPN by PC5/6A could modify the function of OPN in bone leading to the bone phenotype, and/or it could contribute to downstream sequential processing of OPN by other enzymes. *Supported by CIHR.*

IPV-like Motif in Secreted Acidic Proteins of Many Species Enables Rapid Exit from the Ca^{2+}-rich ER.

Zofia von Marschall, Anna S. Nam, Larry W. Fisher*. NIDCR, NIH, Bethesda, MD, USA.

Introduction: Most of the proposed extracellular biomineralization processes include the secretion of proteins that interact with mineral ions and/or mineral surfaces. Typically these proteins are acidic or have acidic domains that interact with multivalent cations in the extracellular environment. We have recently shown that >95% of the DSPP mutations that cause nonsyndromic genetic dentin diseases start their dominant negative affects by failing to rapidly exit the endoplasmic reticulum (ER). Two distinct classes of mutations cause the retention: 1) introduction of a membrane-association domain into the normally hydrophilic protein; 2) changes in the first 3 amino acids of the mature protein (Isoleucine-Proline-Valine, IPV) resulting in failure of the DSPP to interact with a hypothesized cargo receptor responsible for the rapid transit out of the ER. **Proposal**: We propose that most acidic, Ca^{2+}-binding proteins challenge the cells' mechanisms for trafficking through the various subcellular compartments (ER, Golgi, secretory vesicles) due to the presence of mM Ca^{2+} within the lumen of these structures. These proteins include ones associated with mineralizing matrices as well as any acidic protein with multiple Ca^{2+}-binding sites that, if permitted to accumulate to critical levels in any Ca^{2+}-rich environment, will form aggregates. Such aggregates would directly result in reduced secretion of these proteins and probably also result in ER stress as well as other cell responses that could change normal cell functions. We propose that an amino terminal IPV-like motif (ϕ-Pro-ϕ or ϕ–Pro-polar but not charged) is necessary for proteins to interact with this cargo receptor and be rapidly trafficked to the Golgi. **Methods**: Search available genomic databases as well as the literature for acidic, secreted proteins with IPV-like motifs immediately carboxy terminal to the leader sequence and note if motif is conserved across species. Express normal and IPV mutant proteins and observe relative efficiency of trafficking. **Results**: We found the IPV-like motif at the predicted amino terminus of many acidic proteins made in the mineralizing or nonmineralizing tissues of many species that included vertebrates, echinoderms, mollusks, and yeast. While we often focused on acidic proteins reported associated with mineralizing structures, proteins associated with hormones and their storage/secretion, digestion, blood functions, as well as milk and other secreted fluids started with variations of the motif. Interestingly Ca^{2+}-binding proteins meant to be retained in the ER often started with negatively charged amino acids at their amino terminus and

mutation of the IPV motif to include an aspartic acid caused normally secreted proteins to traffic out of the ER much less efficiently. **Conclusions**: The rapid trafficking of multivalent cation-binding proteins out of the ER before they form Ca^{2+}-driven aggregates is important not only for mineral-associated proteins but appears to be conserved for many other acidic proteins secreted by soft tissues. Supported by IRP of the NIH, NIDCR.

Bones and Stones- Why are Inhibitory Proteins Involved in Both?

Douglas Rodriguez[1], Archana Chidambaram[1], Saeed Khan[2], Laurie Gower*[1]. [1]Department of Material Science and Engineering, [2]Department of Pathology, University of Florida, Gainesville, FL, USA.

Introduction: Acidic proteins are commonly found to be intimately associated with biominerals, ranging from the calcium carbonate in the exoskeletons of invertebrates, to the calcium phosphate (CaP) in vertebrate bones and teeth, to the calcium oxalate and phosphate in kidney stones. For many years scientists characterized such proteins as being either inhibitors or promoters of crystal growth. Things became more complicated when researchers realized that this inhibitory/promotory activity often depends on whether they are in soluble form or bound to a surface, or their degree of phosphorylation, or the degree of enzymatic cleavage. Things became even more interesting when the field began to realize that many of these biominerals are formed from an amorphous precursor, so the role of these acidic proteins needed to be re-evaluated. Our group proposed that the role of these acidic proteins might be to act as a process-directing agent to promote the formation of a hydrated amorphous precursor called a polymer-induced liquid-precursor (PILP) phase, which is one mechanism by which mineral can be molded and shaped into an endless array of non-equilibrium morphologies. **Purpose:** In this talk, I will discuss the possible role(s) of osteopontin (OPN) in biomineralization, which historically has a confusing assortment of literature relating to its inhibitory or promotory activity. **Methods:** A variety of collagen-based scaffolds have been mineralized with OPN additive, including reconstituted collagen sponges, demineralized bone and dentin, and decellularized porcine bladder. The reactions were performed in the presence of OPN, with comparison to polyaspartate, a polypeptide known to induce the PILP process, and with a negative control of no polymer, where the mineralization occurs via the classical crystallization process. **Results:** The OPN was found to be highly effective at achieving intrafibrillar mineralization, and with faster kinetics than polyaspartate, leading to nanostructures found in bone and dentin. In addition to being a non-collagenous protein associated with bone, OPN is also found to be intimately associated with kidney stones. So our recent work in emulating stone formation will be discussed, which includes the first stage of stone formation, the mineralization of interstitial tissue with CaP to form Randall's plaque, to the second stage of stone formation, the overgrowth of plaque with calcium oxalate mineral. **Conclusions:** This work demonstrates that it is the inhibitory activity of OPN that can aid in the intrafibrillar mineralization of collagen, as well as concentrically laminated concretions, as found in stones. The talk will conclude with our hypothesis on the possible role of OPN in the formation of these pathological precipitates, which hopefully ties together some of the perplexing issues regarding the involvement of "inhibitory" proteins in both bones and stones.

Dentin Phosphoprotein Binds Annexin 2 and is Involved in Calcium Transport in Rat Kidney Ureteric Bud cells:

Keith Alvares[#1], Paula H. Stern[*] and Arthur Veis[#]. Departments of Cell and Molecular Biology[#] and Molecular Pharmacology and Biological Chemistry[*], Feinberg School of Medicine, Northwestern University, Chicago, IL. 60611

Introduction: Dentin Phosphophoryn (DPP) is a highly phosphorylated serine- and aspartic acid-rich protein. DPP contains 35 to 45 residue % aspartic acid and 40 to 55 residue % serine, of which as many as 90% of the serine residues are phosphorylated. Dentin Phosphoprotein is the most abundant non-collagenous protein in the dentin, where it plays a major role in the mineralization of dentin. However in addition to being present in the dentin, we and others have shown that DPP is also present in non-mineralizing tissues like the kidney, lung and salivary glands, where it conceivably has other functions. **Purpose**: To determine the functions of DPP in non-mineralizing tissues. **Methods**: We expressed phosphorylated DPP in the baculovirus system. Baculovirus synthesized DPP was linked to Sepharose and used to isolate DPP binding proteins from rat ureteric bud cells (RUB1). The proteins isolated were identified by MS/MS analysis and confirmed by western blots. Association of DPP with the isolated proteins was demonstrated by co-immunoprecipitation and co-localization in RUB1 cells and embryonic rat kidney using immunofluorescence analysis. Calcium uptake studies were performed by suspending the cells in calcium free buffer and then raising the calcium concentration to 2 mM, either with or without the prior addition of ionomycin, using a Perkin-Elmer LS5 luminescence spectrophotometer for fluorometric determination. **Results:** Two major bands at ~76 and 40 kDa were isolated when the RUB1 cells solubilized membrane fraction was passed over a DPP-Sepharose column. MS/MS analysis identified these two bands as Annexin 2 and 6 with greater than 95% accuracy by Mascot. This was confirmed by western blots. DPP was also present in the immunoprecipitate brought down by anti-annexin 2 antibody. Immunofluorescence studies show that Annexin 2 and DPP co-localize in the RUB1 cells. In addition DPP and annexin 2 also colocalize in the ureteric bud branches of embryonic metanephric kidney. In the RUB1 cells and ureteric bud branches of embryonic kidney, co-localization was restricted to the cell membrane. Studies on calcium influx into RUB1 cells show that in the presence of anti-DPP, there was a 40% reduction of calcium influx into these cells either with or without the prior treatment with ionomycin. **Conclusions**: The results indicated that in the rat ureteric bud cell line and embryonic kidney tissue, DPP is associated with annexin 2 along the cell membrane. We hypothesize that DPP has different functions in the kidney as compared to the odontoblasts. In the odontoblasts, its primary

function is in the extracellular mineralization of dentin, while in the kidney it may participate in calcium transport by forming complexes with annexin 2. Supported by NIH Grant DE001374 (to A.V.)

Binding Affinity and Effect on Hydroxyapatite Mineralization of the Enamel Protein Amelotin

Nastaran Abbarin*, Symone San Miguel, James Holcroft, Bernhard Ganss
Matrix Dynamics Group, Faculty of Dentistry, University of Toronto, Toronto. ON, Canada

Introduction: We have recently identified amelotin (AMTN), a novel protein that is specifically expressed during the maturation stage of dental enamel formation. It is located at the interface between enamel mineral and the apical surface of ameloblasts. Transgenic mouse models developed in our lab, which overexpress or lack AMTN, have shown specific defects in the structure and organization of the enamel hydroxyapatite (HA) microstructure. Thus, one of the biological roles of AMTN may be to regulate HA mineralization directly. **Purpose:** The first goal of this study was to determine the binding affinity of recombinant human AMTN protein to hydroxyapatite. The second goal was to study the effect of recombinant AMTN protein on the kinetics of calcium phosphate mineral formation *in vitro* and to determine shape and phase of calcium phosphate mineral deposits. **Methods:** Recombinant human AMTN protein was expressed in *Escherichia coli* cells and affinity purified to near-homogeneity. Protein adsorption experiments were carried out on synthetic hydroxyapatite powder using the "Langmuir isotherm equation". About 90µg/ml AMTN was added to a modified SBF solution (molar ratio Ca/P=1.67 and physiological pH) and incubated at 37°C for 48hours. Calcium phosphate deposits were then imaged using SEM and the mineral phase analyzed by electron diffraction. Phosphorylated osteopontin from bovine milk (OPN) and myoglobin from equine heart (MG) were used as positive and negative controls, respectively. **Results:** Adsorption isotherms of the proteins used in this study on HA showed an excellent fit with the Langmuir model (N=30, R^2 =0.97 for AMTN). The adsorption affinity of AMTN for HA binding sites was determined to be $4.15*10^5$ M^{-1}, lower than that of phosphorylated OPN, but higher than that of myoglobin. The maximum number of adsorption sites on HA among the three proteins was the highest for AMTN molecules ($5.98*10^{-8}$ mol/m^2). Our in vitro crystallization and electron diffraction results indicate that AMTN accelerated hydroxyapatite formation significantly. While extensive mineral precipitation was observed in the presence of AMTN, control experiments using OPN or MG or without addition of protein did not show any mineral precipitation from the buffer after 48 hours. **Conclusion:** These findings suggest a direct interaction between AMTN and HA at the enamel surface during the final stages of enamel formation, and during enamel mineralization. The induction of hydroxyapatite precipitation *in vitro* and the effect of AMTN overexpression on the enamel microstructure *in vivo* may indicate a role for AMTN in establishing the densely mineralized, aprismatic surface enamel. Supported by the Canadian Institutes of Health Research (CIHR) and the National Science and Engineering Research Council (NSERC) of Canada.

DSP-PP Precursor Protein Cleavage

Robert T. Yang[‡1], Glendale L. Lim[‡1], Zhihong Dong[‡], Arthur M. Lee[‡], Colin T. Yee[‡], Robert S. Fuller[§], and Helena H. Ritchie[‡*‡]*Department of Cariology, Restorative Sciences and Endodontics, School of Dentistry and the* [§]*Department of Biological Chemistry, School of Medicine, University of Michigan, Ann Arbor, Michigan 48109*

Introduction: Mineralizatin of dentin requires the two highly acidic proteins dentin sialoprotein (DSP) and phosphophoryn (PP) that are produced by proteolytic processing of a common secreteory precursor, DSP-PP, by cleavage at a single site. Because of the difficulty of obtaining sufficient DSP-PP from mammalian cells and dentin matrix, chemical evidence that G_{447}^D_{448} is the DSP-PP cleavage site has been elusive. Moreover, only Western blot analyses substantiate the claim that bone morphogenic protein 1 (BMP1) can correctly cleave DSP-PP. **Purpose:** To use baaculovirus expression system and Sf9 cells to obtain chemically identifiable amounts of DSP-PP;to determine the exact site at which baculovirus-expressed DSP-PP is cleaved; to identify the endogenous DSP-PP processing activity expressed by Sf9 cells; and to determine whether mutation of conserved residues near and distant from the cleavage site can affect cleavage. **Methods:** A baculovirus expression system was used to express human DSP-PP240 protein. MALDI-TOF/TOF and Edman degradation were used to determine the N-terminal sequence of the PP240 cleavage product. Point mutations were generated to test their effects on DSP-PP protein cleavage. **Results:** When expressed in Sf9 cells using a baculovirus vector, rat DSP-PP_{240} was accurately cleaved into DSP and PP_{240} after secretion into the medium by a Zn-dependent activity secreted by Sf9 cells. The cleavage site was identified by tandem MS analysis of the C-terminal cleavage product, PP_{240}, as occurring between G_{447} and D_{448} in the P4-P4' sequence SMQG^DDPN. The expression of a *Spodoptera frugiperda*Tolloid Related-1 Protein (TLR1) mRNA correlated with the expression of the DSP-PP_{240} processing activity, suggesting that this BMP1 homolog was responsible for DSP-PP_{240} cleavage. Recombinant human BMP1 also accurately cleaved the baculovirus-expressed precursor, further supporting the role of BMP1 in DSP-PP processing. Mutation of conserved residues near and distant from the SMQG^DDPN processing site had dramatic effects on the efficiency of DSP-PP_{240} processing both by the Sf9 cell activity and by recombinant BMP1. **Conclusions**: This is the first direct evidence that G447^D448 is the DSP-PP processing site. Comparison of a partial cDNA clone corresponding to the catalytic domain of Sf9 TLR1 to the crystal structure of BMP1 demonstrated that residues lining the substrate binding cleft are perfectly conserved, helping to explain why the Sf9 activity so efficiently processed the human precursor. The effects of mutations of conserved residues outside those immediately adjacent to the cleavage site suggests that exosite recognition is important for correct processing. This work was supported by NIDCR DE18901 to HHR.

Phosphorylation-dependent incorporation of osteopontin peptides into calcium oxalate crystals

Jared S. Gleberzon[2], Bernd Grohe[1], Harvey A. Goldberg[1,2] and Graeme K. Hunter*[1,2]
[1]School of Dentistry and [2]Department of Biochemistry, University of Western Ontario, London, Canada

Introduction: Our previous studies have shown that synthetic phosphopeptides based on sequences in osteopontin (OPN) adsorb to and decrease the growth of calcium oxalate monohydrate (COM) crystals. However, residual crystal growth results in the incorporation of adsorbed peptide into the COM lattice, with consequent loss of inhibition. Understanding the relationship between adsorption and incorporation will be important in the design of peptide-based reagents to treat ectopic calcification.
Purpose: To determine the factors governing adsorption of OPN peptides to, and incorporated into, COM crystals.
Methods: Peptides P0 (SHESTEQDAIDSAEK), P1 (SHESTEQDAIDpSAEK) and P3 (pSHEpSTEQDAIDpSAEK) were labeled with the fluorescent dye AlexaFluor-488 (green) or AlexaFluor-555 (red). For adsorption studies, COM crystals were grown for 20 h prior to addition of various concentrations of AlexaFluor-488-labelled peptides and incubation for a further 1 h. Bound and free peptide were then quantified by fluorimetry. For incorporation studies, a similar protocol was used, except that peptides were added to crystals during the initial 20-h incubation. Binding and incorporation data were fitted to one-site binding curves to calculate maximum amounts of peptide associated with COM. In addition, crystals grown in the presence of AlexaFluor-555-labelled peptide and then incubated with AlexaFluor-488-labelled peptide were examined by confocal microscopy.
Results: By fluorimetry, P0 exhibited minimal adsorption or incorporation. For P1, the maximum amounts adsorbed and incorporated were 0.081 and 10.3 ng/µg crystal, respectively. For P3, maximum amounts adsorbed and incorporated were 0.461 and 79.6 ng/µg, respectively. From crystals incubated with dual-labeled peptides, the following findings were obtained: P0 – weak adsorption to {100} and {121} faces; P1 – strong adsorption to {100} and {121} faces, incorporation into {100} faces; P3 – strong adsorption to and incorporation into {100} and {121} faces (see Figure).
Conclusions: OPN peptides adsorbing weakly to COM faces are not incorporated. P3 exhibits ~6-fold more adsorption to COM crystals than P1, and ~8-fold more incorporation. Incorporation of P3 into COM reaches a plateau when the peptide is ~8% (w/w) of the crystal. These studies suggest that net charge determines both the adsorption of acidic peptides to and their incorporation into COM crystals. Supported by the Canadian Institutes of Health Research.

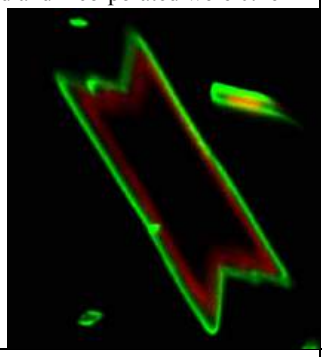

FAM20C Plays Critical Roles in Biomineralization

Xiaofang Wang, Mary Tandang, Gay Groppe, Jian Q Feng, Chunlin Qin. Texas A&M University Baylor College of Dentistry, Department of Biocmedical Sciences add Center for Craniofacial Research & Diagnosis.

Introduction: FAM20C is a molecule highly expressed in osteoblasts/osteocytes, odontoblasts and ameloblasts. In previous studies, we indicated that inactivation of FAM20C in mice leads to hypophosphatemic rickets and severe dental defects. Our studies also showed that FAM20C may regulate phosphate (Pi) homeostasis through direct mediation of FGF23 or via the mediation of DMP1. It remains unclear if the hypophosphatemia in the global *Fam20C*-KO mice significantly contributed to the dentin and enamel defects and if these defects were independent from each other or correlated through the reciprocal interaction between dental epithelium and dental mesenchyme. Recently, *in vitro* biochemical analyses identified FAM20C as a Golgi-enriched kinase that can phosphorylate SIBLING proteins. This kinase role of FAM20C has not been confirmed by *in vivo* approaches. Studies are also warranted to show whether FAM20C is the only kinase responsible for the phosphorylation of SIBLING proteins. **Purpose:** 1) To determine if the dental defects in *Fam20C*-KO (KO) mice are associated with hypophosphatemia and the reciprocal interactions between dental epithelium and dental mesenchyme. 2) To determine if *Fam20C*-KO mice had phosphorylation failure in SIBLING proteins. **Methods:** *Fam20C*-floxed mice were crossed with K14-Cre and Wnt1-Cre mice to specifically remove FAM20C from dental epithelium and dental mesenchyme, and the mineralization defects and changes in serum biochemistry in these mice were examined in comparison with WT and the universal knockout mice. Non-collagenous proteins (NCPs) were extracted from *Fam20C*-KO mice and the attached Pi to the phosphoproteins were determined. We separated SIBLING proteins from the NCPs with FPLC, and compared the SIBLING proteins between WT and *Fam20C*-KO mice with Stains-All staining and Western Immunoblotting analyses. **Results:** The K14Cre-mediated KO mice showed enamel defects, while the dentin, long bones, and serum Pi level were not significantly affected. The Wnt1Cre-mediated KO mice showed dentin defects, normal enamel, very mild defects in the long bone, along with a lower serum Pi level than normal but higher than that in the universal KO mice. NCPs in the KO mice had a lower phosphorylation level than in the WT mice. OPN extracted from *Fam20C*-KO mice had lower molecular weight and less Stains-All staining than normal. **Conclusions:** These results indicate that the dental defects in the *Fam20C*-KO mice are not associated with hypophosphatemia in the KO mice. . FAM20C is not involved in the reciprocal interactions between dental epithelium and dental mesenchyme. The NCPs from *Fam20C*-KO mice had lower level of phosphorylation than those from the WT mice.. OPN in the *Fam20C*-KO mice may have lower phosphorylation level than that in WT. FAM20C might be a primary kinase critical for the phosphorylation of SIBLING proteins.

Thursday, October 31, 2013 Session 11

Mineralization of dense collagen hydrogel scaffolds regulated by human dental pulp stem cells

Benjamin R. Coyac,*1,2,4,5 Florencia Chicatun,3 Betty Hoac,1 Valentin Nelea,1 Showan N. Nazhat,3 Catherine Chaussain,4,5 and Marc D. McKee1,2. 1Faculty of Dentistry, 2Department of Anatomy and Cell Biology, 3Department of Mining and Materials Engineering, McGill University, Montreal, QC, Canada, 4Faculty of Dentistry, Paris Descartes University, Montrouge, France, 5Odontology Department, Bretonneau Hospital, AP-HP, Paris, France

Introduction: While advances have been made in recent years on biomineralization, unanswered questions persist on bone- and tooth-cell differentiation, on outside-in signaling from the extracellular matrix, and on the link between protein expression and mineral deposition. Purpose: To validate the use of a bioengineered three-dimensional (3D) dense collagen hydrogel scaffold as a cell culture model to explore these questions. Methods: Dental pulp stem cells from human exfoliated deciduous teeth (SHEDs) were previously shown to display a highly proliferative capacity combined with the ability to differentiate into an osteo/odontogenic cell type. The bioengineering method of collagen hydrogel plastic compression was shown to produce dense scaffolds with increased mechanical properties and extracellular matrix-like characteristics. In the present study, SHEDs were seeded into an extracellular matrix-like collagen gel whose fibrillar density was increased through plastic compression. SHED viability, morphology and metabolic activity, as well as scaffold mineralization, were investigated over 24 days in culture. Additionally, measurements of alkaline phosphatase enzymatic activity, together with immunoblotting for mineralized tissue cell markers ALPL (tissue-nonspecific alkaline phosphatase), DMP1 (dentin matrix protein 1) and OPN (osteopontin) were performed. The mineral phase was analyzed by electron microscopy including electron diffraction and energydispersive X-ray spectroscopy, combined with Fourier-transform infrared spectroscopy and biochemical analyses (calcium and phosphate assays). Results: Our compressed collagen scaffolds sustained SHED cell viability throughout the gel. Alkaline phosphatase activity and the production of odonto/osteoblastic marker proteins over time demonstrated osteo/odontogenic cell differentiation coincident with accumulation of calcium and phosphate in the cultures. Our elemental analyses of the matrices were consistent with the formation of apatitic mineral in the scaffolds. The mineral phase was located in the extracellular matrix along collagen fibrils and as spherulitic mineral deposits, presumably resulting from radial expansion of originally smaller mineralization foci. Conclusion: Use of a 3D dense collagen scaffold promoted SHED osteo/odontogenic cell differentiation and mineralization. SHEDs behave similarly to rodent cell lines used previously showing cell differentiation, but with the important additional feature of now potentially allowing for the use of patient cells for clinical repair of osseous and dental defects. Bioengineered mineralized tissue repair strategies might also benefit from this work, as might patients having genetic disorders detrimentally affecting bone and dentin mineralization.

Intracellular Mechanism of Osteogenic Effect of Magnesium Ion on Bone Marrow Stromal Cells

Sayuri Yoshizawa* [1,2,4], Andrew Brown [1,2,3,4], Aaron Barchowsky[5], Charles Sfeir [1,2,3,4]
[1]Department of Oral Biology, [2]The Center for Craniofacial Regeneration, [3]Department of Bioengineering, [4]The McGowan Institute for Regenerative Medicine, [5]Department of Environmental and Occupational Health, University of Pittsburgh, Pittsburgh, PA, USA

Introduction: Biodegradable magnesium (Mg) alloys are currently under investigation for craniofacial and orthopedic bone fracture fixation due to their initial mechanical strength and high biocompatibility. The biological effect of these alloys on human bone marrow stem cells (hBMSC) is, however, not fully understood. **Purpose**: To assess the osteogenic effect of biodegradable Mg alloys on hBMSCs, we analyzed degree of extracellular matrix (ECM) mineralization by Alizarin red staining, comprehensive mRNA expression by quantitative PCR (qPCR) array, and protein expression by Western blotting in the presence of varying Mg^{2+} concentrations. **Methods**: hBMSCs were cultured for three weeks in α-MEM containing 5% FBS, with or without osteogenic factors (100nM dexamethasone, 50μM ascorbic acid, and 10mM β-glycerophosphate). Mg^{2+} concentration in the medium was adjusted to either 0.8 (physiological concentration), 5, 10, 20 or 50mM by adding $MgSO_4$ to culture medium. Extent of ECM mineralization was assessed using Alizarin red stain, quantified by dissolving Alizarin red into 10% CPC. Total RNA was extracted from the cells, and osteogenic marker expression was analyzed by qPCR array. The mRNA expression level of collagen type X mRNA (*col10a1*) was confirmed by qPCR. To further analyze the intracellular signaling pathway, mRNA expression of hypoxia-inducible factor-1α (*hif1a*) and *hif2a* (transcription factors of *col10a1*) was analyzed. Furthermore, the protein expression of collagen type X, vascular endothelial growth factor (VEGF), HIF-1α, HIF-2α, and peroxisome proliferator-activated receptor gamma coactivator 1-alpha (PGC-1α) of hBMSCs cultured in 0.8mM or 10mM $MgSO_4$ was analyzed by Western blotting. **Results**: Mineralization of ECM was significantly enhanced at 10mM of $MgSO_4$. PCR array data showed the significant increase of *col10a1* and insulin-like growth factor 2 mRNA (*igf2*) of hBMSCs cultured in 10mM of $MgSO_4$, and decrease of integrin alpha 3 mRNA (*itga3*) compared to the cells cultured in 0.8mM $MgSO_4$. The mRNA expression of *hif1a* and *hif2a* did not change in the 10mM $MgSO_4$, however, the protein expression was enhanced in 10mM $MgSO_4$. Moreover, protein expression of VEGF and PGC-1α was also enhanced at 10mM $MgSO_4$ compared to the cells cultured in 0.8mM $MgSO_4$.

Conclusions: These results indicate that Mg^{2+} (5-10mM) enhance the production of collagen type X and VEGF via activation of HIF-1α and PGC-1α expression. Mg^{2+} degraded from the bone fixation devices may promote the bone regeneration by enhancing the production of collagen type X and VEGF from osteogenic cells in fractured bone.

Dual functioning peptides encourage human bone marrow cell specific attachment to mineralized biomaterials

Harsha Ramaraju[1*], Sharon Segvich Miller[1], David H. Kohn [1,2] [1]Department of Biomedical Engineering, [2]Department of Biologic and Material Sciences, University of Michigan, Ann Arbor, MI, USA.

Introduction: Cell instructive mineralized biomaterials pose a promising alternative to conventional auto-, allo-, and xenograft therapies for the reconstruction of critical sized defects. In order to mediate cell specific interactions on biomineral surfaces, we identified a sequence with high affinity towards apatite (VTKHLNQISQSY) and clonally derived human bone marrow stromal cells (DPIYALSWSGMA) using phage display. Combining the sequences conserves dual-specificity to apatite surfaces and human bone marrow stromal cells. **Purpose:** Improve human bone marrow stromal cell specific interaction on apatite surfaces using high affinity dual-functioning phage derived sequences. **Methods:** Cell specific peptide sequences were identified by screening a12 mer Ph.D.12 Phage Display Library against clonally derived hBMSC (Passage 3-6), and analyzing sequences using the bioinformatics tool Receptor Ligand Contacts (RELIC) and immunohistochemistry. Mineral binding sequences were identified using a 12 mer Ph.D.12 Phage Display Library, computational modeling, RELIC, and *in vitro* binding assays. Cell binding (RGD) and mineral binding (E7) controls were also tested in conjunction with the single and dual functioning peptide affinity to cells and apatite. To assess affinity to apatite, Langmuir isotherms representing peptide binding affinity (K1) and monolayer adsorption concentration (Cm1) were constructed for each of the peptides under physiologically relevant conditions. HBMSC, MC3T3 and mouse dermal fibroblast (MDF) on biomimetic apatite functionalized with single and dual peptide sequences was evaluated using a centrifugal force of 300rpm for 5 min under physiologically relevant conditions. **Results:** Although charged and acidic residues are documented to interact with the HA crystal lattice, the predominantly charge neutral and hydrophobic dual peptide DPI-VTK had the highest binding affinity (K1) 198.3 ± 7.61 μM compared to 13 ± 2.13 μM of RGD-E7. Although RGD-E7 peptide had lower binding affinity to the apatite, (Cm1) at 328.9 ± 12.3 nmol/mm^2 whereas DPI-VTK has a packing efficiency of 30.2 ± 2.4 nmol/mm^2. Cell detachment assays demonstrated that DPI-VTK had the highest affinity towards HBMSCs with 25% more cells adhered than compared to controls. RGD-VTK and VTK encouraged 20% and 15 % more fibroblast attachment compared to no peptide controls while pre-osteoblast adhesion was unaltered. **Conclusions:** These results suggest that combining page derived apatite and cell specific sequences conserves their dual functionality. Material specific sequences can be used to control delivery of cell specific signals without constraining conformation through immobilization techniques. Interestingly, net charge, acidic residue content, and molecular weight of the peptides does not directly correlate with apatite binding affinity of these phage derived peptides. Understanding the properties that mediate apatite affinity and appropriate delivery of cell specific signals on mineralized materials can improve cell based tissue reconstruction strategies. Supported by NIH DE015411 & DE13380

Amelogenin-chitosan matrix forms an organized mineralized layer with a dense interface with enamel

Qichao Ruan[*1], Yuzheng Zhang[2], Xiudong Yang[1], Steven Nutt[2], Janet Moradian-Oldak[1]. [1]Center for Craniofacial Molecular Biology, [2]Mork Family Department of Chemical Engineering and Materials Science, University of Southern California, Los Angeles, CA, USA

Introduction: Enamel reconstruction is of significant interest in material science and dentistry as a novel approach for treatment of dental caries. During amelogenesis, the initial formation of organized crystals occurs in an amelogenin gel-like matrix. **Purpose:** Our objectives were 1) to investigate the interaction between chitosan and amelogenin, and 2) to re-construct enamel utilizing the amelogenin-chitosan (CS-AMEL) hydrogel system. **Methods:** Chitosan-amelogenin interactions were investigated by Circular Dichroism and Fluorescence spectroscopy. Two methods were designed to prepare the CS-AMEL hydrogel and to re mineralize enamel: (I) Ca^{2+} and HPO_4^{2-} were added into chitosan solution followed by addition of amelogenin; (II) Amelogenin and HPO_4^{2-} were mixed with chitosan, followed by addition of Ca^{2+} via diffusion. The complex hydrogel was applied onto acid-etched human tooth enamel surface, as a model for early carious lesions, prior to mineralization in artificial saliva. The mineral phases and morphologies of newly-grown layers on the enamel were characterized by X-ray diffraction and electron microscopy. The interface between the newly-grown layer and enamel was analyzed using a focused ion beam technique and TEM. The hardness and elastic modulus were tested with a nanoindenter. **Results:** The interaction between chitosan and amelogenin was pH dependent. At lower pH values, chitosan interacted with amelogenin through electrostatic interaction, whereas at pH higher than 5.5, the interaction was weak because of chitosan's low solubility and deprotonation. After mineralization in artificial saliva, organized fluoridated hydroxyapatite crystals were formed on the enamel surface treated by CS-AMEL hydrogel. Furthermore, both the hardness and modulus of etched enamel were markedly increased following remineralization with amelogenin. The repaired layer formed using Method I had better orientation and mechanical properties. In Method I, the Ca^{2+} and HPO_4^{2-} were added under a fixed supersaturation promoting the formation of amorphous calcium phosphate (ACP) in the CS-AMEL hydrogel. Amelogenin assemblies stabilized ACP clusters and guided their arrangement into linear chains. These amelogenin-ACP composite chains fused with enamel crystal and eventually evolved into enamel-like co-aligned crystals, anchored to the natural enamel substrate through a cluster growth process. The continuous growth of crystals formed an excellent bond between the

newly-grown layer and the enamel. **Conclusions:** Our studies introduce amelogenin-containing chitosan matrix as a promising biomaterial for enamel repair and demonstrate the potential of applying protein-directed assembly to biomimetic reconstruction of complex biomaterials.

Plithotaxis, a collective cell migration, regulates the sliding of proliferating pulp cells located in the root apical papilla niche.

Azumi Hirata[1], Sasha Dimitrova-Nakov[2], Hector Ardila[2], Stéphane Simon[3], Stéphane-Xavier Djole[3], Odile Kellermann[2], Michel Goldberg *[2]. [1]Osaka Med Univ, [2]Univ Paris Descartes & INSERM U747, [3]Univ.Paris Diderot & INSERM U 872.

Introduction: Pulp cells are mobile, and migrate from the central part of the pulp toward the lateral sub-odontoblastic cell layer. The cell transfer initially implicates lateral movements, and afterward, ascending cell sliding from the root to the crown. **Purpose & methods:** The aims of the present investigations were to identify the apical niche at the origin of proliferating stem cells, their fate and terminal differentiation. In order to shed some lights on these events, we investigated the structure and ultrastructure of resident pulp cells, and map their kinetic with the proliferating cell nuclear antigen (PCNA). **Results**: 1) **Histological findings:** Resident pulp cells are ciliated. As shown histologically, the cytoskeleton displays tall bundles of microtubules and numerous actin-containing microfilaments located along the plasma membrane and in close association with gap junctions. The cells are linked by desmosome-like and gap junctions, forming a syncytium-like structure, required for cell migration within a 3-D extracellular matrix (Friedl & Bröcker *Cell Mol Life Sci* 2000; Vincent et al., *Biotechnol J* 2013). There is no individual motility, pulp cells being moving collectively. In addition to thin collagen fibrils, glycosaminoglycans (C4S, C6S, DS, KS and hyaluronic acid) contribute to the viscosity of the intercellular matrix allowing cell migration. 2) **PCNA labeling:** In rats' molar, a pulp exposure initiate cells proliferation, and allows detecting zones of proliferating cells. We have identified two intensely labeled zones (zones I and II), located in the crown near the pulp exposure. Inflammatory and PCNA- positive cells were located in the same areas. In the apical zone (zone III), there were no inflammatory cells, but shortly after a pulp exposure, labeled cells proliferate in the apical cell-rich zone. When agarose beads were implanted within the pulp, a burst of PCNA positive cells was observed in the apical papilla mesenchyme. After implantation of beads loaded with stem cells or with bioactive molecules, the number of PCNA-positive cells was increased in the central part of the apical pulp. After eight days, PCNA-positive cells were present in the root beneath the odontoblast/sub-odontoblast layer. They became undetectable after 2 weeks in the root, but appeared to be exclusively located in the coronal pulp. **Conclusion**: We suggest that 1) firstly, the cells issued from the root apical part slide from the center to the lateral sub-odontoblastic area, then 2) secondly, PCNA-positive cells disappearing at day 15 from the root moved to the crown. Plithotaxis, implying a collective cell migration (Trepat & Fredberg, *Trends Cell Biol* 2011) seems to play a key role in the sliding of potential stem cells grouped within the apical niche. This is an emergent mechanism governing pulp healing and regeneration.

Differential responses of osteoblast lineage cells to nanotopographically-modified, microroughened titanium-aluminum-vanadium (TiAlV) alloy surfaces

Gittens RA*[,1], Olivares-Navarrete R[2], McLachlan T[3], Cai Y[3], Hyzy SL[2], Schneider JM[4], Schwartz Z[2,5], Sandhage K[3], and Boyan BD[2] , [1]Biomedical Instrumentation and Bioengineering Center, Instituto de Investigaciones Científicas y Servicios de Alta Tecnología (INDICASAT AIP), Panama, Panama; [2]Department of Biomedical Engineering, Virginia Commonwealth University, Richmond, VA; [3]School of Materials Science and Engineering, Georgia Institute of Technology, Atlanta, GA; [4]Titan Spine, Mequon, WI; [5]Department of Periodontics, University of Texas Health Science Center at San Antonio, San Antonio, TX.

Introduction: Higher failure rates of dental implants in challenging cases, such as in patients compromised by age and disease, are driving efforts to reduce healing times and improve osseointegration. Tailored surface microstructures of implants can promote osteoblast differentiation without use of exogenous growth factors. Recently, surface nanomodification has drawn much interest clinically. However, questions remain about nanostructure effects on human mesenchymal stem cells (hMSCs), one of the first cell types to infiltrate an implantation site. **Purpose:** To evaluate surface nanostructural effects on hMSC differentiation and local factor production in comparison to human primary osteoblasts (hOBs) using a novel nanomodified Ti alloy surface. **Methods:** Ti alloy (Ti6Al4V) samples were nanomodified at 740°C for 45m under air and characterized using SEM, XPS, LCM, and contact angle analyses. hMSCs and hOBs were cultured on smooth (sTiAlV), nanomodified smooth (NMsTiAlV), rough (rTiAlV), nanomodified rough (NMrTiAlV) disks, and tissue-culture polystyrene. Cell number, alkaline phosphatase, and production of osteocalcin, osteoprotegerin, and VEGF were assayed (mean ± SEM, n=6 cultures/variable, ANOVA/Tukey's modified Student's t-test). **Results:** The nanomodification treatment significantly increased surface nanoroughness and rearranged surface chemistry. hOB cell numbers were lower, and differentiation markers and local factor production were synergistically higher on NMrTiAlV compared to all other groups. For hMSCs, cell numbers were lower and differentiation markers were higher on rough samples compared to smooth, with no further enhancement produced by the superposition of nanostructures found on NMrTiAlV surfaces, except for higher production of the angiogenic factor VEGF. **Conclusions:** The results show that in the absence of any exogenous soluble factors, osteoblastic maturation of hOBs but not osteoblastic differentiation of hMSCs is strongly influenced by nanostructures superimposed onto a microrough Ti alloy surface. Our results suggest that the differentiation state of osteoblast-lineage cells determines the recognition of surface nanostructures and subsequent cell response, which has implications for clinical evaluation of new implant surface nanomodifications.

Abstracts for Poster Session- TUESDAY

Bond strength of dentin and bleach-treated enamel from two different AI mouse models.

Megan K. Pugach*[1,2], Fusun Ozer[1], Rajappa Mulmadgi[1], Yong Li[1], Cynthia Suggs[3], Ashok B. Kulkarni[4], John D. Bartlett[2], J. Timothy Wright[3], Carolyn W. Gibson[1], Rochelle G. Lindemeyer[1]. [1]School of Dental Medicine, University of Pennsylvania; [2]Mineralized Tissue Biology, The Forsyth Institute; [3]School of Dentistry, University of North Carolina; [4]NIDCR, NIH

Introduction: Amelogenesis imperfecta (AI) is a group of heterogeneous hereditary disorders that affects the structure and appearance of dental enamel. Adhesive restorations have shown high failure rates in areas of poorly mineralized AI enamel. To distinguish which cases of AI may have good clinical outcomes with bonded materials, we evaluated bond strength of enamel and dentin in mouse models, comparing wild-type (WT) with those having mutations in amelogenin (*Amelx*) and matrix metalloproteinase-20 (*Mmp20*), which mimic 2 forms of human AI, hypoplastic (HPAI) and hypomature (HMAI), respectively. Our previous study using a novel system to test shear bond strength (SBS) to mouse incisors showed that *Amelx*KO and *Mmp20*KO enamel surfaces had significantly different SBS from each other and that SBS was improved by using a self-etching (SE) bonding system instead of the traditional etch-and-rinse bonding system. Due to the increased organic content in HMAI enamel, we tested whether pretreatment of the bond interface with NaOCl would improve the adhesion to enamel. Furthermore, because HPAI and HMAI both have thin and poorly mineralized enamel, we tested the adhesion to underlying dentin. **Purpose:** To evaluate the influence of 5% NaOCl treatment on SBS of *Amelx*KO and *Mmp20*KO enamel and determine the SBS to dentin. **Methods:** *Amelx*KO and *Mmp20*KO genotypes were confirmed by PCR. Incisor enamel surfaces were treated with 5% NaOCl for 1 minute, followed by SE primer application. Incisor dentin surfaces were treated with the SE only. Composite inlay sticks were prepared with Clearfil Majesty Anterior (Kuraray, Japan) and bonded to enamel and dentin surfaces using Clearfil SE Bond. SBS was measured using a Micro-shear tester (Bisco, Michigan, USA). To analyze the phenotype of *Amelx*KO and *Mmp20*KO dentin, density and volume were evaluated by micro-CT, and mechanical properties determined by nanoindentation. Data were analyzed using ANOVA ($p<0.05$). **Results:** Treatment of KO and WT enamel with NaOCl prior to bonding with the SE system did not significantly improve enamel shear bond strength. SBS of *Amelx*KO and *Mmp20*KO dentin were not significantly different from WT. *Amelx*KO and *Mmp20*KO dentin displayed no differences in density from WT, and *Mmp20*KO volume was slightly higher than WT. Likewise, *Amelx*KO and *Mmp20*KO dentin demonstrated no differences from WT in elastic modulus, but *Amelx*KO dentin hardness was slightly decreased from WT. **Conclusions:** In patients with HPAI or HMAI enamel, removal of the thin layer of remaining enamel prior to dentin bonding may be a recommended treatment to prevent restoration failure.
Supported by DE019968, DE011089, DE016276 and DE022624.

Aggregatibacter actinomycetemcomitans Lipopolysaccharide Regulates Bone Sialoprotein Gene Transcription

Yorimasa Ogata*[1,2], Liming Zhou[1,3], Hideki Takai[1,2], Masaru Mezawa[1,2], Xinyue Li[1,4]. [1]Department of Periodontology, [2]Research Institute of Oral Science, Nihon University School of Dentistry at Matsudo, Chiba, Japan. [3]Anhui Medical University of Stomatology Hospital, Anhui, China. [4]Tianjin Stomatology Hospital, Tianjin, China

Introduction: Periodontitis is an oral infectious disease that may result in tooth loss. It is caused by Gram-negative anaerobic bacteria including Porphyromonas gingivalis (P. gingivalis), which is associated with chromic periodontitis, and Aggregatibacter actinomycetemcomitans (A. actinomycetemcomitans), which is associated with aggressive periodontitis characterized by a rapid bone loss. A. actinomycetemcomitans lipopolysaccharide (LPS) has a similar structure to E. coli LPS, and they are Toll-like receptor-4 agonists. Bone sialoprotein (BSP) is a mineralized tissue-specific protein that is highly expressed during the initial mineralization of bone. **Purpose:** To determine the molecular mechanism of A. actinomycetemcomitans LPS regulation of BSP gene transcription, we analyzed the effects of A. actinomycetemcomitans LPS on the expression of BSP in osteoblast-like ROS17/2.8 cells. **Methods:** To investigate the effects of A. actinomycetemcomitans LPS on BSP expression, we conducted Northern and Western blot, real-time PCR, transient transfection analyses with chimeric constructs of the rat BSP gene promoter linked to a luciferase reporter gene and gel shift assays. **Results:** Using ROS17/2.8 cells, we revealed that BSP mRNA levels were decreased by 0.1 μg/ml and increased by 0.01 μg/ml A. actinomycetemcomitans LPS at 6 h. Results of luciferase assays showed that 0.1 μg/ml decreased and 0.01 μg/ml A. actinomycetemcomitans LPS increased BSP transcription in -116 to +60 BSP construct. The effects of A. actinomycetemcomitans LPS were abrogated by triple-mutations in cAMP response element (CRE), FGF2 response element (FRE) and homeodomain protein-binding site (HOX). Tyrosine kinase, ERK1/2 and PI3-kinase inhibited the effects of A. actinomycetemcomitans LPS. Furthermore, 0.1 μg/ml LPS decreased CRE-, FRE- and HOX-protein complexes formation, whereas 0.01 μg/ml A. actinomycetemcomitans LPS increased the nuclear protein binding to CRE, FRE and HOX. Chromatin immunoprecipitation assays revealed increased binding of CREB1, JunD, Fra2 and c-Fos to a chromatin fragment containing the CRE, and Runx2, Dlx5 and Smad1 to the FRE and HOX by 0.01 μg/ml A. actinomycetemcomitans LPS. **Conclusions:** These studies indicated that 0.1 μg/ml suppressed and 0.01 μg/ml A. actinomycetemcomitans LPS increased BSP transcription mediated through CRE, FRE and HOX elements in the BSP gene promoter. Supported by a Grant-in-Aid for Scientific Research (C; No. 22592319), and a grant for Supporting Project for Strategic Research in Private Universities by the Ministry of Education, Culture, Sports, Science, and Technology, Japan (MEXT), 2008-2012.

Variations in the Bone Mineral Composition in Mouse Models of Osteogenesis Imperfecta: An FTIRI Study

Adele Boskey*,[1,2], Lyudmila Spevak[1], Cathleen Raggio[1,3], Marco Masci[2], Rhima Colema[4] . [1] Research Division and [3]Department of Orthothopaedics, Hospital for Special Surgery, New York, NY; [2]Weill Medical School of Cornell University, New York, NY; [4] Department of Biomedical Engineering, University of Michigan, Ann Arbor, MI

Introduction Osteogenesis Imperfecta, OI, is a rare, heterogeneous, genetic disease that is due to mutations leading to alterations in type I collagen structure or production, and is characterized by brittle bones. Depending on the mutation the collagen may be hypo- or hyper-mineralized. The disease is heterogeneous and the exact reason for the mineralization defects is uncertain. We hypothesize that alterations in collagen structure affect noncollagenous protein (NCP) binding to collagen and alter both mineral nucleation and growth. **Purpose**: To compare mineral variations in different mouse models of OI and obtain insight as to their origins. **Methods:** Fourier transform infrared imaging was used to measure relative HA, carbonate, and acid phosphate content, crystallinity, collagen maturity (XLR), and their spatial distributions in 6 different OI model tibias at various ages. Models studied were: 1) oim/oim, a naturally occurring mutant with a premature stop codon in colIa2 (2 & 6 mo), 2) Brtl/+ mouse with a knock-in mutation mimicking patients with Silence type IV OI (2&6 mo), 3) OOA mouse with mutation resembling that in a large population of old order Amish (2&6 mo), 4) PEDF KO mouse resembling mutation in type VI OI (3 mo), 5) osteopotentia KO (OPT,10 d) and 6) mutagenesis induced fro/fro mutation (3&6 mo). Data from fro/fro animals were already published (Coleman et al, Bone, 2012). Controls for each study were age- matched wild type liter mates. **Results:** In all OI mutant models studied, mineral to matrix (M/M) ratio exceeded that of the wild type. There were also age dependent differences in M/M, with smaller differences at the older range. There were other differences among mutants of similar ages. For example OAA bones increased in XLR only in cancellous bone, not seen in oim/oim. **Discussion**: The observed increase in M/M ratio in all OI bones relative to age-matched controls, is a reflection of the reduced collagen contents in these bones. The persistence of acid phosphate around the forming surfaces of most of the mutant bones reflects an attempt to synthesize new mineral. Altered XLR can be explained in terms of the nature of the different mutations. In contrast, where collagen structure per se is not altered, the synthesis and release from the osteoblast (PEDF and OPT), may slow down. Alteration in acid phosphate, may be due to delayed nucleation as the NCPs must also show delayed binding. Unpublished results show that in these models mineralization depends on the presence of properly aligned NCPs. **Conclusion:** The heterogeneity in collagen structure in OI is reflected in heterogeneous mineral characteristics. Supported by AR046121. Brtl/+ & OOA mice supplied by J. Marini; PEDF mice from T. Clemens; OPT mice from M Sohansky.

Remineralization of Dentin Lesions via the Polymer-Induced Liquid-Precursor (PILP) Process

Neha S. Saxena[1]*, Anora K. Burwell[2], Taili Thula-Mata[1], Michael Kurylo[2], Sunita P. Ho[2], Yung-Ching Chien[2], Jing Cheng[2], Nancy F. Cheng[2], Stuart A. Gansky[2], Sally J. Marshall[2], Stefan Habeliz[2], Grayson W. Marshall[2], Laurie B. Gower[1]. [1] Materials Science and Engineering Department, University of Florida, Gainesville, Florida, [2]Department of Preventive and Restorative Dental Sciences, University of California San Francisco, San Francisco, California

Introduction: In the United States, dental caries remains the most prevalent chronic disease. Although the incidence of dental caries has decreased in the past 50 years, recent studies by the Centers for Disease Control and Prevention show a statistically significant increase in the occurrence of dental caries in children aged 2 – 11 years. Much work has been done on developing a process to remineralize dentin to prevent tooth loss due to caries. In the polymer-induced liquid-precursor (PILP) process developed by our group, anionic polymers are used to sequester ions. This results in liquid-liquid phase separation, forming droplets that can infiltrate collagen fibrils and induce mineralization. **Purpose:** To evaluate the efficiency of the PILP process in the remineralization of artificial dentin lesions. **Methods:** 140 μm deep dentin lesions were created via exposure to acetate buffer at pH 5 for 66 hours. The lesions were then remineralized via the PILP process, using 27 kDa poly-aspartic acid (pAsp) for 7, 14, and 28 days. The specimens were dehydrated to measure shrinkage via optical microscopy and wet nanoindentation was performed to determine the recovery of the elastic moduli. Micro-XCT and EDS were conducted to determine mineral content throughout the lesions. TEM was performed to examine the mineral-collagen relationships within the specimens. **Results:** The shrinkage measurements decreased drastically, from over 20 μm for demineralized specimens, to less than 2 μm for specimens remineralized for 14 and 28 days. After remineralization for 14 days, the elastic moduli at the surfaces of the lesions resulted in a 91% improvement over those of the demineralized lesions, but were only about 51% of that for native dentin. Micro-XCT showed full mineral recovery of the lesions after remineralization for 14 days. EDS data showed very little difference between the bottom and top of a lesion remineralized for 14 days. TEM showed an increase in mineral content between 0, 7, and 14 day remineralization times, but the mineral organization in the fibrils at the surface of the lesion did not appear to be fully recovered. **Conclusions:** The bottom halves of the lesions recovered to normal levels of elastic moduli, while the top portions recovered about 50% of their mechanical properties, even though full remineralization was achieved, according to the micro-XCT profiles. **Current Work:** Other reaction conditions are being explored to determine the influence on the structural organization of the tissue, such as degree of intra- versus extra-fibrillar mineral, which we believe may relate to the lower mechanical recovery of the outer remineralized zone.

Asporin in epithelial and mesenchymal mineralized tissues

Sophia Houari[1,2, 3, 4], Tillman Wurtz[2, 3, 4], Didier Ferbus[1,2, 3, 4], Danielle Chateau[1,2, 3], Ariane Berdal[1,2, 3, 4], Sylvie Babajko*[1,2, 3, 4] [1]Centre de Recherche des Cordeliers, INSERM UMRS 872, Paris, 75006 France, [2]Université Paris-Descartes, Paris, France, [3]Université Pierre et Marie Curie-Paris, Paris, France, [4]Université Paris- Diderot, UFR d'Odontologie, Paris, France

Introduction: Fluoride protects enamel from caries, but excessive fluoride intake leads to enamel hypomineralization as well as defects in other tissues. We have previously studied fluoride effects on gene expression in cultured odontoblastic cells by microarrays (Wurtz et al., 2008). Among fluoride target genes identified, asporin appeared particularly relevant as it is involved in the mineralization process. Asporin/PLAP-1 is an extracellular matrix (ECM) protein that belongs to the small leucine-rich repeat proteoglycan (SLRP) family and is expressed in osteoarthritic articular cartilage, dentin and periodontal ligament. **Purpose**: to determine the involvement of asporin in different mineralized tissues including dentin, enamel and alveolar bone **Methods:** Wistar rats were treated with 2.5 mM to 7.5 mM fluoride (NaF) in drinking water during 6 weeks. Asporin expression was investigated in the dental tissues by quantitative procedures as RT-qPCR and western-blotting. Concomitantly, asporin localization in the incisor and mandibular bone was followed by confocal and transmission electron microscopy (TEM). **Results:** Asporin was expressed by odontoblasts as expected, and also by dental epithelial cells. Opposite fluoride expression modulations were observed depending on the tissues considered. Asporin expression was decreased 2-fold in the dental mesenchyme and enhanced in dental epithelium. Confocal observations showed asporin in epithelial cells, odontoblasts and predentin. Further TEM analysis showed asporin co-localization with collagen 1 in the predentin. Asporin was accumulated in pericellular microenvironment suggesting a specific function around the cells. **Conclusion**: Asporin, the only SLRP sensitive to NaF, could induce mineralization in dentinal compartment by the binding to collagen 1 and inversely, could reduce it in enamel where collagen is absent. In addition, asporin may have a protective function for cells that synthesize a mineralized ECM suggested by its pericellular accumulation. Wurtz T, Houari S, Mauro N, MacDougall M, Peters H, Berdal A. Fluoride at non-toxic dose affects odontoblast gene expression in vitro. Toxicology. 2008 Jul 10;249(1):26-34.

Self-Assembled Recombinant Elastic-Like Polypeptides Based Hydrogel: A Novel Approach for Calcium Phosphate Mineralization with Complex Morphology

Y.P. Li,[1*] X. Chen,[1] J.C. Rodriguez-Cabello,[2] C. Aparicio[1], [1]Minnesota Dental Research Center for Biomaterials and Biomechanics, Department of Restorative Sciences, University of Minnesota, Minneapolis, MN USA; [2]University of Valladolid, Valladolid, Spain.

Introduction: Biological minerals are organic-inorganic hierarchical nanocomposites with unique mechanical properties. In biomineralization processes, mineral deposition is under the control of organic molecules, e.g., self-assembled collagen fibrils serve as the template for the deposition of hydroxyapatite nanocrystals. Amorphous precursor pathways and self-assembled polymer matrices play the key roles in the morphological control of the final complex morphology. Although calcium phosphate mineralization in conventional polymeric hydrogels is receiving significant attention, limited progress was made in combining inorganic polymers and hydroxyapatite, differing in morphology and composition at nano scale. **Purpose**: Using recombinant elastin-like hydrogels carrying a bioactive peptide with known affinity for enamel hydroxyapatite and self-assembled nanoscale sheets to template calcium phosphate mineralization and obtain inorganic-organic nanocomposite. **Methods**: Triblock elastin-like recombinamers (St-ELR) (B1:$((VPGIG)_2$VPGKG$(VPGIG)_2)$DDDEEKFLRRIGRFG$((VPGIG)_2)$; B2:$(VPAVG)_{20}$; B3=B1).were synthesized according to previously published procedures. Each of the side blocks include the SN_A15 peptide (DDDEEKFLRRIGRFG), which is derived from the salivary protein statherin with known affinity for enamel hydroxyapatite crystals. The hydrogels were obtained by mixing a solution of the ELP (20mg/mL) with 50mM 1-ethyl-3-[3-dimethylaminopropyl] carbodiimide hydrochloride and 25mN N-hydroxysuccinimide. ELPs hydrogels were mineralized via the polymer-induced liquid-precursor (PILP) process. The mineralization solution was prepared by mixing equal volumes of 9 mM $CaCl_2{\cdot}2H_2O$ and 4.2 mM K_2HPO_4 in Tris-buffered saline (pH7.4). Poly-L-aspartic acid (27,000 Da) was added to calcium solution as 50-ug/mL before mixing. Hydrogels were incubated in the mineralization solution at 37 °C for 14 days. Gelatin and chitosan hydrogels were used as controls. **Results**: The transparent St-ELR hydrogels turned turbid in the mineralization solution indicating the spontaneous self-assembly of St-ELR since they have a lower critical solution temperature (LCST) below 37°C. SEM and microCT revealed that mineral penetrated from the surface of hydrogel into inner side up to 50 μm. EDS and XRD confirmed the mineral is hydroxyapatite. They were needle-shaped nanocrystals which were densely packed within the frame wall of the hydrogels without compromising microporosity of hydrogels. Mineralization of non-crosslinked St-ELRs resulted in the mixture of round hydroxyapatite nanocrystals and self-assembled nanosheets. No mineral formed in gelatin and chitosan gels. The produced St-ELR-hydroxyapatite microporous composite exhibited high elastic modulus and strength. **Conclusion**: The use of self-assembled St-ELR hydrogels with tunable self-assembling properties as well as mineral affinity open the possibility to both obtain hybrid biomaterials and study *in vitro* model systems that reproduce biomimetic processes. Complex hybrid biomaterials can be developed through templatation since St-ELR can be fabricated as fibers, thin films, as well as 3D complex matrices. **Funding**: Supported by 3M Foundation and University of Minnesota Office of Research

NanoCrystallite Models for Amorphous Calcium Carbonate

Sourabh Sinha and Peter Rez, Department of Physics, Arizona State University, Tempe, AZ 85287-1504, USA

Introduction: It is now well established that calcium carbonate biominerals are initially deposited as a transient amorphous phase that subsequently transforms to calcite. Amorphous calcium carbonate (ACC) can also be prepared synthetically in the laboratory. The evidence for the amorphous phase is the lack of optical birefringence, the suppression of the ν4 absorption relative to the ν2 absorption in IR and both electron and X-ray diffraction. The atomic structure of the amorphous phase and the mechanisms by which is transforms to a crystalline phase are still subject to controversy. Both continuous random networks and aggregations of nanocrystallites are consistent with amorphous diffraction patterns. In contrast to amorphous semiconductors or silica it is hard to see how it is possible to generate a continuous random network in calcium carbonates. **Purpose:** To determine

the size of nanocrystals whose diffraction might be classified as amorphous **Methods:** Crystal shapes corresponding to the standard calcite rhomb bounded by {10-4} facets and a needle shaped crystal bounded by {12-1} facets were generated on a real space grid. Fourier transforms representing the shape function were calculated on a grid that could be appropriately scaled to the size of the crystal. Diffraction intensities were calculated for both 200 keV electron diffraction, appropriate for an electron microscope, and Cu Kα X-ray diffraction. In the case of electron diffraction averaging over the full range of orientations of nanocrystallites was achieved by summing over diffraction from 7 well populated zones with appropriate multiplicities. For X-ray diffraction the complete range of orientations was sampled by considering all reflections within a sphere whose radius was double that of the Ewald sphere. Sorting by the magnitude of the reciprocal lattice vector gave calculated diffraction profiles. These could be directly compared with experimental measurement or use to infer a RDF. **Results:** Nanocrystallites were specified in terms of single cells bounded by the planes that defined the shape. Clear diffraction peaks were distinguishable for nanocrystallites whose size was greater than about 3 nm. The profiles from crystallites of dimension 1-2 nm gave broad peaks and were comparable to experimental observations of Michel at al[1] for synthetic ACC. The profiles for rhomb shaped were broader than those from the needle shaped nanocrystallites when specified in terms of the fundamental unit cell since the rhomb shaped fundamental cell is smaller. RDFs extracted from these diffraction profiles could erroneously give the impression of wide spread in nearest neighbor distances. **Conclusions:** Nanocrystallites 1-2 nm across give amorphous diffraction profiles consistent with ACC. 1. Michel, F.M. et al, Chem. Mater., 20, 4720-4728, (2008)

Investigating Bone Mineral Precursors In Osteoblastic Cells

Dongbo Wang[1], Wojtek Tutak[2], Ming Tung[2], Alex Fernandez-Martinez[3], Adam Wallace[4], Carl Simon[1], Marcus Cicerone[1], Sheng Lin-Gibson[1], Young Lee[1]; [1] NIST Biosystems and Biomaterials Division, Gaithersburg, Maryland; [2] American Dental Association Foundation, Gaithersburg, Maryland; [3] Institut des Sciences de la Terre, Grenoble, France; [4] Berkeley National Labs, Berkeley, California

Introduction: Formation of bone and teeth are ubiquitous among mammalian organisms. Bone is a primary focus of tissue engineered approaches for treatment of diseased or damaged tissue. Our primary focus is to understand the cells responsible for bone formation – osteoblasts and specifically to characterize the biomineralization process. Evidence from *in vivo* and cell culture systems shows that osteoblasts concentrate ions as stabilized amorphous calcium phosphate (ACP) precursors prior to the formation of the bone mineral, apatite. This evidence points to the importance of a condensed phase for the formation of mineralized tissues, however the details remain unclear. **Purpose:** We are focusing understanding the spatial (intra and extra cellular) and temporal distribution of ACP and apatite associated with osteoblastic cells; **Methods:** To address the problem we are using Broadband Coherent Anti Stokes Raman Spectroscopy (BCARS) imaging. This technique allows us to spectroscopically identify osteoblast produced mineral (ACP or apatite) along with relevant organelles such as nuclei and matrix vesicles. **Results:** We have validated the ability to use BCARS imaging to spectroscopically differentiate between ACP and apatite. Then we have applied such analysis to fixed human Bone Marrow Stromal Cells (hBMSC) induced towards an osteogenic phenotype. To date we have used BCARS imaging to spectroscopically detect the presence of intracellular ACP in hBMSC. **Conclusions:** Our experiments demonstrate that a BCARS is a useful technique for studying biomineralization in tissue culture systems. There are experiments underway to further elucidate and validate our results and better understand the spatial distribution of ACP and apatite as they are associated with mineralizing cells.

Evaluation of Bone Mass, Osteoblast Function and Treatment Results in Murine Models of Rett Syndrome.

Mary E. Blue[1, 3, 4], Charlotte Eyring[1], Adele Boskey[6], Steven Doty[6], Neal S. Fedarko[5], Mir Ahamed Hossain[1, 3], Ludmilla Lukashova[6], Jay R. Shapiro*[1, 2], [1]Hugo W. Moser Research Institute at Kennedy Krieger, Inc., Depts. [2]Rehabilitation and Physical Medicine, [3]Neurology, [4]Neuroscience, [5]Gerontology and Geriatrics, Johns Hopkins Medical Institutions, Baltimore MD, [6]Hospital for Special Surgery, Weill Cornell Medical College, New York, NY

Introduction: While 50% of children and young adults with Rett Syndrome (RTT) have osteoporosis, the effect of *MECP2* mutations on bone cell function is unknown, and there is no recognized treatment for osteoporosis in RTT. **Purpose:** To determine the effects of MeCP2 deficiency on osteoblast function *in vitro* and *in vivo* and to assess the effectiveness of treatment on bone mass with teriparatide (anabolic, TP) or zoledronic acid (antiresorptive, ZA). **Methods:** We conducted femur and tibia micro-CT, histomorphometry analyses and established osteoblast cell cultures from WT and *Mecp2*-null male and WT and *Mecp2*-HET female mice using the Bird model of MeCP2 deficiency. Untreated mice were sacrificed at 5 weeks (*Mecp2*-null and WT males) or 8 weeks of age (HET and WT females). Starting at 3 (WT and *Mecp2*-null M mice) or 8 weeks (WT and HET F mice), TP (40 mg/kg/day) ZA (20 mg/kg/week) or vehicle (saline), were injected for 6 weeks. **Results:** On MicroCT, trabecular and cortical bone parameters were significantly decreased in *Mecp2*-null mice, while trabecular bone separation was increased compared to WT. Cortical bone volume was decreased in HET but trabecular volume was increased. Osteoblasts from *Mecp2*-null mice did not express MeCP2 and had accelerated logrithmic growth rates compared to WT. Osteoblast morphology was altered and immunostained alkaline phosphatase decreased in *Mecp2*-null mice. In WT and *Mecp2*-null male mice, ZA treatment increased bone volume fraction and tissue mineral density in trabecular and cortical bone, increased trabecular number and decreased trabecular bone separation to a greater amount than did TP. In HET, ZA increased trabecular bone volume and trabecular number more than TP. **Conclusions:** Our preliminary results indicate a defect in osteoblast morphology and function, that osteoblast growth is altered by MeCP2 deficiency, and suggest that ZA may be more effective than TP in promoting increased bone growth and preventing bone loss in this RTT mouse model. **Support**: International Rett Syndrome Foundation and Rett Research Trust

Biomimetic" Randall's Plaque to Develop an In-Vitro Model System for Studying the Role of Acidic Proteins in Renal Stone Formation

Archana Chidambaram[1], Laurie Gower[1], Saeed Khan[2]. [1]Department of Material Science and Engineering, [2]Department of Pathology, University of Florida, Gainesville, FL, US.

Introduction: Understanding kidney stone formation is difficult due to the complexity of the urinary environment, and thus there is a need for the development of an in-vitro model system to study the two stages of idiopathic nephrolithiasis: 1) the deposition of calcium phosphate (CaP) in the form of Randall's plaque (RP); and 2) the subsequent overgrowth of calcium oxalate (CaOx) on RP to form a composite stone. Our group has found that many of the unusual morphologies found in RP and stones, such as mineral concretions, concentrically-laminated spherulites, and collagenous tissue, can be reproduced in-vitro via the polymer-induced liquid-precursor (PILP) process, in which acidic polypeptides induce a liquid-phase amorphous precursor. Purpose: Given that there are many acidic proteins present in urine, the PILP model system can be used to mimic stone formation and to study what role these macromolecules may play. In our initial experiments to be presented here, the development of "biomimetic" RP was investigated, which will then serve as a nidus for CaOx overgrowth studies. Methods: One main theory of RP formation is that CaP deposits initially form in the basement membrane of the thin loops of Henle, which then spread into the interstitial tissue. Thus, MatriStem® (ACell, Inc.), a decellularized porcine urinary bladder matrix was used, as it has both an intact epithelial basement membrane surface and tunica propria surface. These lyophilized tissue sheets were mineralized using a 4.5 mM calcium and 2.1 mM phosphate solution (pH of 7.4). To induce the PILP process, 50 μg/ml of poly-D-aspartic-acid (27,000 kDa) was added. Samples were removed at after 7 days and examined using SEM. Results: In samples mineralized via the conventional process, hydroxyapatite clusters were found nucleated on both the luminal side and on the surface of the collagen fibers, similar to crystallization via the classical process. In the PILP scaffolds, fibers appear thicker and the mineral coating is smooth due to coalescence of the fluidic CaP precursor. While identifiable crystal features are not seen on the collagen, the corresponding energy dispersive spectroscopy spectra detected a large presence of CaP inside the fibers. On the luminal side, faint, tiny spherule structures can be seen and the intensity contrast is suggestive of higher z-contrast expected from mineral. These may be similar to the concentrically laminated, plaque deposits found in the basement membrane, which is currently being verified with TEM. Conclusions: Kidney stones may involve non-classical crystallization pathways induced by the large variety of species in the urinary environment, and thus mineralization of native tissue scaffolds is useful to develop a model of stone formation. Supported by NIDDK grant RO1DK092311.

Collagen Structure Controls Water Diffusion Within Intra-Fibrillar Space: Implications for Ca2+ and HPO42- Ion Transport and Calcium Phosphate Nucleation In Bone Biomineralization.

Zhijun Xu1, Weilong Zhao1, Yang Yang2, Qiang Cui3, Nita Sahai1,*. 1Department of Polymer Science, University of Akron, Akron, OH, USA, 2Department of Chemistry and Biochemistry, Rowan University, Glassboro, NJ, USA, 3Department of Chemistry, University of Wisconsin-Madison, Madison, WI, USA.

Introduction: The self-assembled structure of Type 1 collagen plays a critical role in bone matrix mineralization, but the detailed mechanisms are not known. The earliest calcium phosphate (Ca-P) solid phase nucleates in the hole zones of the collagen fibrils, in the a and e bands. The mechanism(s) by which Ca2+ and inorganic PO4 ions are transported from bulk solution to the intra-fibrillar space, and eventually to the hole zones, is a major unresolved question. Proposed models in the literature include, (i) diffusion of individual ions; (ii) diffusion of Ca-P "pre-nucleation" clusters directly or aided by polyanionic non-collagenous proteins (ANCPs) or delivery by matrix vesicles, and subsequent release into the intra-fibrillar space; or (iii) Ca-P nucleation templated by ANCPs occluded within the collagen fibrils. To distinguish between these scenarios, we extended Paul Price's size exclusion model by determining the intra-fibrillar lateral space between adjacent collagen molecules compared to the size of the earliest formed Ca-P clusters. Aim: The goal of our study was to determine the mechanisms for water, Ca2+ and HPO42- transport into the intra-fibrillar space of collagen. Methods: Molecular Dynamics (MD) simulations were performed using the GROMACS 4.5 software with CHARMM and TIP3P force fields. We constructed an atomic-level model of the entire collagen molecule and of the self-assembled, pseudo-hexagonal array within a fibril, and optimized the side-chain residue configurations. The system was solvated with explicit water molecules and contained 0.1M NaCl. Simulations were run for 100ns. Results: The collagen molecules within a fibril were tightly packed with small lateral spaces (~1.5nm) from center-to-center of each molecule, near the overlap area and the a1-a3 and e1 bands. Larger lateral spaces (~3-4.5nm) were obtained at the end of the hole region near the d and c3 bands. The collagen structure results show that the space between the side-chains of the molecules available for water or ion diffusion is even smaller. Consistent with the lateral space results, the water density distribution showed that for some bands, such as a1 and a2, only a single, partial water layer was observed between the molecules; however, a bulk-like water phase existed for the d and c3 bands. Thus, the water diffusion and density distribution strongly depended on the location in the bands of the fibril. The smallest, prenucleation Ca-P clusters observed experimentally are ~1nm and large clusters of 10-80nm have been reported outside or within matrix vesicles. Our results suggest that the transport of large Ca-P clusters would be difficult anywhere in the intra-fibrillar region. Small clusters could diffuse with difficulty into the intra-fibrillar space, and even so, only near the end of the hole region. Conclusions: Only individual ions or very small (<1nm) Ca-P clusters can diffuse into the intra-fibrillar spaces and hole zones of collagen. These results provide some constraints on the proposed models for Ca2+ and PO4 transport and Ca-P nucleation in bone biomineralization.

Primary Cilia and Cartilage Development in Hypothyroidism.

Jessica Kemppainen[1], Robin Jacquet[1], Dennis Weiner[2], William Landis[*1]. [1]Department of Polymer Science, University of Akron, Akron, OH, [2]Department of Pediatric Orthopedics, Akron Children's Hospital, Akron, OH, United States.

Introduction: Primary cilia appear to be key contributors to proper organ development. It is increasingly clear that specific receptors and ion channel proteins of primary cilia initiate signaling pathways that control cell motility and/or link mechanical or chemical stimuli to intracellular transduction cascades to regulate cell differentiation, migration, and growth. Discoveries regarding primary cilia have led to design of drugs currently being evaluated in a wide range of human diseases. **Purpose**: This work is intended to examine possible changes in primary cilia number and orientation and in primary cilia-related gene expression that may contribute to the etiology of hypothyroidism and shorter long bone length associated with this endocrine disorder. **Methods:** Two male Sinclair miniature swine, 10-wks-old, were administered low concentrations of 6-propyl-2-thiouracil (PTU) and glucose (to enhance taste) in their drinking water to induce hypothyroidism in this animal model of the pathology. Two male age-matched control swine had no PTU or glucose. Animals at 25 wks of age were euthanized and their hind limb distal femoral (dF) and proximal tibial (pT) physes were dissected and examined by histology, quantitative histomorphometry, fluorescence immunohistochemistry (IHC) with acetylated α-tubulin antibody, and RT-qPCR analyses of primary cilia-signaling and cartilage matrix gene expression. Data were considered statistically significant at $p \leq 0.1$. **Results:** Quantitative histomorphometric analysis of the physeal zones (resting, proliferating, hypertrophic) of dF and pT of hypothyroid-induced (Hypo) and control miniature swine revealed statistically significant increased height of resting zones between the two animal groups at each anatomic location (dF: Control = 226 ± 37 μm, Hypo = 741 ± 193 μm, $p \leq 0.01$; pT: Control = 222 ± 43 μm, Hypo = 470 ± 47 μm, $p \leq 0.01$). IHC identified single primary cilia protruding from growth plate chondrocytes of both Hypo and control animals. Differences in primary cilia number and orientation were not conclusive between the two groups. For Hypo compared to control animals, initial RT-qPCR analyses of primary cilia-specific genes suggested downregulation of *smo*, *gli2*, and *gli3* as well as *PTHr1,* results implying reduced chondrocyte proliferation and differentiation in Hypo compared to control miniature swine. **Conclusions:** The study examines the first hypothyroid model in miniature swine, potentially useful for understanding the human condition. The work finds hypothyroidism in immature miniature swine causes changes critical to growth plate molecular biology, biochemistry and structure. Possible downregulated gene levels and reduced chondrocyte proliferation and differentiation resulting from primary cilia gene changes appear to underlie the weak physeal structure in the model. This work was supported by funding from the Austen BioInnovation Institute in Akron.

Freshwater acidic inputs on the coastal ocean alter the chemical composition of marine bivalves periostracum.

Laura Ramajo[1,2], Alejandro Rodriguez-Navarro*[3], Nazaret Dominguez-Gasca[3], Luis Prado[1], Rodrigo Torres[4] & Nelson Lagos[1]. [1]Laboratorio de Ecología y Cambio Climático. Universidad Santo Tomás, Chile.[2]Departamento de Cambio Global, Instituto Mediterráneo de Estudios Avanzados (CSIC-UIB), Spain.[3]Departamento de Mineralogía y Petrología, Universidad de Granada, Spain. [4]Centro de Investigaciones de Estudios de la Patagonia (CIEP), Coyhaique, Chile.

Introduction: Important impacts, at regional/continental and global scales, have been described on the coastal global carbon cycle as consequence of processes such as riverine freshwater inputs. Some coastal ecosystems receive persistent or episodic acidic inputs as a result of interactions with river water. These inputs produce a significant reduction of pH and carbonate saturation state along salinity gradients. Such river-dominated coastal marine habitat and calcifying organisms inhabiting there could be more susceptible to these chermical changes than organisms living in localities dominated by the interaction of open and coastal process, such as upwelling ecosystem. **Purpose:** Illustrate the effect of the freshwater input of the Maipo River run-off (central Chile) on mineralogical composition and periostracum chemical composition on mussel *Perumytilus purpuratus*. **Methods:** Two sites were characterized environmentally (SST, salinity and carbonate system parameters). Individuals of mussel *P. purpuratus* were collected in two closely geographic sites in central coast of Chile (Las Cruces and San Antonio). Changes in mineralogical composition (DRX analysis) and chemical composition of periostracum (FTIR analysis) were determinated. **Results:** DRX analysis showed that P. purpuratus shell is mainly composed of aragonite (>95%), which is a $CaCO_3$ mineral phase more susceptible to corrosive waters. Changes in the periostracum due to water chemistry were evidenced when comparing specimens from both sites. At the acidic site (San Antonio), the bivalves had a periostracum which was thinner and with a composition richer in polysaccharids and proteins. A reciprocal transplant of individual between both sites evidenced the environmentally-induced phenotypic plasticity of this organic layer. **Conclusions:** Our results indicate the role that the acidic environment has on the expression and development of the periostracum as a protective layer for calcifying organisms. Phenotipic plasticity in shell periostracum of mussels could be adaptive and evolved to confront stressful acidic conditions, avoiding shell dissolution, promoting shell growth and reducing mussel mortalities. Supported by Project Fondecyt 1090624 (TOA-SPACE), ANILLO ACT-132 and Becas Chile Program.

The Search for the IPV Motif-Binding ER Cargo Receptor used to Traffic Acidic Proteins.

Ying Yin* & Larry W. Fisher. Matrix Biochemistry Section, NIDCR, NIH, Bethesda, MD, USA.

Introduction: In 2008 we proposed that all of the apparently diverse 5' mutations in the *DSPP* gene that caused the nonsyndromic genetic diseases of dentin could be considered ultimately (with one exception) as simple changes in the starting three amino acids of the mature protein, isoleucine-proline-valine (IPV). More recently we have shown that all of these changes (ISV, ITV, ILV, IPD etc.) result in inefficient trafficking of the highly acidic mutant DSPP proteins out of the Ca^{2+}-rich endoplasmic reticulum and, therefore, retention within the cell. Furthermore, we showed that the mutant DSPP that accumulated

in the ER caused the secretion of co-expressed normal DSPP to be reduced thereby offering an explanation of the dominant negative effects caused by these mutations. We have also noted that many other acidic, Ca^{2+}-binding proteins secreted from cells also start with an IPV-like motif (Hydrophobic-Pro- Hydrophobic or Hydrophobic-Pro-polar but not charged) and have proposed that a currently unknown cargo receptor that binds to all of these proteins and enables transit out of the ER at a rate much greater than bulk flow. **Proposal**: Most proteins currently thought to be associated with mineralization events are acidic, multivalent cation-binding proteins that should have similar problems accumulating in the Ca^{2+}-rich (1-10 mM) ER unless rapidly trafficked out. We would like to identify our proposed IPV-binding cargo receptor in the ER. Our approach is to first identify the receptor in a yeast model system and then search for orthologs in human cells. Yeast make a nascent acidic protein in the ER that starts with an IPV-like motif. **Methods**: Express wildtype and mutant DSPP constructs in yeast and observe their relative efficiency of secretion. Then express the same constructs in a battery of *Saccharomyces* mutants from available single gene knockout and knockdown gene collections with a focus on proteins expressed in the ER. We expect that yeast with missing or low expression of the proposed cargo receptor will traffic the wildtype protein as poorly as those starting with the IPV-associated mutations. **Results**: Preliminary results show that wildtype yeast can express DSPP-related constructs with IPD mutant proteins beginning to accumulate within the cell at an earlier time than the wildtype protein. The accumulating form is biochemically consistent with one retained within the ER. **Conclusions**: Although baker's yeast does not develop a mineralized matrix, like many other hard and soft tissue cells in higher eukaryotes, these single celled creatures do make acidic proteins in their endoplasmic reticulum. Yeast appear to conserve an IPV-like start to their acidic proteins and they can serve as a model system for dissecting both the ER trafficking and required destruction of mutant acidic proteins involved in the production and/or maintenance of mineralized matrices. Supported by Intramural Research Program of the NIH, NIDCR.

Three-dimensional structure of the collagenous network of human lamellar bone: a new understanding of the hierarchical organization

Natalie Reznikov *[a], Ron Shahar [b], Steve Weiner [a] ;a- Department of Structural Biology, Weizmann Institute of Science, Rehovot, 76100, Israel; b- Koret School of Veterinary Medicine, Faculty of Agriculture, Food and Environment, The Hebrew University of Jerusalem, Rehovot, Israel.

Introduction: Lamellar bone is the most widespread type of bone in many mammals, including humans. Plywood-like arrays of mineralized collagen fibrils constitute the basic organizational unit of individual lamellae. Using a dual-beam electron microscope and the Serial Surface View (SSV) method we previously elucidated the 3D organization of collagen in rat lamellar bone and identified 3 structures: a plywood-like fanning sub-lamella, a unidirectional sub-lamella and a disordered sub-lamella. Methods: Here we present the results of studies of 12 SSV volumes (about 30 lamellae) from femora of 3 differently aged human individuals. Results: We identify the same 3 sub-lamellar components in human bone as in the rat. The ordered (i.e., fanning and unidirectional) sub-lamellae show two preferred directions, mainly perpendicular to the long axis of the bone, and aligned within 10-12 degrees of the long axis. The proportion of unidirectional/fanning fibrils, as well as the direction of fanning, varies in different lamellae. At a higher organizational level, the ordered collagen fibrils are organized into 'rods' around 2 to 3 microns in diameter, and the long axes of these 'rods' are parallel to the lamellar boundaries. Each rod is enveloped in a thin layer of loosely organized fibrils – the structural equivalent of the disordered sub-lamella in the rat bone. The loosely organized collagen fibrils and their ground substance stain heavily with osmium tetroxide and alcian blue indicating the presence of another abundant organic component in addition to collagen. The canalicular network is located solely within this disordered envelope, along with voids and individual collagen fibrils that are also aligned perpendicular to the lamellar boundaries. The organization of the ordered fibril arrays into rods, wrapped in loose collagen was not observed in rat lamellar bone and might be related to a different mode of loading in human bones. Conclusions: We thus conclude that human lamellar bone is basically similar in 3D structure to lamellar bone from other animals, but contains an additional hierarchical level of organization, which may reflect mechanical adaptation and loading history of the bone.

Lentiviral Overexpression of Bone Sialoprotein Does Not Influence the Osteogenic Outcome of MC3T3-E1 Cells

Rima M. Wazen*[1], Patricia Adachi[2], Thomas Dougnac-Galant[1], Marianne Ariganello[1], Antonio Nanci[1]. [1]Faculty of Dentistry, Department of Stomatology, Université de Montréal, [2]Ribeirão Preto Dental School, USP - University of São Paulo, Ribeirão Preto, SP, Brazil.

Introduction: Bone sialoprotein (BSP) is a highly acidic, phosphorylated noncollagenous matrix protein abundantly expressed in mineralized tissues. It has been demonstrated to be involved in cell attachment and signaling, hydroxyapatite binding and nucleation, and collagen binding. Two polyglutamic-acid (poly[E]) motifs have been implicated in the mineral binding and apatite nucleation capacity of BSP. Also, it has been reported that low levels of expression impair osteoblast differentiation, resulting in reduced mineralization. **Purpose:** Evaluate whether overexpression of BSP enhances the osteogenic outcome of MC3T3-E1 cells. **Methods:** Cells were seeded and infected in large culture flasks with lentiviral vectors (LV) encoding for full-length rat BSP, or a mutated form in which both poly[E] domains were replaced by polyalanine. Uninfected cells, and cells transfected with LV encoding for green fluorescent protein (GFP), alkaline phosphatase (ALP), or ameloblastin (AMBN; a matrix protein involved in enamel mineralization and suggested to also influence bone formation) were used as controls. At 48h post-infection, cells were trypsinized and replated at equal density, and cultured under standard osteogenic conditions. Transgene expression was confirmed by fluorescence microscopy. Mineralization was assessed by alizarin red staining, qualitatively and quantitatively following cetylpyridinium chloride extraction. **Results:** Phase contrast analysis revealed no evidence of cell loss as the cultures progressed, and the early appearance of mineral in LV-ALP infected cultures. At day 21, cultures overexpressing

ALP showed abundantly more mineral than uninfected cultures. There was no significant difference in mineral deposition in cultures overexpressing AMBN, GFP, BSP or its mutant form compared to the uninfected culture. **Conclusions:** The data indicate that overexpression of BSP does not influence the osteogenic outcome of MC3T3-E1 cells. These in vitro results are consistent with the subtle mineral and bone phenotype observed in BSP knockout mice, which suggests a limited role in osteoblast differentiation but also an involvement as a mediator of osteoclast generation. Supported by CIHR, NSERC, and RSBO-FRSQ.

Quantitative Amelogenin-Enamelin Co-localization in Developing Mouse Enamel

Victoria Gallon, Lisha Chen and Janet Moradian-Oldak. Center for Craniofacial Molecular Biology, University of Southern California, Health Sciences Campus, 2250 Alcazar Street, Los Angeles, California 90033

Introduction: Our most recent *in vitro* investigations suggest that enamelin cooperates with amelogenin to control crystal nucleation, morphology and organization. **Purpose:** To quantitatively analyze co-localization of enamelin and amelogenin by using confocal microscopy and to provide evidence for amelogenin-enamelin interactions *in vivo*. **Methods:** Antibodies against a peptide located within the 32kDa enamelin, against the full-length recombinant mouse (rM179), and against a peptide at the C-terminus of amelogenin were used to examine molars from postnatal 1-8 days mouse mandibles. By measuring the co-localization in small areas [regions of interest (ROI)] a picture of the amount of co-localization in reference to the maturity of the enamel can be seen. Quantitative co-localization analysis (QCA) was performed in different configurations using large (45 µm height, 33 µm width) and small (7 µm diameter) ROIs to elucidate any patterns. ROIs were taken in three different ways; a large ROI incorporating the entire thickness of enamel; a small ROI following the mineralization front from the cervical loop to the tip of the tooth; and a small ROI following the direction of crystal elongation. **Results:** Amelogenin and enamelin were secreted into the extracellular matrix on the cuspal slopes of the molars at P1 and secretion continued to at least P8. At early ages, when enamel was initially developing, there was a greater percentage of amelogenin co-localizing with enamelin than enamelin co-localizing with amelogenin, therefore there was more 'free' enamelin than 'free' amelogenin. As the enamel matured this pattern became reversed; on P4 and P5, the percentages of co-localization of enamelin and amelogenin were similar, and then the percentage of co-localizing enamelin becomes greater than the percentage of co-localizing amelogenin (P6-8), indicating there is now more 'free' amelogenin than 'free' enamelin. Co-localization patterns in P8 samples revealed that enamelin and amelogenin co-localize near the secretory face of the ameloblasts and appear to be secreted approximately in a 1:1 ratio. The degree of co-localization decreases as the enamel matures, both along the secretory face of ameloblasts and throughout the entire thickness of the enamel with the C-terminal region of amelogenin located along the secretory face of the ameloblasts. **Conclusions:** The percentage of co-localization between enamelin and amelogenin varies with the postnatal age of the mouse. Immuno-reactivity against enamelin is concentrated along the secretory face of ameloblasts supporting the theory that this protein together with amelogenin is intimately involved in mineral induction at the start of enamel formation. NIH-NIDCR DE-13414,DE-020099.

X-ray absorption spectroscopy at the Oxygen K-edge in forming sea urchin spicules

Ross T. DeVol1*, Rebecca A. Metzler2, Alejandro Fernandez-Martinez3, Assaf Gal4, Boaz Pokroy5, Catherine Jenkins6, Ian C. Olson1, Christopher E. Killian1, P.U.P.A. Gilbert1.
1University of Wisconsin-Madison, USA, 2Colgate University, USA, 3Universite Josef Fourier, Grenoble, France, 4Weizmann Institute of Science, Rehovot, Israel, 5Israel Institute of Technology, Haifa, Israel, 6Advanced Light Source, Berkeley, USA.
*presenting author

Studies of the formation of embryonic and adult sea urchin mineralized structures have provided valuable insight into the underlying mechanisms of biomineralization. Previous analysis using x-ray absorption spectromicroscopy at the calcium L-edge revealed that the first deposited mineral in forming sea urchin spicules is hydrated amorphous calcium carbonate ($ACC{\cdot}H_2O$)(1), which then dehydrates into ACC and finally crystallizes into calcite ($ACC{\cdot}H_2O \rightarrow ACC \rightarrow$calcite)(2). Here we further examine these phase transitions in spicules, using spectroscopy at the oxygen K-edge for the first time. In calcium carbonate ($CaCO_3$), oxygen is three times more abundant than calcium, resulting in stronger signals for oxygen spectroscopy. Furthermore, dichroism is observed at the O K-edge but not at the Ca L-edge, hence O spectroscopy provides simultaneously chemical and orientational analysis of forming calcite spicules. We will discuss the results, which provide a much deeper understanding of the mechanisms leading to the formation of calcite biominerals (3).

1. Y Politi et al. PNAS 2008.
2. YUT Gong et al. PNAS 2012.
3. R DeVol et al. unpublished.

The Osteoinductive Property of Calcium Phosphate is Mediated by Connexin 43

Fatima N Syed-Picard[1,2], Samer Zaky[2,3,*], Thottala Jayaraman[2,3], Raymond S Lam[2,3], Elia Beniash[1,2,3], and Charles Sfeir[1,2,3].
1. Department of Bioengineering, University of Pittsburgh 2. Center for Craniofacial Regeneration, University of Pittsburgh
3. Department of Oral Biology, University of Pittsburgh * Presenting author

Introduction: Recently few reports alluded to the osteoinductive properties of calcium phosphate, yet the cellular processes behind this are not well understood. Purpose: We have conducted a study to investigate the molecular and cellular mechanism by which progenitor cells may respond while being in contact with a calcium phosphate substrate.
Approach: To gain insight into the molecular mechanisms of this phenomenon, we have conducted a series of in vitro and in vivo experiments using a scaffoldless three dimensional (3D) dental pulp cell (DPC) construct as a physiologically relevant model.

Results: We demonstrate that amorphous calcium phosphate (ACP) alters cellular functions and 3D spatial tissue differentiation patterns by increasing local calcium concentration, which modulates connexin 43 (Cx43)-mediated gap junctions. To the best of our knowledge this is the first report proposing a chemical mechanism of osteoinductivity of calcium phosphates. Conclusion: These results provide new insights for possible roles of mineral phases in bone formation and remodeling and are expected to aid in development of novel tissue engineered materials. These data also emphasize the strong effect of scaffold materials on cellular functions.

Context-Dependent Function of Trps1 in the Mineralization Process

Maria Kuzynski[*1,2], Callie Mobley[2], Tony Winters[2], Manisha Yadav[3], Anne Poliard[4], Odile Kellermann[5], Jose Luis Millan[3], Dobrawa Napierala[2]. [1]Cell, Molecular, and Developmental Biology Theme, [2]Institute of Oral Health Research, Department of Oral and Maxillofacial Surgery, School of Dentistry, University of Alabama at Birmingham, Birmingham, AL, [3]Sanford-Burnham Medical Research Institute, La Jolla, CA, [4]UFR d' Université Paris Descartes, France, [5]INSERM UMR-S 747, Université René Descartes Paris 5, Paris, France.

Introduction: Trps1 is a GATA-type transcription factor that acts as a transcriptional repressor. In humans, either *TRPS1* deficiency (tricho-rhino-phalangeal syndrome, TRPS) or dysregulation (Ambras syndrome) results in skeletal and dental abnormalities, thus suggesting that proper endochondral ossification and odontogenesis require precisely controlled levels of *TRPS1*. In the perichondrium of endochondral bones as well as in developing odontoblasts, *Trps1* is highly expressed in progenitor cells and its down-regulation coincides with the onset of mineralization. This expression pattern suggests that *Trps1* is involved in the maturation of cells destined to produce the mineralizing matrix or that it prevents premature mineralization. **Purpose:** Our previous studies suggest that the role of *Trps1* in the mineralization process is context-dependent. However, little is known about the molecular determinants of the context-dependent *Trps1* activity in the mineralization process. **Methods:** To address this, we used 17IIA11 cell line as a cellular model of mineralization. We generated *Trps1* –deficient and *Trps1*– overexpressing cell lines and analyzed their mineralization and expression of osteogenic genes prior to and during the mineralization process. We performed a series of analyses including alizarin red staining and quantification, tissue non-specific alkaline phosphatase activity, qRT-PCR, and western blot analysis. **Results:** We discovered that downregulation of *Trps1* results in loss of mineralization potential associated with decreased expression of genes critical for the initiation of mineralization. In contrast, upregulation of *Trps1* results in delayed mineralization as well as reduced expression of phosphate homeostasis genes during the propagation phase of mineralization. **Conclusion:** Based on these data we have concluded that *Trps1* is required for the maturation of cells destined to produce mineralizing matrix and therefore *Trps1* supports the initiation of mineralization. However, in mature cells *Trps1* represses the extent of extracellular matrix mineralization, thus in mineralized-matrix producing cells *Trps1* acts as a repressor of mineralization.

Abstracts for Poster Session- WEDNESDAY

Identification of Membrane Proteins in the Spicule Deposition Vesicles (SDV) of sea urchin primary mesenchyme cells (PMCs)

Huey-Ming Mak*[1], Regina Knapp[1], and Derk Joester[1].[1] Department of Material Science and Engineering, Northwestern University, Evanston, Illinois.

Introduction: The formation of the endoskeleton in the sea urchin embryo by primary mesenchyme cells (PMCs) is an excellent example of biologically controlled single crystal growth. During embryogenesis, PMCs migrate along the inner ectodermal wall and fuse to form two syncytial clusters. Inside a spicule deposition vesicle in each of the syncytia, spiculogenesis commences with the formation of a tri-radiate calcite rudiment. While PMC initially elongate the rudiment along the three crystallographic *a*-axis, later growth is parallel to the calcite c-axis. Remarkably, PMCs cultured retain their ability to grow spicules in vitro [1]. However, lacking guidance cues provided by ectodermal factors, the complex branching pattern of the spicules is not reproduced. In the embryo, vascular endothelial growth factor (VEGF) has been identified to play an essential role in PMC patterning and spiculogenesis [2]. We recently demonstrated that recombinant sea urchin VEGF (rVEGF) induces the formation of linear, H-shape or tri-radiate shape spicule in PMCs culture in a concentration-dependent manner [3]. The crystal growth direction switches from c-axis to *a*-axis as spicules branch from linear to tri-radiate shape. However, the underlying mechanism of how VEGF switches spicule growth direction is not understood. We hypothesize that specific proteins in the spicule deposition vesicle (SDV) membranes play a decisive role in controlling spicule growth direction in a VEGF-dependent fashion. Purpose: To identify a) any membrane proteins specific to the SDV; and b) any difference in SDV membrane protein composition that depends on the growth direction of the spicule. Methods: PMCs were treated at different VEGF concentrations to induce formation of a) linear and b) tri-radiate spicules. PMC were harvested, collected by centrifugation, and lysed. Spicules with intact SDV membranes were enriched by centrifugation. Membrane proteins of enriched SDV were denatured with guanidinium hydrochloride and precipitated. Precipitated proteins were separated by SDS-PAGE and detected with silver staining. In parallel, isolated spicules were demineralized and similar electrophoresis procedure was performed on spicule matrix protein for comparison. Membrane proteins present in the SDV-enriched fraction will be identified by MS-based proteomics. Comparison between membrane proteins from spicules of shape a) and b) will be made. Results: We will report on the composition of the SDV sub-proteome, its comparison with other membrane protein fractions, and any changes in response to treatment of PMCs at different rVEGF concentrations. Conclusion: In a first step, we anticipate learning which proteins are specific to the SDV. In the second step, we anticipate which are differentially regulated by VEGF. This will help identify targets for further functional analysis, for example by knockdown in the embryo.

[1] Okazaki, K. Amer. Zool. 1975, 15, 567-581. [2] Duloquin, L. Lhomond, G. Gache, C. Development. 2007, 12, 2293-302. [3] Knapp, R. Wu, CH. Mobilia, K. Joester, D. J. Am. Chem. Soc. 2012, 43, 17908-17911.

In vitro studies of the migratory behavior of sea urchin PMC in VEGF gradients

Irene Y. Chang, Regina Knapp, Ching-Hsuan Wu, and Derk Joester. School of Engineering, Department of Materials Science and Engineering, Northwestern University, Evanston, IL.

Introduction: The embryonic cytoskeleton of the sea urchin is preceded by the migration and patterning of primary mesenchyme cells (PMC). PMC then fuse and spiculogenesis commences inside a syncytium, with deposition of the triradiate rudiment. This process relies on guidance cues from the embryonic ectoderm that may include a variety of extracellular matrix proteins and growth factors.[1-4] Inhibition of signaling between vascular endothelial growth factor (VEGF) and its receptor (VEGFR) has been shown to disrupt PMC patterning.[3] Since VEGFR is present only on PMC,[3] the coincidence of VEGF expression and PMC migration[3] suggests that VEGF is a chemo-attractant. Furthermore, we have recently shown that a functionally active recombinant *S. purpuratus* VEGF (rVEGF) produced in our lab[5] controls the crystallographic growth direction and branching of spicules in a concentration-dependent manner.[6] Purpose: To investigate the role of VEGF in directing PMC migration, spicule branching, and crystal growth control, we tested PMC response to gradients of rVEGF in vitro.[3] Methods: Boyden chamber assays were conducted to study PMC migration at different rVEGF concentrations and exposure times. Dynamics of PMC migration and formation of syncytia were investigated using a microfluidic device, by time-lapse imaging of cell movement and analysis of cell trajectories. Results: Boyden chamber assays showed that PMC movement could be detected after ~3 hours of exposure to rVEGF. Low rVEGF concentrations (~12.5 ng/mL) promoted PMC migration, while higher concentrations did not. Time-lapse experiments showed that PMC tend to migrate over relatively short distances inside a microfluidics device. Across a gradient, cell-cell fusion was more evident at high rVEGF concentration. Conclusions: The results indicate that PMC migrate toward a VEGF gradient, confirming the hypothesis that VEGF acts as a chemo-attractant. Migratory activity is enhanced in the lower concentration range and decreases with increasing concentrations. This provides a simple, yet effective means for PMC to migrate to the top of the gradient and stay there. Supported by the US National Science Foundation.

[1] Hodor, P.G. et al.. Dev. Biol., (2000) 222:181-194. [2] Tesoro, V. et al.. Develop. Growth Differ., (1998) 40:527-535. [3] Duloquin, L. et al.. Development, (2007) 134:2293-2302. [4] Rottinger, E. et al.. Development, (2008) 135:353-365. [5] Knapp, R.T. et al.. JACS, (2012) 134:17908-17911. [6] Wu, C.-H. et al.. JACS, (2011) 33:1658-1661.

Vascular endothelial growth factor (VEGF) directs single crystal growth in vitro

Regina T. Knapp, Ching-Hsuan Wu, Kellen C. Mobilia, Derk Joester. Department of Materials Science and Engineering Northwestern University, Evanston, Illinois 60208, USA

Introduction: A striking example of biologically controlled single crystal growth is the formation of the endoskeleton (spiculogenesis) in sea urchin embryos by primary mesenchyme cells (PMC). Spiculogenesis starts with the deposition of a triradiate spicule rudiment in parallel to the three crystallographic a-directions. Later in development, two of the radii change their growth directions by 90°, from a- to c-axis. The intricate endoskeleton of the pluteus larva results from further elongation of spicules and additional branching. Remarkably, PMC remain able to deposit single crystalline spicules in vitro. However, spicules deposited in PMC culture lack the complex branching behavior observed in the embryo.[1,2] In vivo, ectoderm-derived vascular endothelial growth factor (VEGF) has an integral role in PMC patterning and induction of spiculogenesis[3]. In other systems, VEGF is involved in branching morphogenesis, for example in angiogenesis and organ development. In analogy, we hypothesized that in the sea urchin embryo VEGF is involved in the control over branching crystal growth. **Purpose:** To study the effect of recombinant sea urchin VEGF on PMC culture. Furthermore we aim to establish a cell culture system for controlled single crystal growth to learn about the underlying molecular mechanisms how PMC and other cells translate atomic scale information into micron scale structures. **Methods:** A recombinant fusion protein containing an N-terminal Maltose binding protein and a C-terminal sea urchin VEGF (rVEGF) was constructed by standard PCR methods and expressed in bacteria. The lysate of rVEGF-expressing bacteria was used to treat PMC cultures. The spicule growth direction was determined by polarized light microscopy, overgrowth experiments, and SEM analysis. **Results:** Confirming our hypothesis, we have recently shown that recombinant sea urchin VEGF (rVEGF) stimulates spiculogenesis in vitro. In addition, depending on the concentration of rVEGF in the medium, PMC deposit linear, "h/H"-shaped, or triradiate spicules.[4] Notably, the change in shape is accompanied by a change in the crystallographic growth direction, from the c-axis in linear spicules to the a-axes in triradiates. **Conclusions:** Recombinant sea urchin VEGF acts as a concentration-dependent molecular switch of the spicule growth direction in vitro. This opens unique opportunities us to further investigate the molecular mechanism by a) transcriptional profiling; b) study of cytoskeletal rearrangement; and c) analyzing the composition of the spicule deposition vesicle (SDV) membrane. Our model system will thus contribute broadly to understanding the molecular mechanisms underlying cellular control of biomineralization.

[1] Wilt, F. H., and Benson, S. C. (2004), Academic Press Inc., San Diego. pp 273-285; [2] Wu, C.-H., Park, A., and Joester, D. (2011) JACS 33, 1658–1661; [3] Duloquin, L. et al., (2007) Development 134, 2293-2302; [4] Knapp, R. T., Wu, C. H., Mobilia, K. C., and Joester, D. (2012) JACS 134, 17908-17911

Location and Orientation of Charged Amino Acid Sidechains in Collagen Hole and Overlap Zones Direct Intrafibrillar Calcium Phosphate (Ca-P_i) Nucleation in Skeletal Biomineralization.

Zhijun Xu[1,*], Yang Yang[2], Qiang Cui[3], William J. Landis[1], Nita Sahai[1]. [1]Department of Polymer Science, University of Akron, Akron, OH, USA, [2]Department of Chemistry and Biochemistry, Rowan University, Glassboro, NJ, USA, [3]Department of Chemistry and Theoretical Chemistry Institute, University of Wisconsin-Madison, Madison, WI, USA.

Introduction: The critical role of the self-assembled structure of collagen for intrafibrillar Ca-P_i mineralization has been recognized for over 50 years based on transmission electron microscopy and recent stereochemical analyses of this protein. However, the atomic-level nucleation mechanism for Ca-P_i remains unknown. Here we propose that the location and orientation of charged amino acid sidechains direct Ca-P_i nucleation in collagen hole and overlap zones. Computational modeling of the atomic-level structure of hole or overlap regions provides an approach to examine this hypothesis. Atomistic modeling of collagen mineralization has been limited previously by the absence of information on collagen structure from Å to 10s of nm length-scales in three-dimensions and by the difficulty of adequately sampling configurations in rare nucleation events. **Purpose:** To investigate the possibility that charged amino acid location and sidechain orientation toward collagen hole zones underlie Ca-P_i nucleation. **Methods:** We use X-ray diffraction results to construct the Cα backbone structure of the e1 and e2 bands in hole zones of type I human collagen in its quarter-staggered, pseudo-hexagonal array within a fibril. The system is solvated with water molecules and the ionic strength is set at 0.1M NaCl. Sidechain configurations are optimized using atomistic Molecular Dynamics (MD) simulations for 20 ns, using the GROMACS software with the CHARMM22 force field for collagen and ions and the TIP3P force field for water. Hamiltonian Replica Exchange MD (HREMD), which is efficient for sampling ion distributions, is used to determine Ca-P_i cluster formation as well as water density profiles within the collagen hole zones. **Results:** Analyses of HREMD data show that a large percentage of charged amino acid sidechains (aspartate, glutamate, lysine, arginine) point into the hole regions of the collagen fibrils and form H-bond networks with sidechains of the opposite charges. In the presence of Ca^{2+} and P_i, these sidechains form stable Ca-P_i clusters in the hole zones. The water density distribution in the e1 band shows the presence of only a single, partial water layer between collagen molecules 1 and 3 and between molecules 2 and 3 in the pseudo-hexagonal array of molecules ordered clockwise as 1-4-1-3-2-3 surrounding the hole zones. Interestingly, a thicker water layer is obtained between molecules 2 and 3 of the e2 band compared to that in the e1 band. This water layer has a lower density than that of normal water and the low-density water phase is proposed to promote Ca-P_i cluster nucleation. **Conclusions:** Detailed atomistic modeling of the three-dimensional staggered array of molecules within a collagen fibril and HREMD simulations demonstrate that charged amino acid sidechain orientations and reduced water density within specific sites of the e1 and e2 bands of the hole zones of type I human collagen promote stable Ca-P_i cluster (nucleus) formation in skeletal biomineralization.

Are exogenous polyphosphates utilized for in vitro mineralization?

Marianne B. Ariganello*1, Sidney Omelon2, Rima Wazen1, Fabio Variola2, Antonio Nanci1. 1Université de Montréal, Montréal, Québec, Canada, 2University of Ottawa, Ottawa, Ontario, Canada.

Introduction: Polyphosphates (polyPs) are inorganic phosphate chains found extracellularly in body fluids and intracellularly in a variety of cell types, including osteoblastic cells, where they are present at higher concentrations. PolyP provides a source of inorganic phosphate (Pi) and acts as an effective calcium reservoir due to chelation. The resulting neutral Ca-polyP complex represents a concentrated store of Ca2+ and PO43- that may be biologically available for use in apatite mineralization. Alkaline phosphatase (ALP) cleaves Pi from polyP in neutral and alkaline environments, thus ALP cleavage of polyP may provide a mechanism for polyP-mediated apatite mineralization. Purpose: To compare exogenous polyP as a Pi-source for mineralization against β-glycerophosphate (βGP), the in vitro standard, and free, inorganic, orthophosphate (Pi). Methods: We conducted experiments with osteoblastic cells expressing different endogenous ALP levels, and also utilized lentiviral vectors (LV) to overexpress the ALP transgene in vitro. SaOS-2 cells (high ALP expression), MC-3T3-E1 cells (standard ALP expression) and MC-3T3-E1 LV-ALP (ALP overexpression) were cultured in the presence of either βGP or polyP. Results: Control (βGP–treated) and Pi-treated SaOS-2 cells were von Kossa (VK, Pi staining) and alizarin red (AlzR, Ca-staining) positive. Despite a high endogenous ALP expression level, SAOS-2 cells treated with polyP did not mineralize, as demonstrated by negative VK and AlzR. PolyP-treated MC3T3s and LV-ALP MC3T3s similarly displayed negative VK staining. However both polyP-treated MC3T3s cell types (control and LV-ALP) yielded a uniform AlzR stain atypical of the standard punctate pattern observed with Pi- and βGP-treated cells. Ca:P ratios generated from energy dispersive X-ray spectroscopy confirmed the apatite-like qualities of the mineral produced after βGP-treatment in SaOS-2 and MC3T3 cells. In contrast, the very low Ca:P ratios (<1.0) of polyP-treated MC3T3 cultures, combined with scanning electron microscopy suggested the presence of residual Ca-polyP material. These results intimate that AlzR binds to residual Ca-polyP in the MC3T3 cultures, resulting in non-specific "false positive" staining. Conclusions: Our results highlight the caution required when evaluating mineralization with AlzR. They also demonstrate that, under standard cell culture conditions, exogenous polyP does not promote extracellular mineralization, suggesting incomplete metabolism of polyP by ALP and/or their involvement in inhibitory events. Future studies should endeavour to explore the role of intracellular polyP stores in mineralization processes. Understanding the role(s) of polyP in physiological nucleation, mineral deposition and inhibition may provide perspective for regulation of normal and pathological mineralization. Supported by the Canadian Institutes of Health Research and Fonds de Recherche Santé Québec.

Regional identity controls osteogenesis in the embryonic skull

Heather Szabo Rogers*[1], Sabrina Schulze[1], Brian J. Cusack[1], Jacqui Tabler[2], Wills Barrell[2] and Karen Liu[2]
[1]Center for Craniofacial Regeneration, University of Pittsburgh, Pittsburgh PA 15261 [2] Department of Craniofacial Development and Stem Cells, King's College London, London, SE19RT

Introduction: Craniosynostosis is a very common congenital anomaly affecting approximately 1/2000 children. Craniosynostosis has a multifactorial etiology with genetic and environmental risk factors. It results from increased osteogenesis in the embryonic skull. While craniosynostosis is diagnosed in infancy, its primary defect arises during embryonic development. Purpose: The skull develops from two distinct tissue types, the neural crest and mesoderm, and we aim to quantify and describe the regional differences that control osteogenesis within the embryonic skull. Methods: We will use a combination of osteoblast culture experiments and traditional embryological techniques including immunohistochemistry and in situ hybridization to characterize the regional differences in the embryonic skull. Results: This proposal aims to characterize the development of the frontal and parietal bones of the skull with respect to their identities In response to increased Wnt signaling, frontal bones increase osteogenesis, while the parietal bones remain unaffected. Wnt signaling is important for regulating bone mass in adults, but little is know about its role embryonically. Using realtime PCR we have shown that members of the Wnt signaling pathway are differentially expressed, including Lef1 during embryogenesis. Intriguingly, the frontal bone-derived osteoblasts respond to increased □□-catenin-dependent Wnt signaling by increasing differentiation and a twofold increase of Supertopflash response compared to the parietal bone-derived cells. We also found that activators of the hedgehog family are also differentially increased in the frontal bone, we hypothesize that hedgehog signaling is pro-osteogenic during late osteogenesis. Conclusions: Wnt and hedgehog signaling effectors are differentially expressed in the embryonic skull.

Synthesis and characterization of biologically relevant hydrated calcium pyrophosphate phases

Pierre Gras*[1], Nicolas Ratel-Ramond[2], Pierre Lecante[2], Christian Rey[1], Stéphanie Sarda[1] and Christèle Combes[1]. [1]CIRIMAT, UMR 5085, INPT-CNRS-UPS, Université de Toulouse, ENSIACET, Toulouse, France, [2]CEMES, CNRS UPR 8011, Toulouse, France.

Introduction: Calcium pyrophosphate hydrates (CPP: $Ca_2P_2O_7 \cdot nH_2O$) have been reported in the joints of patients suffering from several types of arthritis including osteoarthritis and CPP crystal deposition disease, also known as pseudogout. Although the physico-chemical reactivities of synthetic and biological calcium phosphate crystals are largely studied in the literature, the formation and evolution of CPP crystals has been less investigated and not fully understood. To date, two different types of CPP crystals have been identified in joint tissues of arthritic patients: monoclinic and triclinic calcium pyrophosphate dihydrate (CPPD: $Ca_2P_2O_7 \cdot 2H_2O$) crystals, m-CPPD and t-CPPD respectively. Nevertheless several other forms of CPP were synthesized *in vitro*, including a monoclinic tetrahydrate m-CPPT β (CPPT: $Ca_2P_2O_7 \cdot 4H_2O$) and an amorphous phase (a-CPP). These phases were both reported to be *in vitro* precursors of the pathological dihydrated phases.[1] **Purpose:** The objective of the present study

was to fully characterize the CPP phases and investigate their evolution *in vitro*. **Methods:** Reference samples of m-CPPD, t-CPPD, m-CPPT β and a-CPP were synthesized using a novel direct synthesis method. They were all characterized by powder X-Ray diffraction (XRD), wide angle X-Ray scattering (WAXS), thermogravimetric and differential thermal analyses (TGA-DTA), scanning electron microscopy (SEM), FTIR and Raman spectroscopies. **Results:** Different domains of pH-temperature have been identified for the formation and stability of each CPP phases. Under physiological pH and temperature, a-CPP presented no evidence of crystallization over one year. The exceptional stability of a-CPP phase compared to amorphous calcium carbonate or calcium phosphate phases, already pointed out by Slater *et al.*,[2] could be explained by the flexible structure (P-O-P angle) and probably the size of $P_2O_7^{4-}$ anion. However small variation in temperature or pH led to the evolution of a-CPP into one of the crystalline forms. The results of structural and spectroscopic studies revealed analogies between the amorphous and m-CPPT β phases. Finally, we investigated the hydrolysis of pyrophosphate ions with nearby water molecules. **Conclusions:** m-CPPT β could be an intermediate during a-CPP crystallization into the m-CPPD and/or t-CPPD phases identified in pathological joints. This study contributes in the understanding of calcium pyrophosphate and more generally of calcium salts formation *in vivo* in the joints.

[1] E. H. Brown *et al.*, *J. Agric. Food. Chem.*, 1963, **11**, 214–222.
[2] C. Slater *et al.*, *J. Mater. Chem.*, 2011, **21**, 18783–18791.

Osteogenic Induction Medium Affect Wnt and BMP Molecules in a Micro-Nanostructure *In Vitro* Osteogenesis Model

R. Olivares-Navarrete[1]*, C.A. Cundiff[2], S.L. Hyzy[1], Z.Schwartz[1], B.D. Boyan[1] [1]Biomedical Engineering, Virginia Commonwealth University, Richmond, VA; [2]School of Biology, Georgia Institute of Technology, Atlanta, GA

Introduction: Osteoblast differentiation is a complex process that involves interplay between extracellular matrix (ECM), soluble molecules, and systemic factors. Several in vitro methods have been created to induce osteoblastic differentiation of progenitor or stem cells to study this differentiation. The gold standard for osteogenic induction, known as osteogenic induction medium (OIM), contains dexamethasone (a synthetic glucocorticoid), β-glycerophosphate, and ascorbic acid. The classical assays to determine osteoinduction by this medium are based on increased alkaline phosphatase activity and alizarin red positive nodules. However, it is not clear how OIM affects signaling pathways involved in osteoblastic differentiation. We have reported a new method for osteoblastic differentiation based on physical modification of the substrate on which the cells grow. These modifications produce micro/nanostructures that regulate important molecules associated with osteoblastic differentiation including specific integrins (ITG) and extracellular matrix components. Cells grown on these modified substrates produce an osteogenic environment rich in BMP2, BMP4, WNTs, and angiogenic factors, without the addition of exogenous molecules or OIM. **Purpose:** Elucidate the effect of OIM on BMP and Wnt signaling on stem cells grown on micro-nanostructured modified surfaces. **Methods:** Surface modifications of titanium (Ti) disks were achieved by top-down methods [sand-blasting and acid etching] and characterized to determine surface roughness, chemical surface composition, and surface energy. Human mesenchymal stem cells (MSCs) were grown on Ti surfaces in mesenchymal basal growth media for 7 days. After incubation RNA isolation and real time-PCR was performed. Additionally, in a parallel experiment conditioned media was harvested for soluble proteins and cell layer for growth factors and extracellular matrix components. **Results:** On smooth surfaces, OIM decreased DNA, increased alkaline phosphatase specific activity, increased osteocalcin production, and decreased osteoprogerin in comparison to growth media (GM); however, on rough surfaces, OIM increased alkaline phosphatase and decreased osteocalcin and osteoprotegerin in comparison to growth medium. BMP2 and BMP4 increased in a surface roughness-dependent manner. Levels of BMP2 in the conditioned media and cell lysate were higher in OIM that in GM. Secreted BMP4 was higher in OIM than in GM. Wnt3a decreased in GM on rough surfaces. However, OIM increased levels in a suface roughness-dependent manner. In GM, Wnt5a increased on rough surfaces in both conditioned media and in cell lysate, but OIM suppressed this effect. Surface roughness increased ITGA1, ITGA2, and ITGB1 mRNA and decreased ITGA5 mRNA in GM. Culture in OIM further enhanced expression of ITGA1 and ITGA2 and increased ITGA5, an effect greatest on rough surfaces. ITGA5 did not alter expression of ITGB1. **Conclusions:** MSCs underwent osteoblastic differentiation in response to surface micro/nanostrucutures in GM without exogenous factors. OIM shifted the expression profile of the MSCs, inducing greater levels of early markers of differentiation on rough surfaces, but decreasing later markers. The data indicate that osteogenic induction medium favors signaling pathways that differ from differentiation by surface structures. We suggest that induction with synthetic factors can overshadow molecules that in vivo may be involved in bone formation. Supported by US PHS AR052102; Ti disks are a gift from Institut Straumann AG (Basel, Switzerland).

X-Ray and Infrared Imaging as Tools to Chemically and Spatially Characterize Matrix-Mineral Deposition in Osteoblasts

Lisa M. Miller,[1,2] Meghan E. Faillace,[3] Alvin S. Acerbo,[4] and Roger J. Phipps[5]
[1]Photon Sciences Directorate, Brookhaven National Laboratory, Upton, NY 11973
[2]Department of Biomedical Engineering, Stony Brook University, Stony Brook, NY 11790
[3]GE Inspection Technologies, San Carlos, CA 94070
[4]Cornell High Energy Synchrotron Source, Cornell University, Ithaca, NY 14850
[5]Husson University School of Pharmacy, Bangor, ME, 04401

Introduction: Mineralizing osteoblasts are regularly used to study osteogenesis and model *in vivo* bone formation. Thus, it is important to verify that the mineral and matrix being formed *in situ* are comparable to those found *in vivo*. However, it has been shown that histochemical techniques alone are not sufficient for identifying calcium phosphate-containing mineral. Purpose: The goal of the present study was to demonstrate the use of Fourier Transform Infrared Imaging (FTIRI) and X-ray Nano Computed

Tomography (NanoCT) as tools for characterizing the spatial distribution and co-localization of the collagen matrix and the mineral phase during the mineralization process of osteoblasts *in situ*. Methods: MC3T3-E1 mouse osteoblasts were mineralized in culture for 28 days. FTIRI was used to evaluate the collagen content, collagen cross-linking, mineralization level and speciation, and mineral crystallinity in a spatially-resolved fashion as a function of time. NanoCT was used to image the initial mineral nodule formation on the nanoscale. To test whether these methods could detect subtle changes in the mineralization process, cells were treated with risedronate (RIS). Results: The data showed that collagen deposition and mineralization progressed over time and that the apatite mineral was associated with a collagenous matrix rather than ectopic mineral. The process was temporarily slowed by RIS, where the inhibition of osteoblast function caused slowed collagen production and cross-linking, leading to decreased mineralization. Conclusions: This study demonstrates that FTIRI and NanoCT are complementary tools to histochemistry for spatially correlating the collagen matrix distribution and the nature of the resultant mineral during the process of osteoblast mineralization. It can further be used to detect small perturbations in the osteoid and mineral deposition process. Supported by the Alliance for Better Bone Health and the US Department of Energy.

Mechanical Vibration Inhibits Osteoclast Formation by Reducing DC-STAMP Receptor Expression in Osteoclast Precursor Cells.

R.N. Kulkarni[*1], P.A. Vogelwede[2], D. Liu[1]. [1]Department of Developmental Sciences/Orthodontics, School of Dentistry, [2]Department of Mechanical Engineering, College of Engineering, Marquette University, Milwaukee, WI, USA

Introduction: It is well known that physical inactivity leads to loss of muscle mass, but it also causes bone loss. Since lesser physical demands are placed on our bodies nowadays, there is higher risk to increase bone resorption. Mechanistically, osteoclastogenesis and bone resorption have recently been shown to be regulated by vibration. However, the underlying mechanism behind the inhibition of osteoclast formation is yet unknown. **Purpose:** To investigate whether mechanical vibration of osteoclast precursor cells affects osteoclast formation by involvement of fusion-related molecules such as dendritic cell-specific transmembrane protein (DC-STAMP), and P2X7 receptor (P2X7R). **Methods:** RAW264.7 (a murine osteoclastic-like cell line) cells were treated with 20ng/ml receptor activator of NF-κB ligand (RANKL). For 3 consecutive days the cells were subjected to 1 hour mechanical vibration with 20μm displacement at frequency of 4Hz or kept under static culture conditions. After 5 days of culture osteoclast formation was determined. Gene expression of DC-STAMP, P2X7R and protein expression of DC-STAMP by RAW264.7 cells was determined after 1 hour mechanical vibration. **Results:** Mechanical vibration of RAW264.7 cells inhibited the formation of osteoclasts. Vibration down-regulated DC-STAMP gene expression by 1.6-fold in the presence of RANKL and by 1.4-fold in the absence of RANKL. Not only gene expression but DC-STAMP protein production was also down-regulated by about 66% in RAW 264.7 cells in response to mechanical vibration. However, vibration did not affect P2X7R gene expression. Mouse anti-DC-STAMP antibody inhibited osteoclast formation in the absence of vibration. **Conclusions:** Our results suggest that mechanical vibration of osteoclast precursor cells reduces DC-STAMP expression in osteoclast precursor cells leading to the inhibition of osteoclast formation.

Influence of VEGF on the Gene Regulatory Network of *Strongylocentrotus purpuratus*

Darcie Patterson *1, Regina Knapp1 and Derk Joester1.1 Department of Material Science and Engineering, Northwestern University, Evanston, Illinois

Introduction: In sea urchins embryos, deposition of a single crystalline calcite endoskeleton (spicules) is controlled by primary mesenchyme cells (PMC).1 Vascular endothelial growth factor (VEGF) has been demonstrated to be critical in spiculogenesis in sea urchin embryos and in signaling certain biomineral-related genes such as MSP 130 and SM30.3 Recently, we showed that the spicule growth direction in PMC culture can be controlled by treatment with varying concentrations of recombinant sea urchin vascular endothelial growth factor (rVEGF) where *c*-axis (linear) spicules result from low concentrations of rVEGF and *a*-axis (triradiate) spicules result from high concentrations2. We therefore hypothesize that VEGF will influence variation in transcription levels of biomineral related proteins such as SM30A-SM30F and SM50 in PMC that ultimately leads to control over spicule growth direction. **Purpose:** To analyze data collected from quantitative real-time PCR (qPCR) to determine the transcriptional profile related to differential regulation controlled by *S. purpuratus* PMC. **Approach:** PMC were treated with fetal bovine serum and varying concentrations of VEGF and allowed to deposit spicules. Total RNA was then isolated from PMC using TRIZOL, and reverse transcribed using a reverse transcription kit. The cDNA will be amplified with alongside targets for the SM30 family, SM50, C-lectin, p58 and other genes that are important in biomineralization. Ubiquitin, ATP synthase, topoisomerase 1, succinate dehydrogenase and ribosomal protein L13 will be used as reference genes against which the transcriptional level the targets will be compared. **Results:** A method has been established for the isolation of pure, intact RNA from whole embryos and PMC from *S. purpuratus* in amounts sufficient for qPCR analysis. **Conclusion:** We anticipate that transcriptional profiling will identify target genes for further analysis of the biological mechanism of cellular control over crystal growth along specific crystallographic directions.

1. *Spicule Formation by Isolated Micromeres of the Sea Urchin Embryo.* **Okazaki, K.** 3, Tokyo : Oxford University Press, 1975, Vol. 15

2. *Recombinant Sea Urchin Vasclar Endothelial Growth Factor Directs Single-Crystal Growth and Branching in Vitro.* **Knapp, R., et al., et al.** s.l. : American Chemical Society, 2012.

3. *Localized VEGF signaling from ectoderm to mesenchyme.* **Dulonquin, L., Lhomond, G. and Gache, C.** 2007, Development

Amorphous-Crystalline Transitions of Biomimetic Ca, Sr, and Ba Carbonates Grown Inside Liposomes

Michael L. Whittaker*, Chantel C. Tester, Derk Joester. Department of Materials Science and Engineering, Northwestern University, Evanston, IL, 60208.

Introduction: Amorphous calcium carbonate (ACC) is an essential precursor phase for mineralized tissues in organisms across many taxonomic phyla. The utility of ACC lies in its metastability and its potential to transform into any of the three crystalline polymorphs of $CaCO_3$. One prevalent strategy in biomineralization is to synthesize amorphous precursor particles within lipid vesicles, which isolate the particle from the external solution and transport it to the growing mineral. Synthetic liposomes are model systems that greatly facilitate the study of the synthesis and phase transformations of amorphous precursor particles, because they eliminate the influence of the numerous cellular processes and components that are present in living systems, and allow the impact of individual factors to be examined uniquely. Previously, we have utilized synthetic submicron phospholipid vesicles (liposomes) to show that ACC will nucleate and remain stable within the membrane of submicron liposomes for over 24 hours, which is likely due to the exclusion of heterogeneous nucleators and a high activation barrier to crystalline transformation. It is of great interest to study this behavior in analogous systems, in order to elucidate factors affecting amorphous stability and the transformation process in bioinspired materials. **Purpose:** To provide evidence for amorphous precursor phases of $CaCO_3$ analogues $SrCO_3$ and $BaCO_3$ and compare their stability and structure to that of ACC. **Methods:** We use synthetic submicron (100-200 nm) and giant (10-50 ◘m) phospholipid vesicles (GV's) to observe the mineral formation process of these three carbonates. Cryo-TEM, polarized light microscopy, confocal Raman spectroscopy, and X-ray diffraction were used to characterize crystallinity and morphology in the resulting materials. **Results:** In submicron liposomes, ACC remained stable for over 24 hours, while $SrCO_3$ and $BaCO_3$ crystallized rapidly. In GV's, many ACC particles formed, grew, and aggregated, but remained stable for over one week, as determined by the lack of birefringence under cross-polarizers. Interestingly, an amorphous strontium carbonate (ASC) phase formed in GV's but quickly transformed into strontianite through dissolution-reprecipitation. Bulk synthesis of ACC and ASC showed evidence of metastability in both phases. In contrast, any amorphous phase in the Ba system was too transient to observe, and witherite nucleated almost instantaneously. **Conclusions:** It is hypothesized that in the absence of all other heterogeneous nucleators, differences contact angle between the lipid membrane and the mineral allowed $SrCO_3$ and $BaCO_3$ to nucleate heterogeneously, while preventing the same transformation in $CaCO_3$. This suggests that lipid head group chemistry may have a significant effect on biogenic crystal growth. Effects of cation radius, relative supersaturation, particle morphology on stability and nucleation rate are also considered.

Adverse Effects of BMP2 on Bone Formation and Osseointegration

Sharon L. Hyzy[1], Rene Olivares-Navarrete[1], Barbara D. Boyan*[1], Zvi Schwartz[1,2]
[1]School of Engineering, Virginia Commonwealth University, Richmond, VA; [2]Department of Periodontics, University of Texas Health Science Center at San Antonio, San Antonio, TX

Introduction: Bone morphogenetic proteins (BMPs) are important in both embryonic and adult tissue formation and repair, and can induce cartilage and bone. Clinically, large bolus doses of BMP2 are used for orthopaedic and dental applications to induce bone formation, and in combination with biomaterials to increase peri-implant bone. Inflammatory (swelling, seroma) and bone related (ectopic bone formation, bone resorption) complications are reported after BMP2 treatment along with bone formation. **Purpose:** To investigate potential deleterious effects of BMP2 on inflammation and apoptosis in osteoblasts. **Methods:** Effects on peri-implant inflammation were examined by quantifying secreted inflammatory interleukin (IL) production of osteoblast-like MG63 cells on tissue culture polystyrene (TCPS) or titanium substrates: smooth (PT) [Ra<0.4μm], sandblasted and acid etched (SLA) [Ra=3.2μm], or hydrophilic-SLA (modSLA) after 24 hour incubation ± 40 ng/ml BMP2. Apoptosis was assessed in confluent human mesenchymal stem cells (HMSCs) and normal human osteoblasts (NHOst) on TCPS treated with 50-200 ng/ml BMP2. Apoptosis was measured by quantitative *in-situ* TUNEL, caspase-3 activity, and BAX/BCL2 expression. Data are mean±SEM of n=6 cultures per variable (ANOVA with post-hoc Bonferroni's t-test). **Results:** Surface roughness and energy decreased pro-inflammatory and increased anti-inflammatory interleukin production by osteoblasts. In contrast, exogenous BMP2 abolished the surface effect, increasing pro-inflammatory IL6, IL8, and IL17 in a surface roughness-dependent fashion and decreasing anti-inflammatory IL10 on rough surfaces. BMP2 had little effect on apoptosis in HMSCs. In contrast, BMP2 increased TUNEL, caspase-3, and BAX/BCL2 in NHOst in a dose-dependent manner. **Conclusion:** The results suggest that while surface features direct an initial controlled inflammatory response, the addition of BMP2 induces a pro-inflammatory response. The apoptotic effects of BMP2 on apoptosis depend on cell maturation state, inducing apoptosis in committed osteoblasts. Addition of BMP2 to microtextured orthopaedic and dental implants may increase inflammation and possibly delay bone formation. Dose, location, and delivery strategies are important parameters to consider when using BMP2 as a therapeutic and must be optimized to minimize complications. Supported by US PHS AR052102; Ti disks are a gift from Institut Straumann AG (Basel, Switzerland).

24R,25-dihydroxyvitamin D3 Protects Rat Articular Chondrocytes from IL-1β Induced Degradation *in vitro*.

Qingfen Pan*, Barbara Boyan, Zvi Schwartz. Department of Engineering, Virginia Common Wealth University, Richmond VA, USA 23220.

Introduction: Osteoarthritis (OA) is the most common degenerative joint disease, which is linked to joint inflammation, cell death, and cartilage degeneration. 24R,25-dihydroxyvitamin D3 (24R,25(OH)2D3) is a vitamin D metabolite that has shown to

have protective effects against growth plate chondrocyte apoptosis and cartilage destruction. **Purpose:** The aim of the present study to examine if 24R,25(OH)2D3 can protect knee cartilage from cell apoptosis and cartilage destruction induced by interleukin 1β (IL-1β). **Methods:** To establish an in vitro model of OA, primary rat articular chondrocytes were isolated from adult Sprague-Dawley rat femurs and stimulated with 1, 5, and 10ng/ml of interleukin 1β (IL-1β),and the change in chondrocytes phenotype and induction of major pro-inflammatory cytokine found in osteoarthritis was examined. To test the therapeutic effects of 24R,25(OH)2D3, articular cartilage cells were plated on 24 well plates and treated with 10ng/ml Il-1β for the first 12 h. For the next 12 h, cells were treated with 10ng/ml IL-1β or IL-1β with 10^{-9}-10^{-7} M 24R,25(OH)2D3. mRNA levels of chondrotypic genes were measured by real-time RT-PCR. Matrix metalloprotease 13 (MMP-13) activity and pro-inflammatory mediator prostaglandin E2 (PGE2) production were measured by ELISA and NO production by 2,3-diaminonapthalene (DAN) assay. **Results:** IL-1β increased the synthesis of catabolic factors such as MMP-13, which degrades type II collagen, the main extracellular component of articular cartilage; nitric oxide (NO), which leads to programmed cell death, and PGE2 levels. IL-1β also decreased the mRNA levels of chondrogenic genes (Collagen II, Aggrecan, and SOX9). A different regiment of co-treatment was examined and the best results was found when the cells treat with 10ng/ml Il-1β for the first 12 h and for the next 12 h, cells were treated with 10ng/ml IL-1β and 24R,25(OH)2D3 for addition 12 hours. The co-treatment of IL-1β with different doses of 24R,25(OH)2D3 showed a dose dependent decrease of MMP-13 activity, NO production as well as levels of PGE2 compare to treatment with only 10ng/ml Il-1β. In addition, treatment with 24R,25(OH)2D3 up-regulated the mRNA levels of aggrecan, type II collagen, and Sox-9 compared to the IL-1β treated groups. **Conclusions:** These data indicate that 24,25(OH)2D3 had important role in protection of chondrocyte from undergoing hypertrophic changes which can lead to cell apoptosis, articular cartilage degeneration, and progression of osteoarthritis. The action of 24,25(OH)2D3 occurs by blocking the deteriorating effects caused by inflammatory cytokines and matrix degradation enzymes and by up-regulating the mRNA level of of chondrocyte genes. These data may indicate that 24,25(OH)2D3 has therapeutic benefits in preventing OA or slowing its progression.

Post-translational modification is critical for biomineralization

C. Sfeir, J. Thottala, E. Beniash
University of Pittsburgh PA, Center for Craniofacial Regeneration

The mineralization of bone and dentin is a highly controlled process which is tightly regulated by cells. The constituents of this mineralizing structure vary by species and tissue, but it is known that the post-translational modification (PTM) of its component proteins represent a primary means by which cells regulate the biomineralization process. To better understand the role of phosphorylation on matrix biomineralization we established various in vitro as well as tissue culture model systems to study the kinases involved and the effect of phosphorylation levels on biomineralization.
Methods: We established stably transfected NIH-3T3 and MC3T3 cell lines with exon 5 of DSPP (Phosphophoryn) and assessed the effect of PP on the extracellular matrix mineralization in these 2 cell types (cells that mineralize their matrix vs cells that do not mineralize their matrix). These cells were cultured in the presence of 32P-□ATP to quantify the amount of phosphorylation of Phosphophoryn (DPP). We also designed bioinspired peptides containing 3 Ser-Ser-Asp repeat motifs, based on the highly phosphorylated DPP protein. We also designed point mutations to block the CK2 recognition phosphorylation sites.
Results: The phosphorylation levels of PP in cells that mineralize their matrix are different than cells that do not mineralize their matrix. This data indicated that cells that mineralize their matrix have unique post-translational machinery compared to cells that do not mineralize their matrix. In addition, we demonstrate that up to 80% of serines in the peptide can be phosphorylated by casein kinases. We further tested the ability of these peptides to induce biomimetic calcium phosphate mineralization of collagen fibrils. Our mineralization studies have revealed that in the presence of these phosphorylated peptides, highly organized mineralized collagen fibrils structurally similar to the mineralized collagen fibrils of bone and dentin. Conclusion: Our results demonstrate that cells that mineralize their matrix have unique post-translational machinery. Using phosphorylated DPP-inspired peptides we can successfully synthesize highly organized biomimetic composite nanofibrils, with integrated organic and inorganic phases.

In situ zymography assay to evidence gelatinolytic activity in decalcified and undecalcified human dentin

Thiago Stape1, Wander J da Silva1 Luis Roberto M. Martins1, Leo Tjäderhane2, Sergio R Line1, Marcelo R Marques*1.
1Piracicaba Dental School, State University of Campinas, Piracicaba, SP, Brazil; 2 Institute of Dentistry, University of Oulu and Oulu University Hospital, Oulu, Finland

Introduction: Gelatinases are a class of the matrix metalloproteinases (MMPs), it is believed that these proteases participate in various physiological and pathological events in coronal dentin, but their exact source and location is not clear. Purpose: The purpose of this study was to evaluate the activity of gelatinases in decalcified and undecalcified human molars crowns by in situ zymography. Methods: Sixteen extracted human noncarious lower third molars of similar size and shape were obtained from volunteers between the ages 18 and 29 and used in this study. Eight teeth were fixed in paraformaldehyde and decalcified in EDTA/glycerol solution for ~ 120 days. After the decalcification, the teeth were cut approximately in the middle and in parallel to the longitudinal axis, and then they were embedded in a low melting point paraffin wax. Longitudinal and transversal sections (5 μm thick) from the teeth crown were performed in and immediately prior to in situ zymography assay, the histological slice were deparaffinized. The remaining teeth (eight undecalcified teeth) were cut in the middle and in parallel to the longitudinal axis. Each part of the tooth was use to perform serial 0.6 mm slabs, whereas one half of the tooth, the slabs were done in parallel to the longitudinal axis, and in the other half of the tooth the slabs were done transversely to the longitudinal axis. Calcified and undecalcified, samples were incubated with a solution containing DQ-gelatin in Tris-CaCl2 during 2h for the decalcified samples

and 24h for the undecalcified sample and the gelatinolytic activity was observed as green fluorescence by confocal fluorescence microscopy. Negative control sections were incubated only with Tris-CaCl2. Results: In the sections incubated with DQ-gelatin, the gelatinolytic activity was observed by the fluorescence throughout the dentin in calcified and undecalcified samples. Negative controls showed only faint dentin auto-fluorescence, which was easily discriminated from the fluorescence caused by the degradation of labeled gelatin. Although gelatinolytic activity was present also in the intertubular dentin, the highest fluorescence was found in the dentinal tubules for both calcified and undecalcified samples. Also for both kind of samples, the pre-dentin region show high fluorescence when compared to mature dentin. Conclusions: The gelatinase activity in decalcified and undecalcified human dentin can be evaluated using in situ zymography. The results showed that these enzymes retain their activities after dentin decalcification by EDTA and are concentrated in different compartments of the dentinal tissue, high gelatinase activity being observed in the dentinal tubules and in the pre-dentin, This method, potentially, may help in new investigations undertaken to understand the roles of gelatinases during teeth development and also in the pathological changes resulting in dentin organic matrix degradation. Supported by CAPES - Coordination for Enhancement of Higher Education Personnel/ BRAZIL

Formation and Growth of Randall's Plaques in Human Kidneys

Saeed R. Khan[*1], Douglas E. Rodriguez[2], Laurie Gower[2] [1]Departments of Pathology and Urology, College of Medicine, [2]Department of Material Science and Engineering, College of Engineering, University of Florida, Gainesville, Florida

Introduction: Calcium oxalate (CaOx) kidney stones are formed on renal papillary tips attached to sub-epithelial plaques of biological calcium phosphate (CaP). It was proposed that these plaques, called Randall's Plaques (RP), start as deposits in the basement membrane of the thin loops of Henle, migrate to just under the renal papillary epithelium and protrude to the surface. Once exposed to the papillary surface the plaques act as encrustation platforms and a substrate for the deposition of CaOx crystals leading to the development of CaOx stones. **Purpose:** It is our hypothesis that formation of RP is similar to vascular calcification involving components of extracellular matrix including membrane bound vesicles and collagen fibers. In order to validate our hypothesis we analyzed cold-cup biopsies of human renal papillae with RP. **Methods:** Tissue samples obtained at the time of stone removal were examined by light and electron microscopic techniques. Energy dispersive x-ray microanalysis and electron diffraction were utilized to identify the crystals. **Results:** Transmission electron microscopy revealed spherules of CaP deposits, the hallmark of RP's, in the renal interstitium as well as basement membrane of the renal tubular epithelium. CaP also appeared organized as bundles of elongated striated fibers. Both types of crystals were seen in association with the collagen fibers and membrane bound vesicles. Vesicles often contained needle shaped crystals. Some of the striated interstitial CaP crystals were closely aligned with the collagen fibers. **Conclusions:** We conclude that formation of RP starts with crystal formation in association with membrane bound vesicles and grows by mineralization of interstitial collagen fibers. This mechanism is similar to what has been proposed for bio-mineralization elsewhere in the body during pathological mineralization.

Estrogen Receptor E36 Mediates the Anti-apoptotic Effect of Estradiol *in vitro* and Associates with Clinical Outcome *in vivo*

*Reyhaan A. Chaudhri1, Agreen Hadadi1, Barbara D. Boyan1,2, Zvi Schwartz2. 1School of Biology, Georgia Institute of Technology, Atlanta, GA, USA, 2School of Engineering, Virginia Commonwealth University, Richmond, VA, USA

Introduction: In breast cancer cells, 17β-estradiol (E2) rapidly increases protein kinase C activity, which is associated with increased breast tumorigenicity, and promotes cancer cell survival, metastatic potential, and osteolytic activity by acting through the ERα variant, ERα36. E_2 also mediates anti-apoptosis against taxol, a common chemotherapeutic drug used to treat breast cancer patients. **Purpose:** The aims of this study were to elucidate the mechanism by which ERα36 promotes cancer cell survival and to determine if ERα36 is associated with clinical outcome. **Methods:** Using signaling inhibitors and activators, we evaluated the role of specific proteins on the protective effect of E2 against taxol-induced apoptosis. In order to evaluate these effects, we used MTT to measure cell viability, TUNEL to measure cell death, and caspase-3 activity to measure apoptotic phenotype. In order to determine if ERα36 may be a potential target in cancer, a tissue microarray containing tumors from 40 breast cancer patients were assayed for presence of ERα36 and vascular endothelial growth factor (VEGF) by immunohistochemistry (IHC) and blindly scored by three independent observers to quantify number of positive cells, intensity, and subcellular localization. We used fisher₀ s exact test to determine correlations of several variables with ER⟨36 or VEGF. We also performed Kaplan-Meier survival analysis and the log-rank test to evaluate the significance of variables associated with mortality. **Results:** Inhibition of phosphatidyl-choline specific phospholipase D (PC-PLD) with wortmannin, lysophosphatidic acid signaling with VPC32183S, and phosphoinositide-3-kinase (PI3K) with LY294002, all blocked the inhibitory effect of E2 against taxol-induced caspase-3 activity, while activation of LPA signaling with exogenous LPA and PI3K signaling with YP-40, promoted anti-apoptosis. We also found that inhibition of Gαs with cholera toxin (CTX) and calcium efflux with thapsigargin from the endoplasmic reticulum were necessary in maintaining cell survival, as both increased caspase-3 activity alone, and E2 reduced these effects. In our cohort study, we found that ERα36 intensity was positively associated with age (p=.0450) and VEGF (p=.0226). When all patients were evaluated by survival analysis, we found HER2 status, tumor stage, and lymph node metastasis were associated with mortality. However, when we stratified our analysis to patients with high ERα36 levels and cytosolic ERα36, we found that progesterone receptor status and tumor size were also associated with mortality. **Conclusions:** Our results show that ERα36 mediates the anti-apoptotic effect of E2 against apoptosis from the cell membrane through activation of PC-PLD, LPA and PI3K. The fact that E_2 reduced the apoptotic effects of CTX and thapsigargin suggests that crosstalk occurs between a cell survival-

maintenance pathway and the PLD-mediated anti-apoptotic pathway. Our TMA results indicate that ERα36 may be a potential predictor of outcome in vivo as ERα36 was positively associated with VEGF, which promotes an aggressive tumor phenotype leading to vascularization and metastasis. These data suggest that ERα36 may be a potential target for diagnosis or treatment in breast cancer.

Cell morphology and proliferation of MG-63 osteoblasts on the (100), (101), and (001) faces of mineral apatite

Marzena Z. Suder*[1] and Katarzyna M. Stadnicka[1]. [1]Department of Crystal Chemistry and Crystal Physics, Jagiellonian University, Krakow, Poland.

Introduction: Synthetic hydroxyapatite is a model biomaterial with well proven biocompatibility. Due to differences in the distribution of positively or negatively charged ions at the surface of (100) and (001) crystal faces, hydroxyapatites found application as a column material for the separation of proteins and nucleic acids in HPLC. That differences may have impact on the protein adsorption from blood, and subsequently on the initial cell attachment and growth on implanted hydroxyapatite biomaterial. Previously, we have observed preferential adhesion and proliferation of human fibroblast cells on the (100) face of mineral apatite (AP) with partial substitution of hydroxyl groups by fluoride ions. Using single-crystal mineral apatites with optimal chemical composition, we investigated the effect of crystal orientation on MG-63 cells attachment and proliferation. Main differences were observed in morphology and mutual arrangement of the osteoblasts after 24h of incubation. MG-63 cells were more firmly attached to (100) face than to (001) probably due to the preferential adsorption of bovine serum albumin to (100) face of AP. **Purpose:** To determine how the differences in the distribution of surface potential on the crystal apatite faces affect the behavior of osteoblastic cells. **Methods:** Crystal structure of the mineral apatite was obtained from single-crystal X-ray diffraction. Mean chemical composition was calculated from SEM-EDXS measurements. Morphology and cell arrangement were documented after Giemsa staining or fluorescent staining of actin filaments and nuclei. The number of viable cells was evaluated with MTT assay and with direct cell counting. **Results:** On (001) faces of AP, MG-63 cells had fibroblast-like morphology and were forming characteristic clusters with proliferating but not well attached cells. In contrast, on the (100) faces MG-63 cells were polygonal in shape, an actin cytoskeleton was more stretched and there was no characteristic mutual arrangement of the cells. At the (101) faces both types of morphologies and arrangements were observed. The number of cells after 24h and 48h was not significantly different between different crystal faces. **Conclusions:** The results suggest that crystal orientation of AP influence initial cell attachment of MG-63 osteoblasts. The differences in the cell morphologies are probably the effect of preferential protein adsorption from fetal bovine serum. In longer incubation times the effect seems to not affect the cell proliferation. However, textured hydroxyapatite biomaterials or hydroxyapatite crystallites with distinctive crystal faces (area ratio) may have strong influence on cellular response to implant *in vivo* as was reported before. This research was supported by the Polish Ministry of Science and Higher Education and the Polish National Science Centre grant no. 2146/B/H03/2011/40.

Notes

Notes

Notes

Notes